

# Stabilization of Polymer Dispersions by Using Ionic Monomers

**Sevilay Bilgin**

Polymerization Processes Group  
University of the Basque Country (UPV/EHU)  
(Donostia-San Sebastián)  
(2017)



**POLYMAT**



## Acknowledgements

First of all, I would like to express my sincere gratitude to my advisors Prof. José M. Asua and Prof. Radmila Tomovska for their guidance and help. It was a precious opportunity for me to work in Polymerization Processes Group.

I would like to extend my gratitude to the former and current members of our research group for creating a nice research environment full of joy, learning and scientific discussions. I would like to thank all faculty members of Polymat for their contribution and Ines Plaza for her help in every aspect.

I would like to thank Dr. Zhenli Wei, Dr. Vesna Daniloska, Dr. Sobhan Bahraeian, Mei Ling Liew and all other members of the Dispersion Team of Synthomer, Malaysia for guesting me 3 months. I also like to thank Dr. Odair Araujo for arranging this internship. It was a great experience.

Special thanks to Sgiker Services of University of the Basque Country. I would like to thank Dr. Gracia Patricia Leal and Dr. Maite Miranda for sample preparation, Dr. Loli Martin and Dr. Mariano Barrado for AFM and TEM analysis, Dr. Alba Gonzalez for moisture permeability tests and Dr. Jose I. Mirando for his help with NMR analysis.

I would like to acknowledge the financial support of Industrial Liaison Program in Polymerization in Dispersed Media.



Finally, I would like to thank my family, my fiancé and my friends for their endless love, support and encouragement.





## Table of Contents

---

<b>CHAPTER 1:</b>	<b>INTRODUCTION</b>	
	1.1. Objectives and challenges of the thesis	18
	1.2. Organization of the thesis	21
	1.3. References	23

---

<b>CHAPTER 2:</b>	<b>EFFECT OF COMONOMER TYPE ON THE CHEMICAL INCORPORATION OF SODIUM STYRENE SULFONATE</b>	
	2.1. Introduction	33
	2.2. Experimental	35
	2.2.1. Materials	35
	2.2.2. Polymerizations	35
	2.2.3. Characterizations	39
	2.3. Results and Discussion	39
	2.4. Conclusions	51
	2.5. References	52

---

<b>CHAPTER 3:</b>	<b>EFFECT OF INITIATOR TYPE ON CHEMICAL INCORPORATION OF SODIUM STYRENE SULFONATE ONTO POLYMER COLLOIDS</b>	
	3.1. Introduction	55
	3.2. Experimental	58
	3.2.1. Materials	58

	3.2.2. Polymerizations	58
	3.2.3. Characterizations	62
	3.3. Results and Discussion	63
	3.4. Conclusions	78
	3.5. References	81
<hr/>		
<b>CHAPTER 4:</b>	<b>EFFECT OF COMONOMER TYPE ON THE CHEMICAL INCORPORATION OF SODIUM STYRENE SULFONATE ONTO POLYMER COLLOIDS AT HIGH SOLIDS CONTENTS</b>	
	4.1. Introduction	85
	4.2. Experimental	86
	4.2.1. Materials	86
	4.2.2. Polymerizations	86
	4.2.3. Characterizations	89
	4.3. Results and Discussion	89
	4.4. Conclusions	101
	4.5. References	102
<hr/>		
<b>CHAPTER 5:</b>	<b>EFFECT OF SODIUM STYRENE SULFONATE CONCENTRATION ON LATEX AND FILM PROPERTIES</b>	
	5.1. Introduction	105
	5.2. Experimental	106
	5.2.1. Materials	106
	5.2.2. Polymerizations	106

	5.2.3. Characterizations	108
	5.3. Results and Discussion	109
	5.3.1. Latex properties	109
	5.3.2. Film properties	117
	5.4. Conclusions	135
	5.5. References	137
<hr/>		
<b>CHAPTER 6:</b>	<b>USE OF OTHER SULFONATE MONOMERS IN EMULSIFIER-FREE EMULSION POLYMERIZATION</b>	
	6.1. Introduction	139
	6.2. Experimental	140
	6.2.1. Materials	140
	6.2.2. Polymerizations	141
	6.2.3. Characterizations	142
	6.3. Results and Discussion	142
	6.4. Conclusions	149
	6.5. References	151
<hr/>		
<b>CHAPTER 7:</b>	<b>EVALUATION OF EMULSIFIER-FREE MMA/BA LATEXES AS BINDERS IN PAINT APPLICATIONS</b>	
	7.1. Introduction	153
	7.1.1. Definitions	154
	7.2. Experimental	155
	7.2.1. Materials	155

7.2.2. Polymerizations	155
7.2.3. Preparation of paints	161
7.2.4. Characterization methods	164
7.3. Results and Discussion	176
7.3.1. Latex (binder) properties	176
7.3.2. Water blanching of latex films	179
7.3.3. Properties of liquid paints	180
7.3.4. Properties of the paint films	185
7.4. Conclusions	195
7.5. References	197
<hr/>	
<b>CHAPTER 8: CONCLUSIONS</b>	199
<hr/>	
<b>List of Publications and conference presentations</b>	205
<hr/>	
<b>Conclusiones</b>	207
<hr/>	
<b>APPENDIX I: PROPERTIES OF NaSS AND POLY(NaSS)</b>	
I.1. Introduction	213
I.2. Experimental	214
I.2.1. Materials	214
I.2.2. Methods	214
I.3. Results and Discussion	219
I.3.1. Partitioning coefficient of NaSS	219
I.3.2. Effect of NaSS amount on monomer partitioning	220

	I.3.3. Homopolymerization of NaSS	220
	I.3.4. Critical micellar concentration of NaSS and P(NaSS)	224
	I.4. References	226
<hr/>		
<b>APPENDIX II:</b>	<b>MATERIALS AND CHARACTERIZATION METHODS</b>	
	II.1. Materials	227
	II.2. Estimation of reactivity ratios of NaSS and various comonomers using Alfrey and Price Q-e scheme	228
	II.3. Characterizations	230
	II.3.1. Characterization of latexes	230
	II.3.2. Characterization of polymer films	238
	II.4. References	242
<hr/>		
<b>APPENDIX III:</b>	<b>III.1. Selection of the seed used in Chapters 3-6</b>	243
	III.1.1. Method	243
	III.1.2. Results	243
	<b>III.2. Effect of initiator concentration and feed time/strategy on the chemical incorporation of sodium styrene sulfonate onto MMA/BA particles</b>	246
	III.2.1. Method	246
	III.2.2. Results	247
<hr/>		
<b>APPENDIX IV:</b>	<b>SUPPORTING INFORMATION FOR CHAPTER 7</b>	255
<hr/>		



## Chapter 1. Introduction

Waterborne dispersed polymers are used in a wide range of applications including paints, adhesives, coatings, additives for paper, textile and construction materials, biomedicine, etc.<sup>1-4</sup> The most important production process for waterborne dispersed polymers is emulsion polymerization.

In this process, surfactants play a critical role. They are instrumental in nucleation and stabilization of polymer particles and enhance mass transport by emulsifying the monomer. In addition, they maintain the colloidal stability during storage and transport as well as in the formulated product (paint, adhesive, ...).

However, emulsifiers are not chemically bonded to the polymer particles, so they can desorb from the particles and hence bring undesired effects on the properties of the latexes and the films prepared from them. Desorption of emulsifier under high shear results in the loss of stability of the dispersion. Migration of emulsifier to air-film interface during/after film formation affects the gloss properties of the film and migration to film-substrate interface reduces the adhesion to the substrate. If the chemical structures of the emulsifier and the polymer are compatible, the emulsifier molecules may distribute in the polymer matrix and act as plasticizers, affecting the mechanical properties of the film. On the contrary, if they are not compatible, emulsifier molecules may aggregate forming hydrophilic pockets within the film, which in turn increases the water sensitivity of the film.<sup>5</sup> The extent of the problem is

## Chapter 1

dependent on factors such as the chemical nature of the emulsifier and the polymer matrix and film casting conditions.<sup>6</sup>

Because of these drawbacks, alternatives to conventional surfactants have been developed based on use of polymeric surfactants, reactive emulsifiers and the use of functional monomers and initiators in emulsifier-free emulsion polymerization.

Polymeric surfactants cannot covalently bind to the polymer particles but their migration during film formation is very limited due to strong adsorption on the polymer particles.<sup>6</sup> This decreases the problems on film properties associated with conventional emulsifiers, but their low desorption rate makes them inefficient for particle nucleation.<sup>7</sup>

Reactive emulsifiers contain a double bond in the structure capable of chemical incorporation on the polymer particles during polymerization, therefore migration is avoided.<sup>8</sup> Reactive emulsifiers can be a combination of surfactant and initiator (inisurf), of surfactant and transfer agent (transurf) or of surfactant and monomer (surfmer). However, these systems have their own disadvantages. The amount of inisurf or transurf in a system affects significantly the polymerization rate and the molecular weight distribution. Surfmers are more promising but they have the limitation that their reactivity should adapt well with the reactivity of the monomers in the formulation and hence a change in the monomers used requires a different surfmer. As the commercial processes are semicontinuous, too reactive surfmers may easily become buried in the polymer particles, whereas less reactive ones

## Chapter 1

remain unreacted. Strategies for their optimal use have been proposed,<sup>9</sup> but they are still specific to particular monomer system and/or process method.

Emulsifier-free emulsion polymerization, in which the colloidal stability is provided by the chemically incorporated ionic fragments of the initiator and/or functional monomers, is an attractive alternative to avoid the use of conventional surfactants because negative effects of migratory species on the latex and film properties are prevented and the leaking of emulsifiers into the environment is avoided.<sup>10</sup>

The use of anionic (e.g. potassium persulfate)<sup>11,12</sup> or cationic (e.g. 2,2'-azobis(2-amidinopropane) dihydrochloride)<sup>13,14</sup> initiators have been reported. There are also examples with nonionic polyethyleneglycol-azo initiators that provide steric stabilization.<sup>15</sup> The main limitations of this type of stabilization are that the reactions are performed at low solids contents (around 10 wt%), the final particle sizes are quite high (0.4-1  $\mu\text{m}$ ), and the initiator amount cannot be varied without affecting the molecular weights and reaction kinetics.<sup>10,16,17</sup> Smaller particles (0.2-0.4  $\mu\text{m}$ ) have been obtained by the application of semicontinuous monomer feeding to the nucleation stage of the emulsifier-free polymerization of butyl acrylate or vinyl acetate<sup>18</sup> at very low solids contents (10 wt%). Sub-100 nm emulsifier-free poly(methyl methacrylate) particles have been synthesized at solids contents lower than 15 wt% however, by addition of cosolvents.<sup>19</sup>

Functional monomers with groups such as carboxyl,<sup>20-23</sup> sulfonate,<sup>21,24-27</sup> and amino,<sup>28,29</sup> can be used in surfactant-free emulsion polymerization. There are also

## Chapter 1

examples in which nonionic monomers bearing hydrophilic moieties such as 2-hydroxyethyl acrylate<sup>30</sup> and acrylamide<sup>31</sup> were utilized, however they have shown to be less effective. Up to the best of authors' knowledge, there is just one example of the use of phosphate or phosphonate functional monomers in emulsifier-free emulsion formulations. Penta(propylene glycol) methacrylate phosphate was used in emulsifier-free seeded semicontinuous emulsion polymerization of methyl methacrylate/butyl acrylate/acrylic acid, however emulsifier was used in seed synthesis.<sup>32</sup> In addition, phosph(on)ate monomers have been incorporated in emulsion formulations to impart special properties such as better adhesion to substrates and anticorrosion.<sup>33,34</sup>

Some of these functional groups present practical limitations. The stabilization efficiency of carboxylic acids is dependent on the pH. The pH of the reaction medium should be well above the pKa value of the acid (which for commonly used carboxylics such as acrylic and methacrylic acids is around 4.5)<sup>35</sup> to ensure the ionic state. In alkaline media, the carboxylic acids ionize substantially and lead to strong electrostatic repulsion between particles, ensuring colloidal stability. However, at pH lower than pKa, the carboxylic acids lose their ionic character and their contribution to stabilization is marginal. On the other hand, sulfates and phosphates are prone to hydrolysis. For instance, sulfate groups hydrolyze to hydroxyls at acid pH and high temperatures (>85°C), which further may oxidize to carboxyls.<sup>36</sup> The stabilization efficiency of phosphates is also pH dependent. The pKa values of phosphates are around 2 and 7,<sup>35</sup> but since phosphate groups hydrolyze in basic media, the working

## Chapter 1

conditions are close to neutral or slightly basic. Similarly, phosphonate groups have pKa values around 3 and 8<sup>35</sup> that limit their surface activity under typical polymerization conditions (the pH is usually about 3). Amines provide cationic stabilization, which have limited applications as most of the natural surfaces are anionic and hence destabilize the cationically stabilized particles. Their stabilization efficiency is also pH dependent, mostly requiring acidic conditions to ensure the cationic state.<sup>35</sup>

Sulfonate that combines a very low pKa with high stability over a wide range of temperature and pH is the most attractive functional group.<sup>27</sup> Sulfonate monomers have been extensively used in free radical polymerization<sup>21,24-27,37-40</sup> and controlled radical polymerization (CRP),<sup>41-46</sup> as well as for the production of sulfonated ionomers,<sup>47,48</sup> clean particles for bio-applications<sup>49</sup> and photonic crystals applications.<sup>50,51</sup>

Sodium styrene sulfonate (NaSS) is particularly interesting because it is commercially available and combines a very low pKa (pKa=1)<sup>52</sup> with a styrenic double bond (Figure 1.1) that copolymerizes well with many of the monomers commonly used in emulsion polymerization.

## Chapter 1

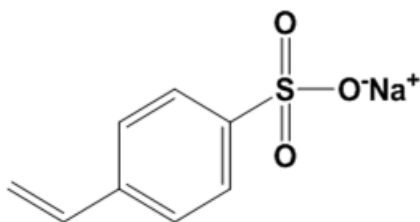


Figure 1.1. Chemical structure of sodium styrene sulfonate (NaSS)

Juang and Krieger<sup>24</sup> studied the batch emulsifier-free emulsion polymerization of styrene using NaSS and 2-sulfoethyl methacrylate (NaSEM) as functional monomers and potassium persulfate (KPS) as initiator. Particle diameter decreased with NaSS and initiator concentration and increased with the amount of styrene and ionic strength. In case of NaSS, batch reactions at 10-25 wt% solids contents with NaSS concentrations of 0.5-1.5 weight % based on monomer (wbm%) yielded particles of 150-500 nm diameter. The amount of coagulum was not mentioned, although it was noted that less coagulation was observed when buffer was utilized in the reactions. In case of NaSEM, batch reactions at 30 wt% solids resulted in high amounts of coagulum (around 20 wt%). Based on the kinetic studies, a mechanism of copolymerization of styrene and NaSS was proposed in which copolymerization takes place in the aqueous phase to form oligomeric radicals that grow until they become insoluble and precipitate to form particle nuclei. No information about the extent of chemical incorporation of ionic monomers in the polymer was given.

## Chapter 1

Chang and Chen used sodium methallyl sulfonate (NaMS) in emulsifier-free emulsion polymerization of styrene with KPS as initiator.<sup>26</sup> Batch reactions up to 20 wt% solids content were performed. 0.07- 0.28 wbm% NaMS resulted in big particles (640-970 nm). It was reported that increasing concentration of NaMS resulted in first a decrease and afterwards an increase of number of particles ( $N_p$ ). Monitoring the evolution of polymer composition by FTIR spectroscopy, they concluded that water soluble polyelectrolytes were formed, which depending on the concentration could either stabilize or destabilize the particles. It was proposed that particle nucleation occurred by a mechanism in which styrene containing oligomers aggregate to form micelles in aqueous phase, which are transformed into particles by absorption of radicals. Based on a bimodal molecular weight distribution, high number of radicals per particle and the S-shape of conversion curve, a “gradient polymerization” within the core (low radical concentration and high viscosity) and the shell (high monomer and radical content and lower viscosity) of the particles was proposed. However, no quantitative information on the extent of chemical incorporation of NaMS and coagulation was provided.

Emulsifier-free batch emulsion copolymerization of styrene (S) and n-butyl acrylate (BA) in 1:1 weight ratio using potassium salt of 3-sulfopropyl methacrylate (KSPM) and potassium persulfate (KPS) as initiator was reported by Guillaume et al.<sup>21</sup> Low solids contents (7 wt%) batch reactions with 3-26 wbm% KSPM yielded particle diameters in the range of 100-475 nm (with loss of monodispersity at high KSPM concentrations). The incorporation of KSPM into the polymer particles was 30%. As

## Chapter 1

KSPM concentration increased, the amount of the species in the aqueous phase decreased and the buried fraction of KSPM increased. This was explained by a higher flocculation of particles at high KSPM concentrations that led to the entrapment of sulfonate units within the particles. The authors explained the batch polymerization mechanism as follows: polymerization starts in the aqueous phase where the growing chains were formed mostly of the hydrophilic functional monomer. The oligoradicals grew until they reached a critical size at which either they become water-insoluble and collapse to form primary particles or achieved a critical size/concentration at which they become surface active and form micelles. Afterwards, generated particles were swollen with BA and S. As copolymerization progressed, the size of the particles increased so more charge was required on the surface for stabilization. This was achieved by chemical attachment of water soluble oligoradicals and/or by adsorption of dead hydrosoluble chains on the particles, which is less effective in stabilization due to possibilities of desorption. In the final stage, when BA and S concentrations decreased in water phase, the oligoradicals contain more functional monomer units. It was proposed that due to the higher content of charges, the propagation and termination rate of these oligoradicals in the aqueous phase also decreased, and hence capture of oligoradicals by the particles becomes dominant. However, it is difficult to understand that entry increased as the hydrophilicity of the polymer produced in the aqueous phase increased. An attempt to increase the incorporation of KSPM onto the poly(styrene/butyl acrylate) particles by a modified seeded batch process method was reported.<sup>21</sup> First, emulsifier-free

## Chapter 1

S/BA/KSPM seed latex was prepared at 25 wt% solids content in batch. The seed particles were allowed to swell by S/BA monomer mixture, and then a shot addition of KSPM and initiator was made. The final solids contents were 30 wt%. Results showed that about 80% of the post added KSPM was fixed on particle surfaces regardless of the amount of KSPM added. The performance of KSPM was compared with that of methacrylic acid (MAA) at pH=6.5 showing the sulfonate to be more efficient in stabilization than MAA due to better stabilizing efficiency of fully ionized sulfonate groups.

A detailed study on emulsifier-free emulsion copolymerization of NaSS and styrene was carried out by El-Aasser and coworkers, using persulfate/ bisulfate redox initiator at 12.5% solids contents by different processes, i.e. batch, seeded batch and semicontinuous.<sup>25,27</sup> They found that for any process the chemical incorporation of NaSS was almost complete up to 1 wbm% NaSS in the formulation. Further increase in NaSS amount resulted in the formation of large amounts of free water soluble polymer and broad (sometimes bimodal) particle size distributions. In order to improve the chemical incorporation of NaSS, a two-stage shot-growth (or in-situ seeding) method which was adapted from Sakota and Okaya<sup>53</sup> was developed.<sup>25</sup> The first stage included batch copolymerization of S/NaSS until a high conversion (90-95%) of S, and then a shot of monomer mixture were injected. As illustrated in Figure 1.2, the incorporation was almost complete in shot-growth method although it could not exceed 2.6% (by weight based on final latex) in batch, seeded batch and semicontinuous methods. The mechanism of incorporation was explained as the

## Chapter 1

surface active oligoradicals formed by NaSS and S in the aqueous phase are adsorbed on the seed particles and become irreversibly attached. The percent conversion at the time of injection and the ratio of NaSS/S in shot growth stage were found to be very critical to achieve monodispersity of the particles (sizes 130-300 nm). If the second stage monomer was added at lower conversions of first stage monomer (around 20%) the bimodal particle size distribution was obtained. Small size secondary particles were still apparent up to 81% conversion, whereas monodisperse particles were obtained if the injection was performed at conversion higher than 93%. Furthermore, as NaSS/S ratio in the second stage determines the hydrophobicity of the polymer chains, it influences significantly the particle size distribution. At values higher than 0.78, secondary nucleation was promoted. Monodisperse particles were obtained when this ratio was in the range of 0.16 - 0.46. Although very high incorporation level was reached by this method, the main drawback of the shot-growth method is that it is only successful for very low solids contents (12.5 %). The authors noted that the maximum solids content achieved without coagulum was 27 wt% at 1 wbm% of NaSS, however no results were provided.

Chapter 1

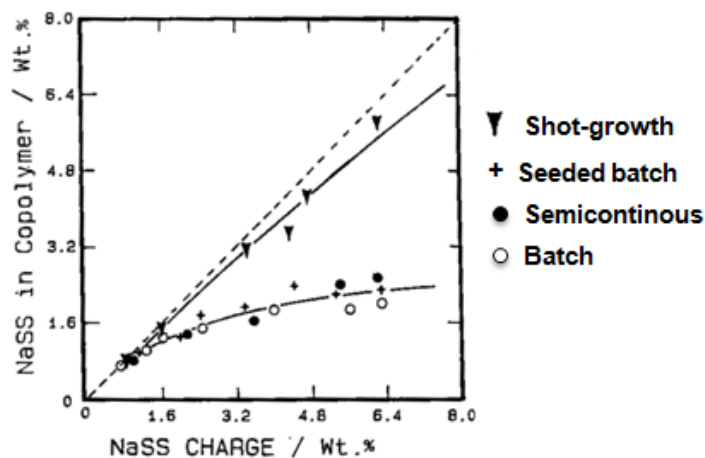


Figure 1.2. The effect of process method on the chemical incorporation of NaSS into the polymer as a function of NaSS amount in the recipe (solids contents: 12.5 wt%).<sup>25</sup> Reproduced with permission of John Wiley and Sons.

The shot-growth synthesis method was adapted by many researchers to prepare highly sulfonated polystyrene particles for different purposes such as to study the colloidal stability of these systems<sup>37,38</sup> and investigate the effect of surface charge density on emulsion kinetics.<sup>39,40</sup> The shot-growth emulsifier-free emulsion polymerization of styrene and NaSS was compared with the batch method by Peula et al. at solids content close to 20 wt% finding that the shot-growth latexes had much better colloidal stability.<sup>37,38</sup> Calculations showed that the hairy layer of these latexes was not thick enough to produce additional steric stabilization, but according to the authors, the electrostatic repulsion was improved by the presence of a layer of immobilized water within the hairy layer.

## Chapter 1

Precise kinetic studies with a reaction calorimeter in the shot-growth emulsifier-free emulsion polymerization of styrene and NaSS at approximately 10 wt% solids content were presented by Cheong et al.<sup>39,40</sup> These latexes were used as a seed for methyl methacrylate (MMA)<sup>39</sup> and styrene<sup>40</sup> emulsifier-free emulsion polymerization, reaching 15 wt% solids content. Potassium persulfate initiator was used. The kinetics was compared at low and high surface charge density of the seed particles. The authors reported that at high surface charge density, the repulsion between the seed particles and newly formed polymer chains was high, which resulted in a lower rate of radical entry, a lower average number of radicals per particle, a significant secondary nucleation and bimodal particle size distributions, especially pronounced at high MMA concentrations. In case of styrene, an oil soluble initiator (azobisisobutyronitrile, AIBN) was used as well, and for this case radical entry/exit rate did not depend on the surface charge density.<sup>40</sup> In presence of electrolyte, the thickness of the electrical double layer decreased and the polymerization rate and radical entry rate increased, whereas no influence on radical exit was noticed.

Wutzel prepared sulfonated polystyrene particles of 30-80 nm size by seeded semicontinuous polymerization.<sup>54</sup> The polystyrene seeds, which were stabilized by conventional emulsifier sodium dodecyl sulfate (SDS), were allowed to grow by feeding S, NaSS and KPS forming a shell around the polystyrene core. Final solids contents were around 10 wt%. It was demonstrated that the surface charge density could be controlled very well by the amount of NaSS. The yield of NaSS incorporation

## Chapter 1

on the polymer particles were reported as 57-74%, yet the amount of conventional emulsifier in the final latex was much higher than that of NaSS.

Copolymerization of NaSS with more hydrophilic monomers, MMA and vinyl acetate (VAc) was performed at 20 wt% solids content by using colloidal silica as stabilizer.<sup>55</sup> In case of MMA, different functional monomers (acrylic acid, NaSS, hydroxyethyl methacrylate and dimethylamino ethylmethacrylate) were utilized and the polymer dispersion which contained NaSS displayed better colloidal stability, demonstrated by the measurement of light backscattered from the dispersion during 3 days. For this dispersion, the highest zeta potential and the lowest average particle size (around 150 nm) with narrowest particle size distribution (polydispersity index was 0.45) was measured. In case of VAc and NaSS, very high particle size was reported (>10  $\mu\text{m}$ ) with wide distribution. However, the extent of incorporation was not studied.

Xu et al. reported the production of stable emulsifier-free polystyrene latexes at 25 wt% solids contents by using NaSS (2.4 wbm%), HEMA (2.4 wbm%), or a combination of both.<sup>56</sup> Monodisperse particles 60 nm in diameter were obtained by seeded semicontinuous emulsion polymerization. The seed particles were prepared at very low solids content by copolymerizing styrene and NaSS with KPS as initiator. Then, these particles were allowed to grow by making very slow addition (6 hours) of styrene with and without HEMA. The latexes were reported as stable during storage for 10 months. The authors reported continuous homogeneous nucleation in the early

## Chapter 1

state of polymerization, which increased with NaSS content. HEMA showed weaker role in particle nucleation, however when used in combination with NaSS it resulted in very stable latexes with smaller particle size, due to the combination of electrostatic and steric stabilization effects exerted by hydrophilic -OH groups, according to the authors. However, the steric stabilization could likely be provided by non-ionic water soluble species rich in HEMA. Higher solids content led to particle coagulation. Although the amount of NaSS incorporated was not measured, XPS analysis of the purified dried particles indicated that half of the surface of the particle was covered by NaSS and/or HEMA. Similar results were observed using the same process for butyl methacrylate polymerization at 27 wt% solids content.<sup>57</sup>

2-acrylamido-2-methylpropane sulfonic acid (AMPS) was used in the production of emulsifier-free S/BA latexes at 40 wt% solids contents.<sup>58</sup> 2-4 wbm% AMPS yielded particles in the range of 250-480 nm. A semicontinuous method was used. AMPS, water, buffer, persulfate initiator and monomer mixture (actual amount was not given) were initially charged in the reactor (no information was offered about the time given for the initial charge to react). The remaining monomer mixture was fed for 3-4 hours. The amount of coagulum during the synthesis was 1% for the reaction with 2 wbm% AMPS. Slightly better salt stability was observed compared to the control latex synthesized by a mixture of nonionic and ionic emulsifiers. Dai and coworkers expanded the same system to 50 wt% solids content.<sup>59</sup> 1-3 wbm% AMPS yielded particles of 230-630 nm diameters. According to the authors, particles were formed by homogeneous nucleation. The amount of coagulum during the synthesis of the

## Chapter 1

latex with 1.5%wbm AMPS was 0.6%. AMPS containing latexes had better salt stability and their films displayed less water uptake than the control analogs prepared by using SDS. All latexes failed in freeze-thaw stability tests. Incorporation of AMPS onto particles was not studied.

Emulsifier-free emulsion polymerization of MMA/BA at 60 wt% solids content was carried out using 3-allyloxy-2-hydroxy-1-propanesulfonic salt (AHPS).<sup>60</sup> The reactions with 1-4 wt% AHPS yielded monodisperse particles in 300-500 nm range. A semicontinuous method was applied in which AHPS, water, persulfate initiator and monomer mixture (actual amount was not given) was used as the initial charge. No information about the time given for the initial charge to react was provided. The remaining monomer mixture was fed for 4 hours. It was reported that no coagulum was formed during the syntheses and no sedimentation occurred during storage for 10 months. The particle size decreased with AHPS concentration because more particles were produced. The contribution of charge groups of KPS to the stability was mentioned but that of OH group was discarded. AHPS incorporation onto the particles was not quantified. Water uptake and tensile properties of the emulsifier-free films were better than the control film prepared from the latex stabilized by SDS. According to the authors, emulsifiers present in conventional emulsion polymers would lead to weakening of interaction between polymer chains, resulting in lower tensile strength.

## Chapter 1

Guo et al. prepared core-shell emulsifier-free latexes using AHPS at 60 wt% solids content.<sup>61</sup> A semicontinuous method was utilized. AHPS, water, and KPS were added as initial charge. Feeding of MMA and BA mixture as the core monomers were followed by that of either MMA/BA or S as shell. 220-260 nm particles were obtained for 1.2 wbm% of AHPS. It was mentioned that the latexes were stable and the stability was accomplished through sulfate groups of the initiator, and sulfonate and hydroxyl groups of AHPS. No quantitative data about incorporation of functional monomer or coagulation were provided.

50 wt% solids content MMA/BA latex was produced by using Sipomer Cops-1 that is the commercial equivalent of 3-allyloxy-2-hydroxy-1-propanesulfonic salt, together with acrylic acid (AA, 1 wbm%).<sup>32</sup> A seeded semicontinuous method was followed, using a commercial emulsifier (alkyldiphenyloxide disulfonate, Dowfax2A1) in the seed synthesis. The seed latex, sulfonate monomer and water were added to the reactor, sodium persulfate (NaPS) initiator was injected and the mixture of monomers (MMA/BA/AA) was fed to obtain a 50 wt% final latex. The incorporation of the sulfonate monomer was about 50% regardless of the concentration used in the formulation. Enhancement in water whitening resistance was reported.

Amphiphilic block copolymers of NaSS and a more hydrophobic monomer synthesized by controlled radical polymerization (CRP) is an elegant way to chemically incorporate sulfonate monomers on the polymer particles.<sup>41-46</sup> The amphiphilic copolymers have been used as surfactants in emulsion polymerization

## Chapter 1

process.<sup>41,45</sup> In this process, the hydrophobic block may be extended with the main monomer ensuring virtually complete incorporation of sulfonate monomer to the polymer particles. However, from the industrial point of view CRP has the following limitations:<sup>62-64</sup>

- (1) Rigorous reaction conditions and multi-step synthesis may be required.
- (2) Use of CRP agents with a distinct color or odor may result in discoloration or an unpleasant odor in the final product.
- (3) CRP agents may interfere with the polymerization of the main monomer lowering the molecular weight.
- (4) Solids contents of emulsion CRP reactions are generally low to moderate ( $\leq 25$  wt%).

In conclusion, batch, semicontinuous and seeded semicontinuous emulsion polymerization have been used to produce emulsifier-free waterborne polymers, in which the stabilization has been provided by copolymerization of major monomers with minor amounts of sulfonate monomer. Using batch polymerization, low solids contents latexes were prepared with low extent of incorporation of sulfonate monomer onto polymer particles. The dependence of incorporation on the reaction parameters was not studied. The reaction locus of the copolymerization has been determined to be in aqueous phase, however, no attempts have been made to transfer it toward the organic particle phase, where most of the emulsion polymerization occurs. The incorporation was improved by modification of batch method, thus, shot-growth emulsion polymerization was developed, in which the mixture of major and sulfonate

## Chapter 1

monomers was added in two steps. However, this method was not able to produce high solids content latexes (maximum solids content reported was 27 wt%). Semicontinuous emulsion polymerization, either with or without seeds resulted in significant augmentation of solids content, thus, stable latexes with up to 60 % solids have been prepared. Some of the properties of the latexes and the films showed improvement when compared to that obtained with conventional surfactants. Nevertheless, there is a lack of quantitative data about the incorporation of sulfonate monomers on polymer particles and no attempts were made to increase the incorporation in high solids content latexes.

### **1.1. Objectives and challenges of the thesis**

The main objective of this PhD thesis is to produce colloidally stable, high solids content and film forming emulsifier-free latexes, in which the colloidal stability is solely provided by chemically incorporated sulfonate moieties onto the polymer particles. For a proof-of-concept, (meth)acrylic monomers (MMA/BA) as major monomers and NaSS as sulfonate monomer were selected.

The implementation of this idea is challenging because MMA and BA are sparingly water soluble monomers mainly located in polymer particles (and monomer droplets) and NaSS is a water soluble monomer that is almost solely located in the aqueous phase. Thus, to realize this aim, it is important to understand well this system. For

## Chapter 1

that, preliminary studies have been performed, to determine how NaSS and its homopolymer distribute between the organic and aqueous phase in absence and presence of co-monomers and to study their surface behavior. The conditions of these preliminary studies and the results are presented in Appendix I. Based on these results, it was confirmed that NaSS is highly water soluble and it tends to be only in the aqueous phase regardless on the temperature and on the presence of monomers, MMA/BA in different ratios (Table I.2). However, distribution of MMA shifted toward the organic phase in presence of NaSS (Table I.3). The NaSS homopolymer is as well highly water soluble, but it shows some surface activity due to the structure of the homopolymer that contain hydrophobic backbone. The homopolymer is not prone to form micelles in aqueous phase (Figure I.6). However, one should have in mind that in the presence of hydrophobic monomers the oligomers formed in aqueous phase are amphiphilic as they contain units of hydrophobic monomers, so they may form micelles. Thus, micellar nucleation has been proposed by some authors,<sup>26</sup> although it has been discarded as an option by others<sup>65</sup> due to highly hydrophilic nature of oligoradicals, especially at the beginning of reaction.

Based on the state of the art and the information from the preliminary studies, the challenges to achieve the main project aim can be summarized as follows:

## Chapter 1

1. Co-polymerization of NaSS with (meth)acrylic monomers, due to different location of these polymers, the former one in aqueous phase exclusively, and the last ones mainly in droplet phase.
2. Elimination/decreasing the amount of water soluble species that may enhance the water sensitivity of the film and even destabilize the latex by acting as flocculants.
3. Ensure high colloidal stability during synthesis and afterwards.
4. Produce high solids content stable latexes.
5. The latexes should be film-forming.

The first two requirements are essential for colloidal stability which will allow increasing of the solids content. They may be achieved by shifting the locus of polymerization from the aqueous phase to the particle phase by altering the hydrophobicity of the oligoradicals growing in the aqueous phase. This can be accomplished by variables such as the nature and concentration of comonomers and initiator.

Finally, the high incorporation of NaSS and absence of water soluble oligomers will ensure improvement of latex properties such as water insensitiveness and good film properties (gloss and adhesiveness to the substrates) due to decrease in the content of the migratory species in the latexes.

## Chapter 1

### **1.2. Organization of the thesis**

This thesis is divided in eight chapters.

In Chapter 1, the state-of-the-art is reviewed and the motivation, objectives and challenges of this PhD thesis are presented. Results of a preliminary study about the phase behavior of NaSS, e.g. distribution of the monomer and homopolymer between the aqueous and organic phase are presented, as well.

In Chapter 2, the effect of comonomer type on the chemical incorporation of NaSS is investigated by model batch reactions at low solids contents. Monomers with different water solubility ((meth)acrylics, styrene) were selected in order to determine the conditions that lead to increased chemical incorporation.

In Chapter 3, the effect of initiator type on the chemical incorporation of NaSS at high solids content reactions is presented. The initiators used were selected to form hydrophilic or hydrophobic radicals in both aqueous and organic phase.

Chapter 4 reports on the effect of comonomer type on the chemical incorporation of NaSS at high solids content in seeded semicontinuous reactions. In both Chapters 3 and 4, the properties of the final latexes and the films are studied.

Chapter 5 reports on determination of effect of NaSS concentration in the formulation on the extent of incorporation on the polymer particles and on the film properties.

## Chapter 1

In Chapter 6, results of use of other sulfonate monomers, such as 3-sulfopropyl methacrylate potassium salt, 2-acrylamido-2-methylpropane sulfonic acid sodium salt and vinyl sulfonic acid in emulsifier-free emulsion polymerization of MMA/BA at high solids content (50 wt%) are presented.

Chapter 7 presents the evaluation of performance of emulsifier-free latexes based on NaSS as binders in the exterior paint formulations. Comparison with commercial binder is presented.

Finally, in Chapter 8 the most relevant conclusions of this thesis are summarized.

## Chapter 1

### 1.3. References

- [1] Force, C.G. In Emulsion Polymerization; Piirma, I., Gardon, J.L., Eds.; Academic Press: New York, 1982.
- [2] Urban D., Schuler B., Schmidt-Thümmes J. In Chemistry and Technology of Emulsion Polymerisation; van Herk, A. M., Eds.; Blackwell Publishing: India, 2005.
- [3] Chern, C-S. Principles and Applications of Emulsion Polymerization, John Wiley & Sons: USA, 2008.
- [4] Barandiaran, M.J., de la Cal J.C, Asua J.M. In Polymer Reaction Engineering; Asua J.M., Eds.; Blackwell Publishing: Malaysia, 2007.
- [5] Keddie, J., Routh A.F. Fundamentals of Latex Film Formation: Processes and Properties. Springer: Dordrecht, 2010.
- [6] Aramendia, E., Mallégo, J., Jeynes, C., Barandiaran, M.J., Keddie, J.L. and Asua, J.M., Distribution of surfactants near acrylic latex film surfaces: a comparison of conventional and reactive surfactants (surfmers). *Langmuir* **2003**, 19(8), 3212-3221.
- [7] Ballard, N., Urrutia, J., Eizagirre, S., Schafer, T., Diaconu, G., de la Cal, J.C. and Asua, J.M., Surfactant kinetics and their importance in nucleation events in (mini) emulsion polymerization revealed by quartz crystal microbalance with dissipation monitoring. *Langmuir* **2014**, 30(30), 9053-9062.
- [8] Asua, J.M. and Schoonbrood, H.A.S., Reactive surfactants in heterophase polymerization. *Acta Polymerica* **1998**, 49(12), 671-686.
- [9] Aramendia, E., Barandiaran, M.J. and Asua, J.M., On the optimal surfmer addition profile in emulsion polymerisation. *Comptes Rendus Chimie* **2003**, 6(11), 1313-1317.

## Chapter 1

[10] Aslamazova, T.R., Emulsifier-free latexes and polymers on their base. *Progress in Organic Coatings* **1995**, 25(2), 109-167.

[11] Guillaume, J.L., Pichot, C. and Guillot, J., Emulsifier-free emulsion copolymerization of styrene and butyl acrylate. I. Kinetic studies in the absence of surfactant. *Journal of Polymer Science Part A: Polymer Chemistry* **1990**, 28(1), 119-136.

[12] Goodall, A.R., Wilkinson, M.C. and Hearn, J., Mechanism of emulsion polymerization of styrene in soap-free systems. *Journal of Polymer Science: Polymer Chemistry Edition* **1977**, 15(9), 2193-2218.

[13] Goodwin, J.W., Ottewill, R.H. and Pelton, R., Studies on the preparation and characterization of monodisperse polystyrene latices V.: The preparation of cationic latices. *Colloid and Polymer Science* **1979**, 257(1), 61-69.

[14] Xu, J., Li, P. and Wu, C., Formation of highly monodispersed emulsifier-free cationic poly (methylstyrene) latex particles. *Journal of Polymer Science Part A: Polymer Chemistry* **1999**, 37(13), 2069-2074.

[15] Tauer, K., Block copolymers prepared by emulsion polymerization with poly (ethylene oxide)-azo-initiators. *Polymers for Advanced Technologies* **1995**, 6(7), 435-440.

[16] Horak, D., Uniform polymer beads of micrometer size. *Acta Polymerica* **1996**, 47(1), 20-28.

[17] Arshady, R., Suspension, emulsion, and dispersion polymerization: a methodological survey. *Colloid and Polymer Science* **1992**, 270(8), 717-732.

[18] Sajjadi, S., Extending the limits of emulsifier-free emulsion polymerization to achieve small uniform particles. *RSC Advances* **2015**, 5(72), 58549-58560.

## Chapter 1

[19] Camli, S.T., Buyukserin, F., Balci, O. and Budak, G.G., Size controlled synthesis of sub-100nm monodisperse poly (methylmethacrylate) nanoparticles using surfactant-free emulsion polymerization. *Journal of Colloid and Interface Science* **2010**, 344(2), 528-532.

[20] Ceska, G.W., The effect of carboxylic monomers on surfactant-free emulsion copolymerization. *Journal of Applied Polymer Science* **1974**, 18(2), 427-437.

[21] Guillaume, J.L., Pichot, C. and Guillot, J., Emulsifier-free emulsion copolymerization of styrene and butyl acrylate. II. Kinetic studies in the presence of ionogenic comonomers. *Journal of Polymer Science Part A: Polymer Chemistry* **1988**, 26(7), 1937-1959.

[22] Kang, K., Kan, C.Y., Du, Y. and Liu, D.S., Control of particle size and carboxyl group distribution in soap-free emulsion copolymerization of methyl methacrylate–ethyl acrylate–acrylic acid. *Journal of Applied Polymer Science* **2004**, 92(1), 433-438.

[23] Abdollahi, M., Effect of carboxylic acid monomer type on particle nucleation and growth in emulsifier-free emulsion copolymerization of styrene-carboxylic acid monomer. *Polymer Journal* **2007**, 39(8), 802-812.

[24] Juang, M.S.D. and Krieger, I.M., Emulsifier-free emulsion polymerization with ionic comonomer. *Journal of Polymer Science: Polymer Chemistry Edition* **1976**, 14(9), 2089-2107.

[25] Kim, J.H., Chainey, M., El-Aasser, M.S. and Vanderhoff, J.W., Preparation of highly sulfonated polystyrene model colloids. *Journal of Polymer Science Part A: Polymer Chemistry* **1989**, 27(10), 3187-3199.

[26] Chang, H.S. and Chen, S.A., Kinetics and mechanism of emulsifier-free emulsion polymerization. II. Styrene/water soluble comonomer (sodium methallyl sulfonate)

## Chapter 1

system. *Journal of Polymer Science Part A: Polymer Chemistry* **1988**, 26(4), 1207-1229.

[27] Kim, J.H., Chainey, M., El-Aasser, M.S. and Vanderhoff, J.W., Emulsifier-free emulsion copolymerization of styrene and sodium styrene sulfonate. *Journal of Polymer Science Part A: Polymer Chemistry* **1992**, 30(2), 171-183.

[28] Ganachaud, F., Sauzedde, F., Elaissari, A. and Pichot, C., Emulsifier-free emulsion copolymerization of styrene with two different amino-containing cationic monomers. I. Kinetic studies. *Journal of Applied Polymer Science* **1997**, 65(12), 2315-2330.

[29] Charreyre, M.T., Razafindrakoto, V., Veron, L., Delair, T. and Pichot, C., Radically initiated copolymers of styrene with 4-vinylbenzylamine and its trifluoroacetamide derivative, 2. Preparation of latex particles bearing amino groups. *Macromolecular Chemistry and Physics* **1994**, 195(6), 2153-2167.

[30] Chen, S.A. and Chang, H.S., Kinetics and mechanism of emulsifier-free emulsion polymerization. III. Styrene/nonionic comonomer (2-hydroxyethyl methacrylate) system. *Journal of Polymer Science Part A: Polymer Chemistry* **1990**, 28(9), 2547-2561.

[31] Ohtsuka, Y., Kawaguchi, H. and Sugi, Y., Copolymerization of styrene with acrylamide in an emulsifier-free aqueous medium. *Journal of Applied Polymer Science* **1981**, 26(5), 1637-1647.

[32] Aguirreurreta, Z., Dimmer, J.A., Willerich, I., de la Cal, J.C. and Leiza, J.R., Water whitening reduction in waterborne pressure-sensitive adhesives produced with polymerizable surfactants. *Macromolecular Materials and Engineering* **2015**, 300(9), 925-936.

## Chapter 1

[33] Gaboyard, M., Jeanmaire, T., Pichot, C., Hervaud, Y. and Boutevin, B., Seeded semicontinuous emulsion copolymerization of methyl methacrylate, butyl acrylate, and phosphonated methacrylates: Kinetics and morphology. *Journal of Polymer Science Part A: Polymer Chemistry* **2003**, 41(16), 2469-2480.

[34] Gonzalez, I., Mestach, D., Leiza, J.R. and Asua, J.M., Adhesion enhancement in waterborne acrylic latex binders synthesized with phosphate methacrylate monomers. *Progress in Organic Coatings* **2008**, 61(1), 38-44.

[35] Williams, R., Jencks, W. and Westheimer, F., pKa data compiled by R. Williams, **2011**, Online access:  
[http://www.chem.wisc.edu/areas/reich/pkatable/pKa\\_compilation-1-Williams.pdf](http://www.chem.wisc.edu/areas/reich/pkatable/pKa_compilation-1-Williams.pdf)

[36] Goodwin, J.W., Hearn, J., Ho, C.C. and Ottewill, R.H., The preparation and characterisation of polymer latices formed in the absence of surface active agents. *British Polymer Journal* **1973**, 5(5), 347-362.

[37] Peula-Garcia, J.M., Hidalgo-Alvarez, R. and De las Nieves, F.J., Colloid stability and electrokinetic characterization of polymer colloids prepared by different methods. *Colloids and Surfaces A: Physicochemical and Engineering Aspects* **1997**, 127(1), 19-24.

[38] Peula, J.M., Fernández-Barbero, A., Hidalgo-Alvarez, R. and de Las Nieves, F.J., Comparative study on the colloidal stability mechanisms of sulfonate latexes. *Langmuir* **1997**, 13(15), 3938-3943.

[39] Cheong, I.W. and Kim, J.H., Effects of surface charge density on emulsion kinetics and secondary particle formation in emulsifier-free seeded emulsion polymerization of methyl methacrylate. *Colloid and Polymer Science* **1997**, 275(8), 736-743.

## Chapter 1

[40] Cheong, I.W. and Kim, J.H., Investigation of seeded emulsion polymerization using a calorimetric method: effects of the surface charge density on polymerization rate and average number of radicals per particle. *Colloids and Surfaces A: Physicochemical and Engineering Aspects* **1999**, *153*(1), 137-142.

[41] Bouix, M., Gouzi, J., Charleux, B., Vairon, J.P. and Guinot, P., Synthesis of amphiphilic polyelectrolyte block copolymers using “living” radical polymerization. Application as stabilizers in emulsion polymerization. *Macromolecular Rapid Communications* **1998**, *19*(4), 209-213.

[42] Nowakowska, M., Zapotoczny, S. and Karewicz, A., Synthesis of poly (sodium styrenesulfonate-block-vinylnaphthalene) by nitroxide-mediated free radical polymerization. *Macromolecules* **2000**, *33*(20), 7345-7348.

[43] Oikonomou, E.K., Pefkianakis, E.K., Bokias, G. and Kallitsis, J.K., Direct synthesis of amphiphilic block copolymers, consisting of poly (methyl methacrylate) and poly (sodium styrene sulfonate) blocks through atom transfer radical polymerization. *European Polymer Journal* **2008**, *44*(6), 1857-1864.

[44] Marchal, F., Guenoun, P., Daillant, J., Holley, D.W. and Mays, J.W., Unprecedented microemulsion boosting effect induced by a charged diblock copolymer: bending modulus and curvature frustration of the surfactant film. *Soft Matter* **2009**, *5*(20), 4006-4014.

[45] Yeole, N., Hundiwale, D. and Jana, T., Synthesis of core-shell polystyrene nanoparticles by surfactant free emulsion polymerization using macro-RAFT agent. *Journal of Colloid and Interface Science* **2011**, *354*(2), 506-510.

[46] Oikonomou, E.K., Bethani, A., Bokias, G. and Kallitsis, J.K., Poly (sodium styrene sulfonate)-b-poly (methyl methacrylate) diblock copolymers through direct atom transfer radical polymerization: Influence of hydrophilic-hydrophobic balance on self-organization in aqueous solution. *European Polymer Journal* **2011**, *47*(4), 752-761.

## Chapter 1

[47] Weiss, R.A., Turner, S.R. and Lundberg, R.D., Sulfonated polystyrene ionomers prepared by emulsion copolymerization of styrene and sodium styrene sulfonate. *Journal of Polymer Science: Polymer Chemistry Edition* **1985**, 23(2), 525-533.

[48] Siadat, B., Oster, B. and Lenz, R.W., Preparation of ion-containing elastomers by emulsion copolymerization of dienes with olefinic sulfonic acid salts. *Journal of Applied Polymer Science* **1981**, 26(3), 1027-1037.

[49] Lu, S., Ramos, J. and Forcada, J., Self-stabilized magnetic polymeric composite nanoparticles by emulsifier-free miniemulsion polymerization. *Langmuir* **2007**, 23(26), 12893-12900.

[50] Reese, C.E. and Asher, S.A., Emulsifier-free emulsion polymerization produces highly charged, monodisperse particles for near infrared photonic crystals. *Journal of Colloid and Interface Science* **2002**, 248(1), 41-46.

[51] Choo, H.S. and Lee, K.C., Optical properties of CCA films prepared with poly [styrene-co-sodium 1-allyloxy-2-hydroxypropane sulphonate] particles. *Materials Research Innovations* **2015**, 19(8), 157-167.

[52] Kharlampieva, E., Tsukruk, T., Slocik, J.M., Ko, H., Poulsen, N., Naik, R.R., Kröger, N. and Tsukruk, V.V., Bioenabled surface-mediated growth of titania nanoparticles. *Advanced Materials* **2008**, 20(17), 3274-3279.

[53] Sakota, K. and Okaya, T., Polymerization behavior of carboxylic monomers in the preparation of carboxylated latexes. *Journal of Applied Polymer Science* **1976**, 20(9), 2583-2587.

[54] Wutzel, H. and Samhaber, W.M., Synthesis and characterization of sulfonated core-shell latices in the size range between 30 and 80nm. *Colloids and Surfaces A: Physicochemical and Engineering Aspects* **2008**, 319(1), 84-89.

## Chapter 1

[55] Oliveira, A.M., Guimarães, K.L. and Cerize, N.N.P., The role of functional monomers on producing nanostructured lattices obtained by surfactant-free emulsion polymerization—A novel approach. *European Polymer Journal* **2015**, *71*, 268-278.

[56] Xu, X.J., Siow, K.S., Wong, M.K. and Gan, L.M., Polymerization of styrene with ionic comonomer, nonionic comonomer, or both. *Journal of Polymer Science Part A: Polymer Chemistry* **2001**, *39*(10), 1634-1645.

[57] Xu, X.J. and Chen, F., Modified emulsifier-free emulsion polymerization of butyl methacrylate with ionic or/and nonionic comonomers. *Journal of Applied Polymer Science* **2004**, *92*(5), 3080-3087.

[58] Chang, W., Liu, L., Zhang, J., Pan, Q. and Pei, M., Preparation and characterization of styrene/butyl acrylate emulsifier-free latex with 2-acrylamido-2-methyl propane sulfonic acid as a reactive emulsifier. *Journal of Dispersion Science and Technology* **2009**, *30*(5), 639-642.

[59] Dai, M., Zhang, Y. and He, P., Preparation and characterization of stable and high solid content St/BA emulsifier-free latexes in the presence of AMPS. *Polymer Bulletin* **2011**, *67*(1), 91-100.

[60] Tang, G.L., Song, M.D., Hao, G.J., Guo, T.Y. and Zhang, B.H., Studies on the preparation of stable and high solid content emulsifier-free latexes and characterization of the obtained copolymers for MMA/BA system with the addition of AHPS. *Journal of Applied Polymer Science* **2001**, *79*(1), 21-28.

[61] Guo, T.Y., Tang, G.L., Hao, G.J., Song, M.D. and Zhang, B.H., Morphologies and dynamic mechanical properties of core-shell emulsifier-free latexes and their copolymers for P (BA/MMA)/P (MMA/BA) and P (BA/MMA)/PSt systems in the presence of AHPS. *Journal of Applied Polymer Science* **2002**, *86*(12), 3078-3084.

## Chapter 1

[62] Qiu, J., Charleux, B. and Matyjaszewski, K., Controlled/living radical polymerization in aqueous media: homogeneous and heterogeneous systems. *Progress in Polymer Science* **2001**, 26(10), 2083-2134.

[63] Oh, J.K., Recent advances in controlled/living radical polymerization in emulsion and dispersion. *Journal of Polymer Science Part A: Polymer Chemistry* **2008**, 46(21), 6983-7001.

[64] Zetterlund, P.B., Thickett, S.C., Perrier, S., Bourgeat-Lami, E. and Lansalot, M., Controlled/living radical polymerization in dispersed systems: an update. *Chemical Reviews* **2015**, 115(18), 9745-9800.

[65] Farias-Cepeda, L., Herrera-Ordonez, J., Estevez, M., Luna-Barcenas, G. and Rosales-Marines, L., New insights on surfactant-free styrene emulsion polymerization in the presence of sodium styrene sulfonate. *Colloid and Polymer Science* **2016**, 294(10), 1571-1576.



## **Chapter 2. Effect of comonomer type on the chemical incorporation of sodium styrene sulfonate\***

### **2.1. Introduction**

In order to provide stability to the polymer dispersions and to avoid the negative effects of the migratory hydrophilic species on the application properties, NaSS should chemically be incorporated onto the polymer particles and the fraction that remains in the aqueous phase as water-soluble polymer should be minimized. Considering that NaSS is located in the aqueous phase and that its homopolymer is a water soluble polyelectrolyte, one way to achieve this goal is to create conditions that will enhance the copolymerization of NaSS with more hydrophobic monomers, which will increase the hydrophobicity of the growing chains in aqueous phase. As a result, the time that growing chains spent in aqueous phase will decrease and the process of entry of radicals into the particles will be enhanced.

\* The content of this chapter has been published in:

Bilgin, S., Tomovska, R. and Asua, J.M., Fundamentals of chemical incorporation of ionic monomers onto polymer colloids: paving the way for surfactant-free waterborne dispersions. *RSC Advances* **2016**, 6(68), 63754-63760.

## Chapter 2

The incorporation of the NaSS to the polymer particles by copolymerization with a more hydrophobic monomer is expected to be largely controlled by the nature of the comonomer. The choice of the comonomer is not obvious as it requires a compromise between two conflicting characteristics. On one hand, a certain water solubility of the comonomer is needed to be present in the aqueous phase in order to copolymerize with NaSS. On the other, hydrophobicity is needed to reduce the water solubility of the copolymer formed. Another important point is the reactivity of the comonomer with NaSS. In this regard, literature is not of much help as most of the works reported are limited to the use of NaSS in the emulsion polymerization of styrene<sup>1-5</sup> and when other comonomers are used, the incorporation of NaSS to the polymer particles was not studied.<sup>6</sup>

In this chapter, the effect of the functionality and water solubility of the comonomer on the chemical incorporation of NaSS onto the polymer particles was investigated using styrene as well as methacrylates and acrylates with different alkyl chain length. Seeded batch emulsion polymerization was used to eliminate the possible effect of the comonomer on particle nucleation. A nonionic surfactant was used to prepare a seed devoid of charges. Tert-butyl hydroperoxide/ ascorbic acid redox pair initiator that forms noncharged hydrophobic radicals in the aqueous phase was utilized in all the reactions.

## Chapter 2

### **2.2. Experimental**

#### **2.2.1. Materials**

The materials are given in Appendix II.

#### **2.2.2. Polymerizations**

##### **2.2.2.1. Seed synthesis**

Poly(butyl methacrylate) seeds were synthesized in batch using the recipe given in Table 2.1. Butyl methacrylate (BMA) was used due to a number of reasons. First of all, BMA has low water solubility and hence formation of free oligomer in the aqueous phase was minimized. The reaction temperature (55°C) was above the glass transition temperature ( $T_g$ ) of poly(BMA) which is 20°C. Therefore, the conversion was not limited by the glass effect which is observed in the case of high  $T_g$  polymers such as polystyrene. Moreover,  $T_g$  of the poly(BMA) is low enough to provide good film forming capabilities at room temperature for coating applications.

A 2 L jacketed glass reactor equipped with reflux condenser,  $N_2$  inlet, temperature probe, feeding inlet and stainless steel 8-bladed frame-type agitator rotating at 200 rpm was used. The procedure was as follows: Butyl methacrylate, Disponil A3065 emulsifier and water were sonicated at 80% duty cycle (0.8 on, 0.2 off) for 10 minutes while magnetically stirred at 500 rpm. The dispersion was transferred into the reactor

## Chapter 2

and heated to 55°C while being stirred under N<sub>2</sub> flow (12 cc/min). After 20 minutes, TBHP was introduced as a shot and the aqueous solution of AsAc (2.5 wt%) was fed at a rate of 1 g/min for 60 minutes. Then, the reaction mixture was allowed to react for 2 additional hours. Complete conversion of BMA was confirmed by <sup>1</sup>H-NMR spectra of the final latex. Therefore, additional monomer removal steps or post-polymerization were not required.

**Table 2.1.** Recipe used to prepare the poly(BMA) seed

Ingredient	Amount (g)	Introduced as
BMA	150.0	initial charge
A3065 (active matter)	5.3	
H <sub>2</sub> O	1356.0	
TBHP	1.5	shot
H <sub>2</sub> O	10.8	
AsAc	1.5	feed
H <sub>2</sub> O	58.5	

The reason to utilize nonionic emulsifier in the seed synthesis is twofold. Firstly, it does not have charges that can interfere with the characterization of final lattices. In addition, since desorption of nonionic emulsifiers from the seed particles is very slow,<sup>7</sup> the probability of secondary particle nucleation due to the presence of emulsifier in the aqueous phase is very low. On the other hand, the slow diffusion of the emulsifier may limit particle nucleation during the seed formation lowering the number of seed particles and hence facilitating secondary nucleation during the

## Chapter 2

seeded emulsion polymerization. Therefore, sonication was applied to reduce the size of the monomer droplets and to increase the availability of the surfactant during seed formation. The temperature of the reactions was kept at 55°C to make sure not to exceed the cloud point of the nonionic emulsifier (75-79°C, 1wt% in 10wt% aqueous solution of NaCl).

### 2.2.2.1. Seeded batch reactions

Seeded batch emulsion polymerizations were performed in 0.5 L reactor equipped with a reflux condenser, N<sub>2</sub> inlet, temperature probe, feeding inlet and stainless steel three-bladed Ekato MIG impeller. The comonomers used in this study and their water solubility are presented in Table 2.2. A representative recipe (based on MMA) is given in Table 2.3. In each reaction, the number of moles of comonomer was kept constant (141 mmol). In the reaction with two comonomers (BA and 2HEA), the amounts were 134 and 7.05 mmol, respectively. Because of the different molecular weights of the comonomers, the solids contents ranged from 13.6 wt% to 15.6 wt%. The poly(BMA) seed latex, the comonomer, the aqueous solution of NaSS and TBHP (this initiator is stable at room temperature) were charged into the reactor and allowed to swell overnight at 130 rpm at room temperature. To prevent the formation of monomer droplets, the amount of monomer was kept below the swelling capacity of the seed which for these monomers is at least 60% by volume (monomer/seed: 60/40).<sup>8</sup> After checking that there was no conversion of the monomers during the swelling, the stirring rate and the temperature were increased to 200 rpm and 55°C,

## Chapter 2

under N<sub>2</sub> purge. After 15 minutes, the aqueous solution of AsAc was fed at a rate of 0.4 g/min for 1 hour.

The reason to use TBHP/AsAc redox couple as initiator is as follows. AsAc is water soluble, whereas TBHP partitions between the aqueous and the organic phase. The tert-butoxy radicals that are formed in the aqueous phase are nonionic and hydrophobic. Therefore, they do not contribute to the hydrophilicity of the oligomers formed by reaction with NaSS and the fraction of the comonomer soluble in the aqueous phase.

**Table 2.2.** Water solubilities of the comonomers

	<b>Comonomer</b>	<b>Solubility in water (mM) at 25°C<sup>9</sup></b>
<b>Methacrylates</b>	Methyl methacrylate (MMA)	150
	Ethyl methacrylate (EMA)	45
	Butyl methacrylate (BMA)	4
<b>Acrylates</b>	2-hydroxy ethyl acrylate (2HEA)	∞ <sup>10</sup>
	Methyl acrylate (MA)	650
	Ethyl acrylate (EA)	150
	Butyl acrylate (BA)	11
<b>Styrene</b>	Styrene (S)	3.5

∞: miscible with water

## Chapter 2

**Table 2.3.** Representative recipe for seeded batch reactions with different comonomers

Ingredient	Amount (g)	Introduced as
Seed latex	200	
Comonomer (MMA)	14.1*	
NaSS	0.48	initial charge
TBHP	0.14	
H <sub>2</sub> O	3.8	
AsAc	0.13	
H <sub>2</sub> O	24	feed

\*141 mmoles of comonomer is used in each reaction

### 2.2.3. Characterizations

The characterization methods are given in Appendix II.

## 2.3. Results and Discussion

Complete conversion of BMA was obtained at the end of seed synthesis. The seed had an average particle size of 141 nm (Figure 2.1) and displayed a relatively narrow particle size distribution with a coefficient of variation (CV) of 13.5% (monodisperse particles have CV less than 10%).<sup>11</sup> Table 2.4 also includes the molecular weights of the poly(BMA).

## Chapter 2

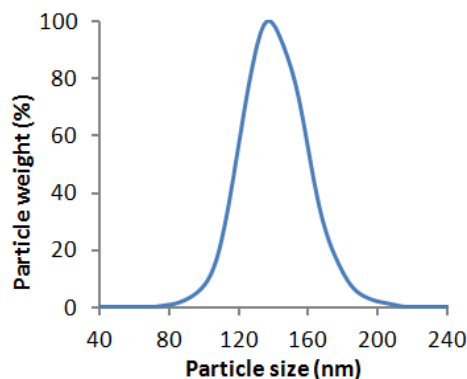


Figure 2.1. Particle size distribution (by CHDF) of the poly(BMA) seed

**Table 2.4.** Characteristics of the seed

$d_{\text{particle}}$ (nm) by CHDF	Coag. (%)	Insoluble polymer (gel) wt%	$M_n$	$M_w$	PDI
$141 \pm 19.0$	6.6	-	198,000	424,000	2.1

Figure 2.2 presents the evolution of the number of particles ( $N_p$ , calculated from DLS measurements) for the polymerizations carried out with different comonomers. It can be seen that after the initial drop,  $N_p$  remained relatively constant for all the comonomers, except for 2HEA. The initial drop indicates that the nonionic surfactant contained in the seed was not enough to stabilize the monomer swollen particles. The in-situ formation of copolymers containing NaSS provided stabilization to the polymer particles. The decreasing  $N_p$  indicated that there was no significant nucleation of new particles.

## Chapter 2

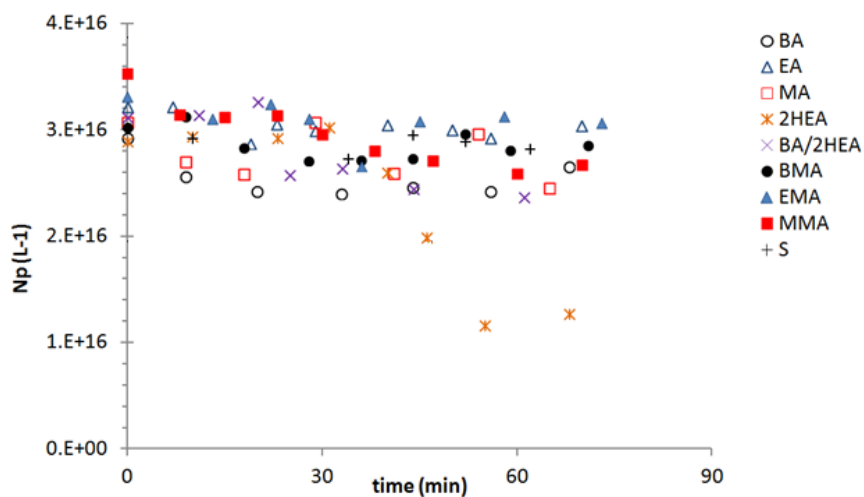


Figure 2.2. Time evolution of the number of particles ( $N_p$ ) in the seeded batch emulsion copolymerizations of NaSS with different comonomers

The significant drop in the number of particles in case of 2HEA in comparison to the other comonomers suggests that the copolymer 2HEA/NaSS formed was too hydrophilic and did not adsorb on the polymer particles. Consequently, the nonionic surfactant contained in the seed was the only surfactant available and it was not able to stabilize the particles. It is worth pointing out that although the calculation of  $N_p$  from measurements of the particle size should be taken with precaution because  $N_p$  is inversely proportional to the third power of the measured size, and hence relatively small errors in the measurement lead to larger errors in  $N_p$ , the low  $N_p$  values obtained for 2HEA are far beyond the experimental errors, namely they are due to the characteristics of 2HEA.

## Chapter 2

The evolutions of the conversion of the comonomers are given in Figure 2.3. They exhibited typical behavior of batch processes. The conversions of MA, EA and BA started very soon, but inhibition periods of ca. 30 minutes were observed for the methacrylates. The polymerization rates in all presented cases have shown significant differences up to ca. 30% comonomers conversion, thus, all the comparison presented below refer to this point. Acrylate monomers have higher homopropagation rates than methacrylates.<sup>12,13</sup> The slow polymerization rate of styrene was due to its low propagation rate coefficient.<sup>14</sup>

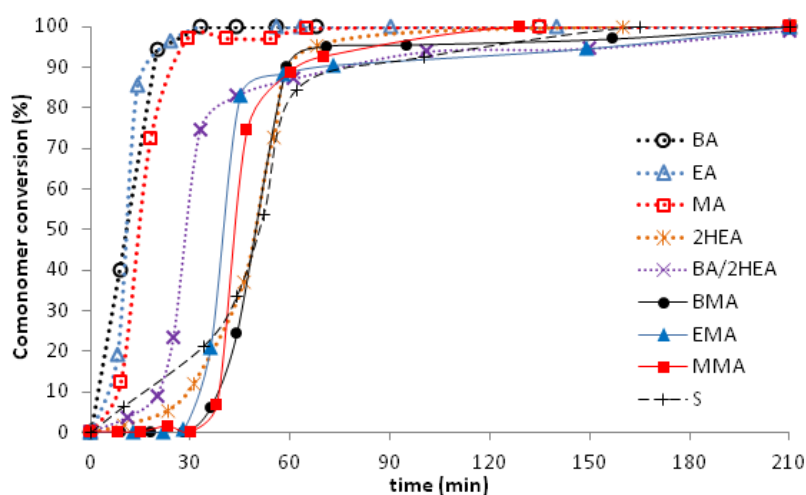


Figure 2.3. Time evolution of the conversion of the comonomers for the seeded batch emulsion copolymerization with NaSS

## Chapter 2

With the exception of 2HEA, within each family, the water solubility of the comonomer did not significantly affect the polymerization rate measured at 50% conversion. The low polymerization rate of 2HEA was due to both the lower number of particles (Figure 2.2) and its lower concentration in the main locus of polymerization (polymer particles) which is a consequence of its high water solubility. This effect can also be seen in BA/2HEA reaction, where 5 mol% of the hydrophobic monomer (BA) was replaced with the hydrophilic one (2HEA) leading to a decrease of the polymerization rate. Figure 2.3 shows that full conversion was achieved for both MMA and S, even though the polymerization temperature was lower than the  $T_g$  of these polymers and under these conditions glass effect is expected. Polymerization in both the aqueous phase and the hydroplasticized NaSS-rich outer layer of the particles may be the reason for the complete conversion of these monomers.

The characteristics of the latexes are summarized in Table 2.5. The theoretical particle sizes were calculated based on the assumption of constant number of particles and agreed well with experimental sizes for most of the latexes, indicating no secondary nucleation and colloidally stable systems. This was supported by the monomodal and relatively narrow particle size distributions (Figure 2.4). On the contrary, in case of 2HEA, the experimental value diverged significantly from the theoretical one. The large particle size and a very broad particle size distribution (Figure 2.4 inset) showed that the system was less stable.

## Chapter 2

**Table 2.5.** Characteristics of the final latexes obtained by seeded batch emulsion copolymerization of NaSS and different comonomers

Monomer	$d_{\text{particle}}$ theoretical (nm)	$d_{\text{particle}}$ by CHDF (nm)	Coag (%)	NaSS conversion (%)	Insoluble polymer (gel) wt%	$M_n$	$M_w$	PDI
MMA	189	187.8 ± 23.4		89.9	*	134,400	475,000	3.5
EMA	195	195.6 ± 22.2	none	86.5	*	136,000	473,000	3.5
BMA	206	200.7 ± 24.3		77.3	*	137,000	480,000	3.5
2HEA	189	475.5 ± 120.3	1	100	46.7	197,000	656,800	3.3
MA	183	192.6 ± 26.5	1.4	97.0	13.9	175,700	670,500	3.8
EA	190	193.6 ± 25.3		90.0	11.9	146,400	440,000	3.0
BA	202	210.6 ± 26.0	none	83.0	35.6	193,000	662,000	3.4
BA/2HEA (19/1)	201	193.1 ± 21.5		99.9	35.7	185,600	464,000	2.5
S	192	197.3 ± 24.3	1	72.4	*	80,200	238,000	3.0

\*Below detection limit

No coagulum was observed in most of the cases, and only for the more water soluble comonomers (MA and 2HEA) as well as for the slowest comonomer (S) a small amount of coagulum was obtained. For the MA and 2HEA, the reason might be the formation of water soluble polymer. On the other hand, the coagulation observed in the reaction of S may be related to the low conversion of NaSS that resulted in less stabilized particles.

## Chapter 2

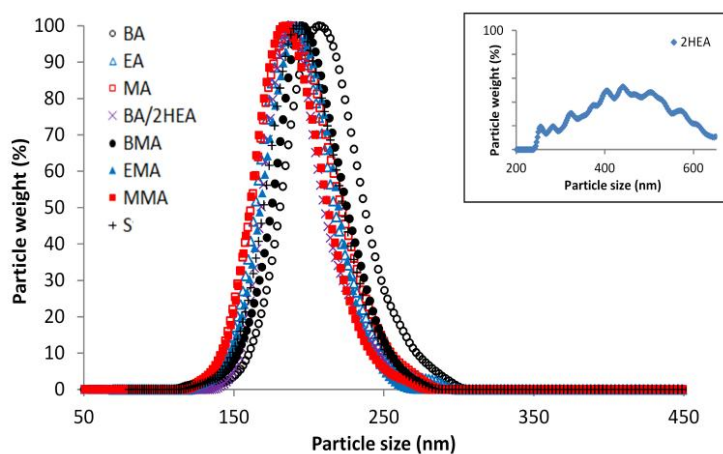


Figure 2.4. Particle size distributions (by CHDF) of the final latexes obtained by seeded batch emulsion copolymerization of NaSS with different comonomers (inset plot is for 2HEA).

This implies that the nonionic emulsifier of the seed particles was not able to stabilize the particles. In order to demonstrate this, a seeded batch polymerization of MMA without NaSS was performed and a huge amount of coagulation (26%) was observed.

The fraction of polymer insoluble in THF (commonly called gel) was only significant for acrylates. These monomers suffer intermolecular chain transfer to polymer that coupled with termination by combination leads to the formation of large macromolecules that may be insoluble in good solvents.<sup>15</sup> In this context, it is worth

## Chapter 2

pointing out that it has recently been reported at the temperature used in the present work (55°C) only about 7% of the terminations occurred by combination.<sup>16</sup> If this is correct, the rate coefficient for intermolecular chain transfer to polymer should be higher than the previously estimated values.<sup>15</sup>

Taking into account that the insoluble fractions were based on the total amount of polymer (i.e., including the seed which represented about 50 wt% of the final polymer), and that the poly(BMA) of the seed does not contain abstractable hydrogens and hence it cannot suffer transfer to polymer, the insoluble fractions found for 2HEA, BA and BA/2HEA were very high. In particular, almost all of the poly(2HEA) was not soluble in THF, likely due to the formation of H-bonds and the incorporation of NaSS in the copolymer. For BA, about 71% of the poly(BA) formed was not soluble in THF. This is substantially higher than what is usually found for batch emulsion polymerization (54 wt%<sup>17</sup>). The reason may be that in the present case, hydrophobic tert-butoxy radicals able to enter rapidly in the polymer particles were generated. These oxygen centered radicals are very efficient in abstracting hydrogen from the polymer backbone, which leads to the formation of long branches and eventually to gel. The lower gel fraction found for MA and EA was likely due to the higher water solubility of these monomers favored the polymerization of the tert-butoxy radicals with monomer yielding carbon-centered radicals which are less efficient for hydrogen abstraction. Neither methacrylates nor styrene suffer any significant transfer to polymer, and hence no gel was formed.

## Chapter 2

Table 2.5 also shows that, within each comonomer family, NaSS conversion increased with the water solubility of the comonomer, which indicates that copolymerization was beneficial for NaSS conversion. The main reason is that the cross propagation rate coefficient of (meth)acrylate radical with NaSS was much higher than the rate coefficient for homopropagation of NaSS (See Appendix II for the estimation of the reactivity ratios using the Q-e scheme). A second reason is that the critical length for both precipitation of the oligoradicals in the aqueous phase and their adsorption on the polymer particles increased with the hydrophilicity of the comonomer. On the other hand, the type of double bond (acrylic/methacrylic/styrene) had no effect on the NaSS conversion.

The results of the NaSS incorporation are given in Table 2.6. It can be seen that incorporation increased with the water solubility of the comonomer and that as in the case of NaSS conversion, the type of double bond had no effect on the incorporation. However, comparison between the NaSS conversion (Table 2.5) and the NaSS chemically incorporated to the polymer particles (Table 2.6) shows that a significant part of the NaSS reacted was not strongly attached to the polymer particles.

Figure 2.5 presents the fraction of the NaSS reacted that was incorporated onto the polymer particles. It can be seen that this fraction also increases with the water solubility of the comonomer suggesting that in the interplay between hydrophobicity of the comonomer and its content in the NaSS copolymer, the content is the main factor controlling the incorporation of the copolymer to the polymer particles.

Chapter 2

**Table 2.6.** Effect of the comonomer type on the incorporation of NaSS into the polymer particles

Monomer	Yield of NaSS incorporation (%)
MMA	75.5
EMA	57.2
BMA	53.8
2HEA	99.7
MA	86.9
EA	77.6
BA	48.7
BA/2HEA (19/1)	78.9
S	42.3

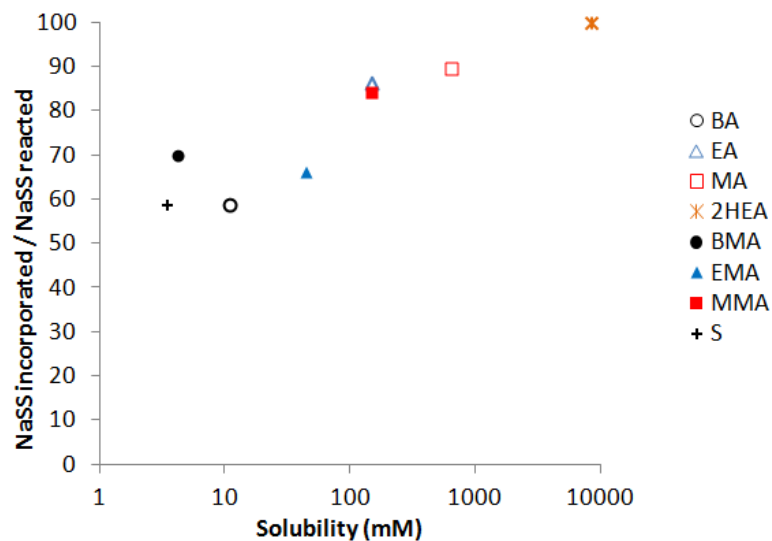
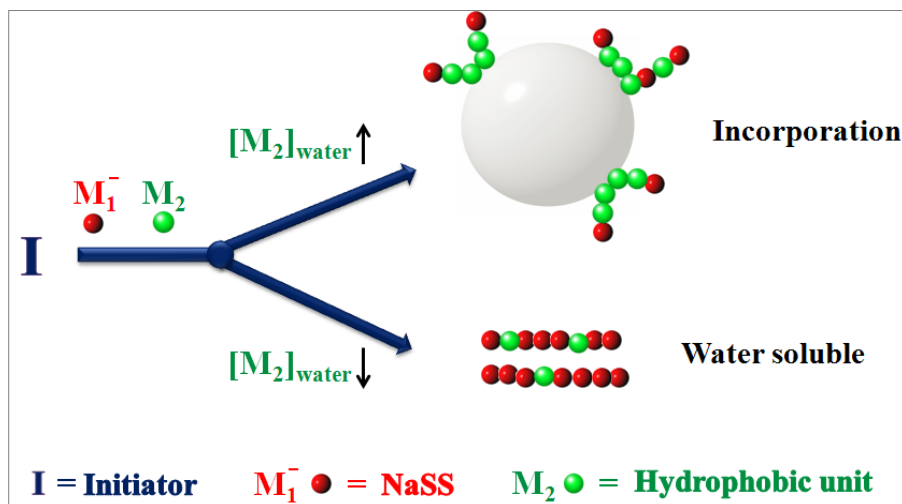


Figure 2.5. Fraction of the reacted NaSS that was incorporated into polymer particles

## Chapter 2

Based on the results described above, the mechanisms leading to the incorporation of NaSS onto the polymer particle can be described as follows: The tert-butoxyl radicals created from the initiator system reacted with the monomers dissolved in the aqueous phase. Direct entry into the particles may be reduced due to the high concentration of monomer in the aqueous phase and the relatively low solids content. The composition of the copolymer formed depended on the relative concentrations of comonomer and NaSS as well as on the reactivity ratios. However, the results in Figure 2.5 and Table 2.6 show that  $[Comonomer]_{aq} / [NaSS]$  was the main factor as methacrylates ( $r_{NaSS}=1.9$ ;  $r_{methacrylate}=0.3$ ) gave the same results as acrylates ( $r_{NaSS}=2.8$ ;  $r_{acrylate}=0.1$ ). Hydrophobicity of the oligoradicals depends on both comonomer content and hydrophobicity of the comonomer. It is expected that the higher the water solubility of the comonomer the more comonomer incorporates into the copolymer, but the contribution of each comonomer unit to the hydrophobicity of the oligoradicals will be lower. Data in Figure 2.5 and Table 2.6 show that the higher amount of comonomer incorporated for the more hydrophilic comonomers compensated their lower hydrophobicity. The copolymer incorporated onto the polymer particles may contain active radicals and continue polymerizing in the particles becoming chemically linked or may be dead chains that adsorbed onto the polymer particles. These chains may suffer further grafting reactions (transfer to polymer in the case of acrylates). The copolymer rich in NaSS stays in the aqueous phase (Scheme 2.1).

Chapter 2



Scheme 2.1. Influence of water solubility of comonomer on the chemical incorporation of ionic monomer as stabilizer in emulsion polymerization

From a practical point of view, the fact that NaSS incorporation is controlled by the concentration of the comonomer in the aqueous phase may be a limitation because in most practical cases, the main monomers and their relative concentrations are given by the application sought. Therefore, it is interesting to investigate if chemical incorporation of NaSS can be improved by using small fractions of hydrophilic comonomers in the formulation. BA was chosen as a case study for the proof of concept finding that substitution of 5% of BA by 2HEA increased the incorporation of NaSS from 48.7% to 78.9%.

## Chapter 2

### **2.4. Conclusions**

In this chapter, the fundamentals of the chemical incorporation of a pH and temperature insensitive ionic monomer (sodium styrene sulfonate, NaSS) to the polymer particles were investigated in an attempt to go beyond the current technology for production of waterborne polymer dispersion, which is based on the use of surfactants to stabilize the dispersion. The reason for avoiding surfactants is that they reduce desirable properties of the films cast from the dispersions such as gloss, adhesion and water resistance. pH and temperature insensitiveness are needed because the dispersions should be stable in the reactor (pH=2-3, T~80°C) and during the application (pH~7 and T~15-40°C).

The necessary condition for the success of this approach is to chemically incorporate the NaSS onto the polymer particles minimizing at the same time the amount of water soluble polymer. To achieve this goal, NaSS was copolymerized with more hydrophobic monomers in the aqueous phase. Using monomers of different functionality (styrene, acrylates, methacrylates) and different water solubilities, it was found that the key factor controlling the chemical incorporation of NaSS was the concentration of the comonomer in the aqueous phase, whereas the functionality did not play any significant role. Of practical importance is the finding that chemical incorporation of NaSS to a rather hydrophobic dispersion can be boosted using small amounts of a relatively water soluble monomer in the formulation.

## Chapter 2

### 2.5. References

- [1] Juang, M.S.D. and Krieger, I.M., Emulsifier-free emulsion polymerization with ionic comonomer. *Journal of Polymer Science: Polymer Chemistry Edition* **1976**, *14*(9), 2089-2107.
- [2] Kim, J.H., Chainey, M., El-Aasser, M.S. and Vanderhoff, J.W., Emulsifier-free emulsion copolymerization of styrene and sodium styrene sulfonate. *Journal of Polymer Science Part A: Polymer Chemistry* **1992**, *30*(2), 171-183.
- [3] Kim, J.H., Chainey, M., El-Aasser, M.S. and Vanderhoff, J.W., Preparation of highly sulfonated polystyrene model colloids. *Journal of Polymer Science Part A: Polymer Chemistry* **1989**, *27*(10), 3187-3199.
- [4] Tamai, H., Niino, K. and Suzawa, T., Surface characterization of styrene/sodium styrenesulfonate copolymer latex particles. *Journal of Colloid and Interface Science* **1989**, *131*(1), 1-7.
- [5] Wutzel, H. and Samhaber, W.M., Synthesis and characterization of sulphonated core-shell latices in the size range between 30 and 80nm. *Colloids and Surfaces A: Physicochemical and Engineering Aspects* **2008**, *319*(1), 84-89.
- [6] Oliveira, A.M., Guimarães, K.L. and Cerize, N.N.P., The role of functional monomers on producing nanostructured lattices obtained by surfactant-free emulsion polymerization—A novel approach. *European Polymer Journal* **2015**, *71*, 268-278.
- [7] Ballard, N., Urrutia, J., Eizagirre, S., Schafer, T., Diaconu, G., de la Cal, J.C. and Asua, J.M., Surfactant kinetics and their importance in nucleation events in (mini) emulsion polymerization revealed by quartz crystal microbalance with dissipation monitoring. *Langmuir* **2014**, *30*(30), 9053-9062.

## Chapter 2

[8] Gardon, J.L., Emulsion polymerization. II. Review of experimental data in the context of the revised Smith-Ewart theory. *Journal of Polymer Science Part A-1: Polymer Chemistry* **1968**, 6(3), 643-664.

[9] Chern, C-S. Principles and Applications of Emulsion Polymerization, John Wiley & Sons: USA, 2008.

[10] Penzel, E., Polyacrylates. *Ullmann's Encyclopedia of Industrial Chemistry* **2000**, DOI:10.1002/14356007.a21\_157

[11] Sugimoto, T. Monodispersed particles, Elsevier: Amsterdam, 2001.

[12] Beuermann, S., Buback, M., Davis, T.P., Gilbert, R.G., Hutchinson, R.A., Olaj, O.F., Russell, G.T., Schweer, J. and van Herk, A.M., Critically evaluated rate coefficients for free-radical polymerization, 2. Propagation rate coefficients for methyl methacrylate. *Macromolecular Chemistry and Physics* **1997**, 198(5), 1545-1560.

[13] Asua, J.M., Beuermann, S., Buback, M., Castignolles, P., Charleux, B., Gilbert, R.G., Hutchinson, R.A., Leiza, J.R., Nikitin, A.N., Vairon, J.P. and van Herk, A.M., Critically evaluated rate coefficients for free-radical polymerization, 5. *Macromolecular Chemistry and Physics* **2004**, 205(16), 2151-2160.

[14] Buback, M., Gilbert, R.G., Hutchinson, R.A., Klumperman, B., Kuchta, F.D., Manders, B.G., O'Driscoll, K.F., Russell, G.T. and Schweer, J., Critically evaluated rate coefficients for free-radical polymerization, 1. Propagation rate coefficient for styrene. *Macromolecular Chemistry and Physics* **1995**, 196(10), 3267-3280.

[15] Plessis, C., Arzamendi, G., Leiza, J.R., Schoonbrood, H.A.S., Charmot, D. and Asua, J.M., Seeded semibatch emulsion polymerization of n-butyl acrylate. Kinetics and structural properties. *Macromolecules* **2000**, 33(14), 5041-5047.

## Chapter 2

[16] Ballard, N., Hamzehlou, S., Ruipérez, F. and Asua, J.M., On the termination mechanism in the radical polymerization of acrylates. *Macromolecular Rapid Communications* **2016**, 37(16), 1364-1368.

[17] Yadav, A.K., Barandiaran, M.J. and de la Cal, J.C., Effect of the polymerization technique and reactor type on the poly(n-butyl acrylate) microstructure. *Macromolecular Reaction Engineering* **2014**, 8(6), 467-475.

## **Chapter 3. Effect of initiator type on chemical incorporation of sodium styrene sulfonate onto polymer colloids**

### **3.1. Introduction**

As explained in the literature survey (Chapter 1), high solids content (up to 60 wt%) emulsifier-free latexes have been produced by semicontinuous emulsion polymerization either in the presence or absence of the seed particles. The use of a seed has the advantage that it offers a better control on nucleation and hence the possibility of new particle formation could be minimized. Seeded semicontinuous method, which is typically preferred in industry for consistent product quality and good control of kinetics and heat removal, was selected as the process strategy. The seed could be produced either by batch or semicontinuous method. Due to smaller particle sizes obtained in batch, MMA/BA/NaSS emulsifier-free seed latex was produced by batch polymerization. Selected seed was used in all seeded semicontinuous emulsion polymerizations.

In Chapter 2, it was shown that chemical incorporation of NaSS onto polymer particles was enhanced by copolymerizing it with monomers that present some

### Chapter 3

solubility in water because copolymerization promotes the formation of amphiphilic oligomers that can be attached to the polymer particles, where they continue polymerizing to complete the incorporation. These results highlighted the importance of the adequate balance between the polymerization in the aqueous phase and in the polymer particles. This balance can be substantially altered by means of the initiator because it determines the loci and rate for radical generation as well as the type of radicals, which in turn affect the time that they spend in the aqueous phase and the amphiphilicity of the oligomers.

The effect of initiator type on the entry of (oligo)radicals into the polymer particles has been studied in the presence of slightly or scarcely water-soluble monomers.<sup>1-4</sup> However, no highly water soluble monomers were utilized in these studies.

Aramendia<sup>5</sup> studied the effect of initiator type/charge on the extent of incorporation of a surfmer and reported no significant effect either on surfmer burial or surfmer conversion for the final latexes at about 50 wt% solids contents.

The studies investigating the effect of initiator type on the chemical incorporation of water soluble monomer into hydrophobic polymers are limited and reported conflicting results.<sup>6-8</sup> Siadat<sup>6</sup> found that the most suitable initiator to be used in the copolymerization of water soluble sulfonate monomers with a hydrophobic monomer (isoprene or butadiene) was a redox system composed of an oil soluble peroxide and a water soluble reducing agent, namely benzoyl peroxide/ ferrous ammonium sulfate or diisopropyl benzene hydroperoxide/ triethylenetetramine. The reactions were

### Chapter 3

performed at 40-46 wt% solids contents and the use of water soluble persulfate initiator resulted mainly in the formation of homopolymers and only a small amount of desired copolymer. In the copolymerization of NaSS and styrene (30 wt% solids content) Weiss and coworkers<sup>7</sup> reported that the water soluble potassium persulfate and the redox initiator including diisopropyl benzene hydroperoxide (oil soluble) and triethylenetetramine (water soluble) led to the same copolymer composition. Luo and Schork<sup>8</sup> studied the copolymerization of butyl acrylate and a water soluble cationic monomer at solids contents around 45 wt% and reported that the copolymer could be formed when a water soluble azo-initiator was replaced by a redox initiator composed of cumene hydroperoxide (hydrophobic) and tetraethylene pentamine (water soluble). However, in all of these studies, either nonionic or ionic surfactants were utilized.

In this chapter, the effect of the initiator system on the chemical incorporation of NaSS onto MMA/BA polymer particles was investigated at 50 wt% solids contents by using emulsifier free seeded semicontinuous emulsion polymerization. Initiators with different water solubilities and decomposition mechanisms were used: potassium persulfate (water soluble) and azobisisobutyronitrile (oil soluble) as thermal, and tert-butyl hydroperoxide/ ascorbic acid (yielding hydrophobic radicals in the aqueous phase) and hydrogen peroxide/ ascorbic acid (yielding hydrophilic radicals in the aqueous phase) as redox initiators. The same seed was utilized in all the reactions to eliminate the effect of differences in particle size (total surface area) and total number of particles on the entry of oligoradicals<sup>9</sup> which may affect NaSS incorporation.

## Chapter 3

### **3.2. Experimental**

#### **3.2.1. Materials**

The materials are given in Appendix II.

#### **3.2.2. Polymerizations**

##### **3.2.2.1 Seed synthesis**

The recipe used to synthesize the seed is given in Table 3.1. A 2 L reactor equipped with a stainless steel 8-bladed frame-type stirrer, a reflux condenser, a N<sub>2</sub> inlet, a temperature probe, a sampling tube and two feeding inlets was first charged with an aqueous solution of NaSS. Then, the MMA/BA mixture was added as a shot and the content was stirred at 200 rpm under N<sub>2</sub> for 20 minutes. Aqueous solutions of TBHP (0.54% weight based monomer (wbm)) and AsAc (0.53% wbm) were fed separately into the reactor for 90 minutes at a temperature of 70°C. The reaction was continued further at the same temperature for 2 hours under stirring.

The reason to use TBHP/ AsAc redox pair in the seed synthesis is that this redox system forms noncharged radicals and hence the only charged species in the seed are due to the NaSS.

## Chapter 3

**Table 3.1.** The recipe for seed production in batch at 10 wt% solids content

	Initial charge	Feed 1	Feed 2
MMA (g)	75	-	-
BA (g)	75	-	-
NaSS (g)	3	-	-
AsAc (g)	-	0.79	-
TBHP (g)	-	-	0.81
H <sub>2</sub> O (g)	1213	89.2	89.2

### 3.2.2.2. Seeded semicontinuous reactions

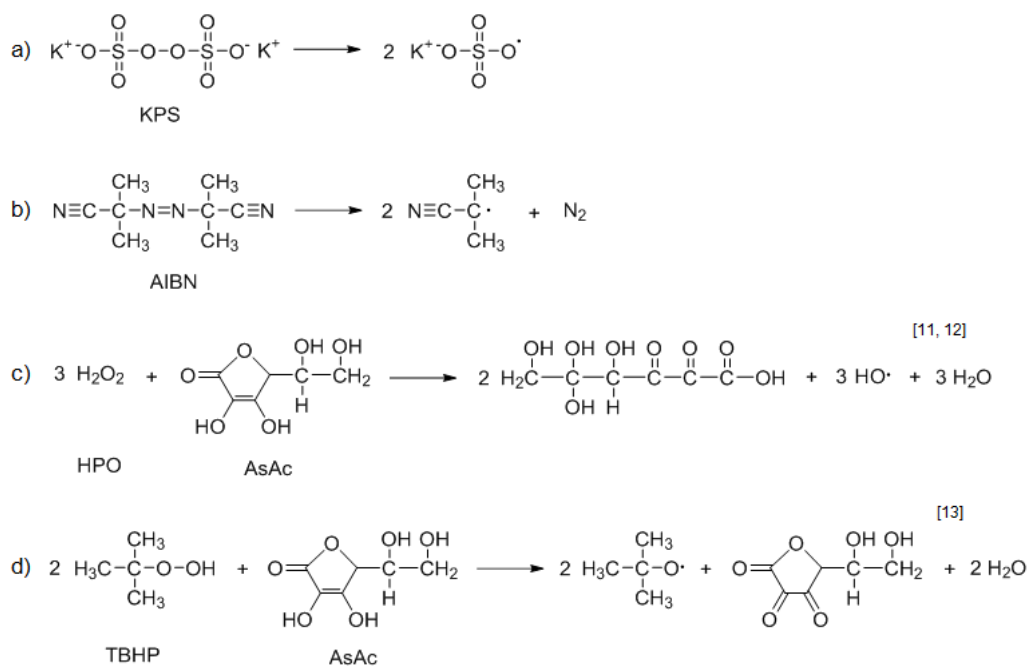
The details of the seeded semicontinuous reactions are given in Table 3.2. Four different initiators were studied:

- 1) Potassium persulfate (KPS) is a water soluble thermal initiator that forms negatively charged hydrophilic radicals in the aqueous phase. In one reaction, a small amount of styrene was added in an attempt to make the sulfate radicals react with styrene and become less hydrophilic.
- 2) AIBN is an oil soluble thermal initiator that mainly forms hydrophobic radicals in pairs in the organic phase. Partitioning of AIBN in water is small and its contribution to the overall polymerization has been reported to be almost negligible.<sup>10</sup>
- 3) Hydrogen peroxide (H<sub>2</sub>O<sub>2</sub>)/ Ascorbic acid (AsAc) is a redox initiator. Both components are water soluble and they form neutral hydrophilic hydroxyl radicals.

### Chapter 3

4) Tert-butyl hydroperoxide (TBHP)/ Ascorbic acid (AsAc) is a redox couple. TBHP distributes between aqueous and organic phases. AsAc is soluble in water. The tert-butoxy radicals formed in the aqueous phase are hydrophobic enough to directly enter into the organic phase.

Radical formation from these initiators is summarized in Scheme 3.1.



Scheme 3.1. Radical formation reactions of the initiators used

### Chapter 3

A 1 L reactor equipped with a stainless steel two-stage three-bladed Ekato MIG impeller, reflux condenser, N<sub>2</sub> inlet, temperature probe, and three feeding inlets, was first charged with the seed and purged with N<sub>2</sub> for 20 minutes at 200 rpm. In the reactions where thermal initiators were used, the initiators were added as a shot when the temperature reached 70°C. KPS was dissolved in water while AIBN was dissolved in butyl acrylate. The feed of the monomers started as the temperature was stabilized again after 2-3 minutes. For the case of redox initiators, the oxidant and the reductant were fed separately and simultaneously based on the stoichiometry of the balanced chemical equations (Scheme 3.1). In the first 5 runs, the feedings were maintained for 3.5 hours and then the systems were allowed to react batchwise for 2 hours. In a sixth run, a different feed strategy was applied; MAA/BA, TBHP and AsAc were fed for 3.5 hours whereas the feeding of NaSS was made for 2 hours.

The components of the redox pair cannot keep together because they react rapidly. Therefore, at least one of them should be fed to the reactor. The optimal strategy to feed the redox system is not straightforward. Thus, for H<sub>2</sub>O<sub>2</sub>/AsAc, it was found that addition of AsAc onto the H<sub>2</sub>O<sub>2</sub> in the reactor provided more free radicals than the addition of H<sub>2</sub>O<sub>2</sub> onto AsAc.<sup>12</sup> As a similar study was beyond the goals of this chapter, a simultaneous feeding of the two components of the redox pair was used in order to facilitate the comparison between the initiator systems used.

### Chapter 3

**Table 3.2.** The recipe for seeded semicontinuous reactions by different initiator systems

Run		1	2	3	4	5
Initiator used		KPS	KPS	AIBN	H <sub>2</sub> O <sub>2</sub> /AsAc	TBHP/AsAc
Initial charge	Seed (g)	225	225	225	225	225
	KPS (g)	1.05	1.05	-	-	-
	AIBN (g)	-	-	0.64	-	-
	S (g)	-	14.5	-	-	-
	BA (g)	-	-	14.5	-	-
	H <sub>2</sub> O (g)	30.4	30.4	-	-	-
Feed 1	MMA (g)	129.2	129.2	129.2	129.2	129.2
	BA (g)	129.2	129.2	114.7	129.2	129.2
Feed rate	(g/min)	1.23	1.23	1.16	1.23	1.23
Feed 2	NaSS (g)	3.21	3.21	3.21	3.21	3.21
	AsAc (g)	-	-	-	0.46	0.69
	H <sub>2</sub> O (g)	55.6	66.9	82.5	52.8	54.5
Feed rate	(g/min)	0.28	0.334	0.408	0.269	0.278
Feed 3	TBHP (g)	-	-	-	-	0.7
	H <sub>2</sub> O <sub>2</sub> (g)	-	-	-	0.265	-
	H <sub>2</sub> O (g)	-	-	-	29.7	29.3
Feed rate	(g/min)	-	-	-	0.143	0.143

### 3.2.3. Characterizations

The characterization methods are given in Appendix II.

## Chapter 3

### 3.3. Results and Discussion

The characteristics of the seed are given in Table 3.3. It is remarkable the high fraction of insoluble polymer found because it is similar to the value found for the batch homopolymerization of BA<sup>16</sup> and no gel was reported for semicontinuous emulsion polymerization of MMA/BA =1/1 initiated with KPS,<sup>17</sup> where the lack of gel was attributed to the combined effect of the low reactivity of the MMA terminated active chains for hydrogen abstraction, the absence of abstractable hydrogens in MMA units and the fact that MMA radicals terminate by disproportionation (whereas BA terminates by combination).<sup>18</sup> A possible reason for the high insoluble fraction is that the presence of the ionic groups of NaSS in the polymer chains limits the solubility of the copolymer in THF. In addition, the use of TBHP that yields oxygen centered radicals that are very efficient in abstracting hydrogens from the polymer backbone may also contribute to the formation of long branches and eventually to gel.

**Table 3.3.** Characteristics of the seed

Particle size (Z-ave, nm)	Coag. (%)	Insoluble polymer (gel) wt%	M <sub>n</sub> (g/mol)	M <sub>w</sub> (g/mol)	Đ
115	0.3	54	169,500	362,300	2.1

The evolution of the conversion of the volatile monomers (MMA, BA and S where applicable) in the seeded semicontinuous reactions is presented in Figure 3.1. Full

### Chapter 3

conversion was achieved at the end of all the reactions, except for AIBN that presented the slowest reaction rate. An explanation for this result is that AIBN forms radicals in pairs within the polymer particles which likely suffer rapid geminate termination, and therefore the number of initiating radicals is reduced significantly. Generation of radicals in the aqueous phase by the water soluble fraction of AIBN can initiate chains as well, but their contribution to the overall polymerization rate is almost negligible.<sup>10</sup> Figure 3.1 shows that there is no difference in the conversion profiles of the reactions performed by using KPS, H<sub>2</sub>O<sub>2</sub>/AsAc and TBHP/AsAc, indicating that the rates of polymerization for these reactions were controlled by the feeding rates, namely, the polymerizations proceeded under monomer starved conditions (Fig. 3.2). On the other hand, the reaction rate was slower at the beginning of the reaction performed with KPS and a small amount of S (Fig. 3.1). This may be due to the presence of S that has a lower propagation rate constant than MMA and BA. In addition, the styrene used in this work was of technical grade, namely containing tert-butyl catechol as inhibitor, which has been reported to have a stronger inhibition effect than the inhibitor (monomethyl ether hydroquinone) contained in MMA and BA.<sup>19-21</sup> After the initial period, the rate of polymerization increased and matched well with the feeding rate (Fig. 3.2).

Chapter 3

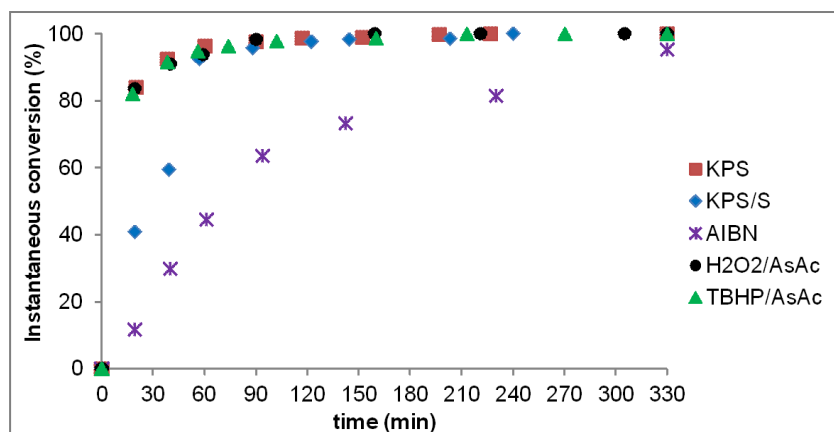


Figure 3.1. Time evolution of the conversion of the monomers for the seeded semicontinuous reactions performed by using different initiators

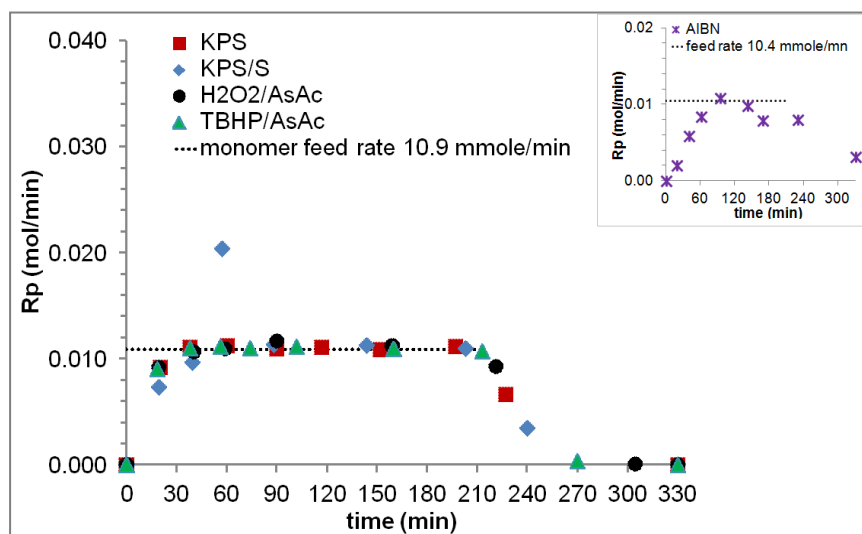


Figure 3.2. Rate of polymerization as a function of time for the seeded semicontinuous reactions performed by using different initiators. In the inset: rate of polymerization as a function of time for AIBN initiator

### Chapter 3

Figure 3.3 shows that in all cases the number of particles ( $N_p$ ) decreased during the first part of the process, the decrease being more pronounced for the systems showing the slowest polymerization rates. The decrease suggested that as the NaSS was semicontinuously added, there was not enough NaSS to stabilize the particles. This effect was more pronounced in the cases where the conversion was lower (AIBN and KPS/S). In order to prove that there was not sufficient amount of NaSS to stabilize the particles, the NaSS feed profile was changed. Instead of 3.5 hours, the feeding of NaSS was performed in 2 hours using TBHP/AsAc as initiator. Figure 3.3 shows that this strategy gave a higher number of particles at the beginning of the reactions (up to 60 min), but later  $N_p$  approached to the value obtained with 3.5 h feeding.

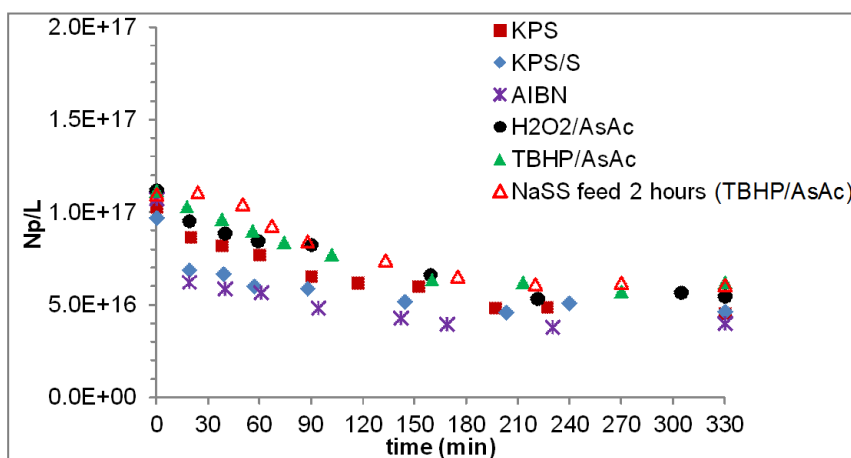


Figure 3.3. Time evolution of the number of particles ( $N_p$ ) in the seeded semicontinuous reactions performed by using different initiators

### Chapter 3

The characteristics of the final latexes summarized in Table 3.4 show that the type of initiator affects the conversion and the chemical incorporation of NaSS.

NaSS conversion increased with the hydrophilicity of the radicals, likely because hydrophilic radicals remained longer in the aqueous phase, and hence the possibility of NaSS to react increased. The lowest conversion was observed for the case of AIBN. In this system, most of the radicals are formed in pairs within the polymer particles, and hence many of them undergo bimolecular termination. Ideally, the radicals that are separated by desorption of one of them from the particles contribute to polymerization. The exited radicals are rather hydrophobic and therefore the time that they spend in the aqueous phase before entering into another particle is short. This led to a low conversion of NaSS that resulted in a low formation of stabilizing copolymer and a high amount of coagulum. This latex was not studied further.

Complete conversion of NaSS was achieved with KPS likely because charged radicals were formed and tended to remain in the aqueous phase where they reacted with the water soluble NaSS. However, the hydrophilic polymer obtained was not prone to attach to the polymer particles leading to a relatively low incorporation (61%) and a high concentration of water soluble polymer (1.6%). The incorporation substantially increased by including a small amount of styrene in the formulation because the presence of S units in the oligomers strongly decreases their water solubility facilitating their attachment to the polymer particles.

Chapter 3

**Table 3.4.** Properties of latexes produced by different initiator systems

	KPS	KPS/S	AIBN	H <sub>2</sub> O <sub>2</sub> /AsAc	TBHP/AsAc	TBHP/AsAc (NaSS feed 2h)
NaSS amount (%wbm)	1.3	1.24	1.3	1.3	1.3	1.3
Monomer conversion (%)	100	100	95	100	100	100
NaSS conversion (%)	100	100	77	97.5	95.0	99.0
NaSS incorporation (%)	60.7	67.7	-	64.1	72.5	73.2
Water soluble species (wt%)	1.6 ± 0.2	1.7 ± 0.1	-	1.2 ± 0.1	0.8 ± 0.2	0.9 ± 0.1
Z-ave particle size (nm)	265	270	-	250	240	240
Coagulation (wt%)	1.9	1.4	11.9	0.7	0.7	1.3
Insoluble polymer (gel, wt%)	66.2	61.8	-	75.8	50.0	51.6
M <sub>n</sub>	131,850	124,500	-	96,240	64,000	47,500
M <sub>w</sub>	374,200	375,900	-	232,800	222,500	206,000

H<sub>2</sub>O<sub>2</sub>/AsAc gave higher NaSS conversion and a higher amount of water soluble polymer compared to TBHP/AsAc, likely due to the higher water solubility of the hydroxyl radicals as compared to the tert-butoxy radicals. As a result, the

### Chapter 3

incorporation was higher for the case of TBHP/AsAc. When the feeding of NaSS was performed in 2 hours, both conversion and incorporation of NaSS improved.

Generally speaking, the changes in incorporation can be linked to the hydrophobicity of the oligoradicals formed in the aqueous phase. The higher the hydrophobicity of the initiator formed in the aqueous phase, the easier the oligoradicals become surface active and attached to the polymer particles. However, the effect of the water solubility of the initiator on NaSS conversion is not straightforward, because the processes discussed above remove radicals from the aqueous phase, where almost all the NaSS is. At first sight, the increase in radical entry should lead to a lower NaSS conversion, which is not what was observed for all the cases. A possible mechanism that accounts for these findings is presented in Scheme 3.2. According to this mechanism, the surface active oligoradicals become attached to the polymer particles but instead of entering within the particles they form a water swollen shell covering the particles. In this way, the radicals are accessible to NaSS that can polymerize. In addition, the attachment to the particles creates a compartmentalization of radicals and as radicals in the surface of different particles cannot terminate between them, the total concentration of radicals accessible to NaSS increased leading to higher NaSS conversions. This mechanism leads to core-shell particles where almost all the NaSS is in the shell and hence contributing to particle stability. This is likely the reason for the good colloidal stability achieved with a modest total concentration of NaSS (1.24 - 1.3 wt% based on monomers). A proof that all the NaSS is in a shell accessible to the aqueous phase was obtained by

### Chapter 3

titrating the dialyzed and ion exchanged latexes with different rates of NaOH (titrant) and almost the same values were obtained whether the addition of NaOH was fast or very slow (Table 3.5).

**Table 3.5.** Effect of titrant addition rate on the calculated values for NaSS incorporation

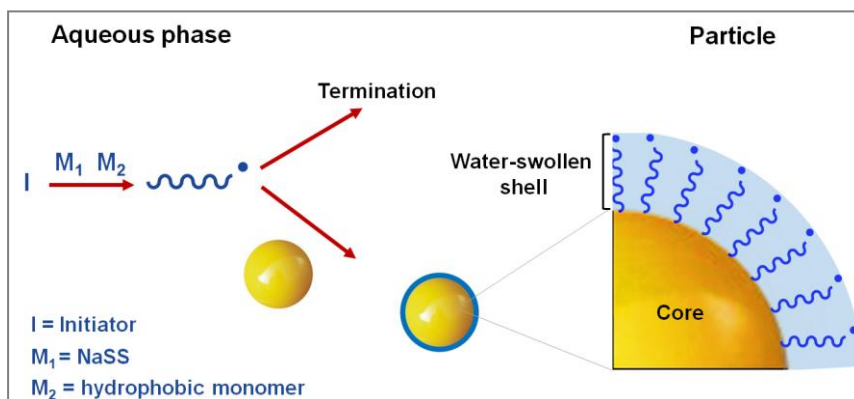
Titrant addition rate	0.1 mL/min	0.2 mL/min	0.4 mL/min
KPS	60.7	60.9	61.2
KPS/S	67.7	67.9	68.3
H <sub>2</sub> O <sub>2</sub> /AsAc	64.1	64.6	64.3
TBHP/AsAc	72.5	72.5	72.7

Scheme 3.2 implies that the polymerization of NaSS occurs in two loci; the aqueous phase that is a solution polymerization and the surface of the polymer particles that behaves as a radical compartmentalized system and it is responsible for most of the polymerization.

In addition to NaSS conversion and incorporation, initiator also affected the polymer characteristics. The insoluble fraction in THF (gel fraction) was found to be high for all investigated systems. Likely, high number of ionic moieties (sulfate and sulfonate groups) is responsible for the limited solubility in THF. The highest gel content was seen for H<sub>2</sub>O<sub>2</sub>/AsAc. In this case, highly reactive hydroxyl radicals

### Chapter 3

capable of entering into the polymer particles<sup>22</sup> and abstracting hydrogens from the polymer backbone may enhance the insolubility.



Scheme 3.2. Polymerization of NaSS occurs in two loci; in the aqueous phase and the surface of the polymer particles (I: initiator, M<sub>1</sub> and M<sub>2</sub> are monomers)

The initiator type has also significant effects on the properties of the latexes and the films prepared from these latexes. The stability of the latexes upon electrolyte addition and freeze-thawing is presented in Table 3.6. The superior stability of the latexes with TBHP/AsAc can be explained by the high incorporation of NaSS. H<sub>2</sub>O<sub>2</sub>/AsAc latex failed in the stability tests because of the low incorporation of NaSS and the absence of charges from the initiator system. KPS/S is (marginally) less stable than KPS in spite of the higher incorporation of NaSS and the similar ionic strength. A possible reason for this result is that in the presence of KPS the

### Chapter 3

estimation of the NaSS incorporation was not accurate. The reason is that in the titration sulfate and sulfonate groups cannot be distinguished and hence the amount of sulfonate groups was calculated from the decomposition rate of KPS. Considering that this reaction is affected by pH of the medium, the accuracy of this estimation is open to discussion.

**Table 3.6.** Salt and freeze thaw stability of the latexes prepared by different initiators

	Salt stability				Freeze-thaw stability		
	0.02 M CaCl <sub>2</sub>	0.05 M CaCl <sub>2</sub>	0.5 M NaCl	0.75 M NaCl	Cycle 1	Cycle 2	Cycle 3
KPS	ok	X	size inc 320nm	X	ok	ok	ok
KPS/S	ok	X	X	X	ok	ok	size inc 330nm
H <sub>2</sub> O <sub>2</sub> /AsAc	X	X	X	X	X		
TBHP/AsAc	ok	X	ok	X	ok	ok	ok
TBHP/AsAc (NaSSfeed 2h)	ok	X	ok	size inc 320nm	ok	ok	ok

The water contact angles of the film-air interfaces before and after rinsing with water are presented in Figure 3.4. It can be seen that for all latexes except those with TBHP/AsAc, the contact angle increases after rinsing with water. This is a proof that hydrophilic species were removed from the films. For TBHP/AsAc, the contact angle was not affected by rinsing, which indicates that the surface of the film was not modified when it was rinsed with water, namely that the hydrophilic species were

### Chapter 3

strongly attached to the polymer. This is in agreement with the high incorporation of NaSS.

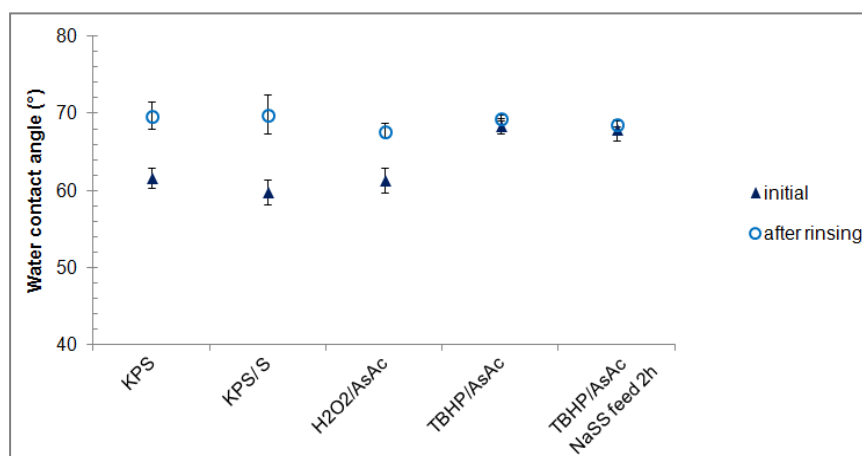
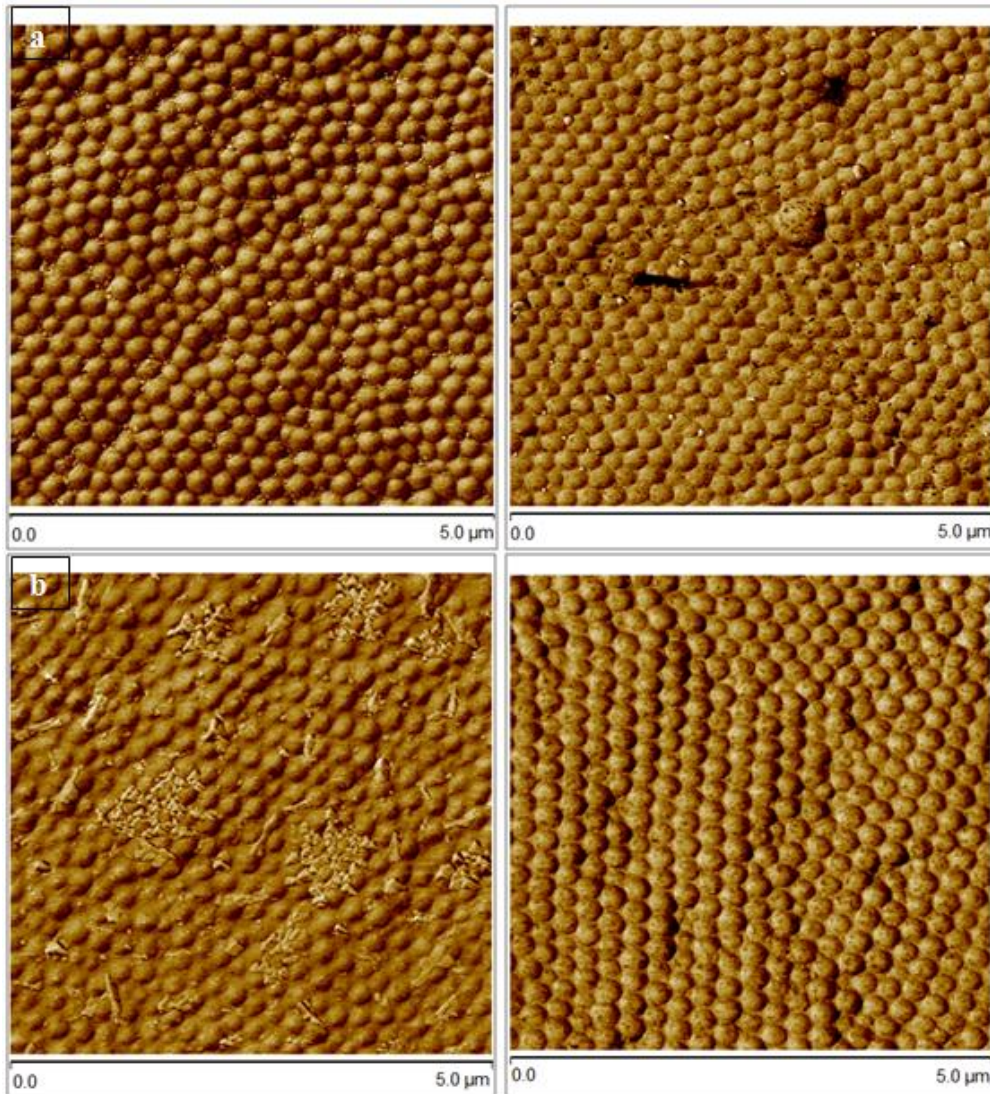


Figure 3.4. Water contact angles of the film-air interfaces before and after rinsing with water

The results of the contact angles (Figure 3.4) are supported by the AFM images of the surface of the films before and after rinsing with water (Figure 3.5). It can be seen that before rinsing with water, in the film prepared with TBHP/AsAc only the polymer particles can be seen, whereas in the films prepared with the other initiators substantial amounts of other presumably hydrophilic materials are apparent. After rinsing, these materials disappeared from the film surface.

Chapter 3



Chapter 3

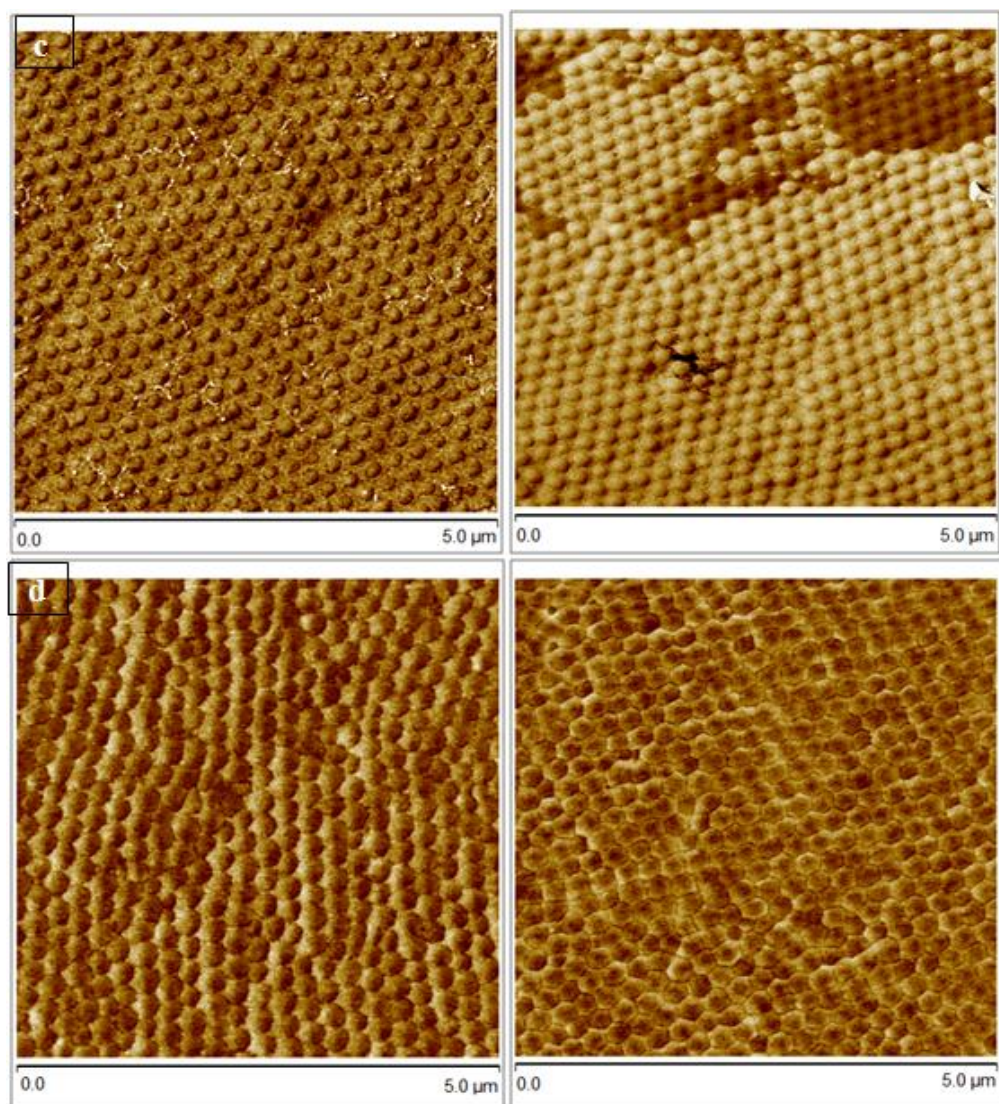


Figure 3.5. AFM phase images of the film-air interface for a)KPS, b)KPS/S, c) $H_2O_2$ /AsAc, and d)TBHP/AsAc, before (left) and after (right) rinsing with water. (Scale:  $5 \times 5 \mu m$ )

### Chapter 3

The water uptake behavior of the polymer films is presented in Figure 3.6. The films containing KPS and KPS/S absorbed more water than the polymers with redox initiators. This is because of a higher concentration of ionic species in these polymers which increase the osmotic pressure as the major driving force for water uptake. As a result of the presence of the water soluble polyelectrolytes, the films with KPS and KPS/S started to disintegrate in water after 3 and 9 days of immersion, respectively. For the case of redox initiators, despite having a lower initial water uptake,  $\text{H}_2\text{O}_2/\text{AsAc}$  with time reached the same value as TBHP/AsAc. The losses in the weight of these polymers were found to be similar, namely 0.9% and 1.1% for  $\text{H}_2\text{O}_2/\text{AsAc}$  and TBHP/AsAc, respectively.

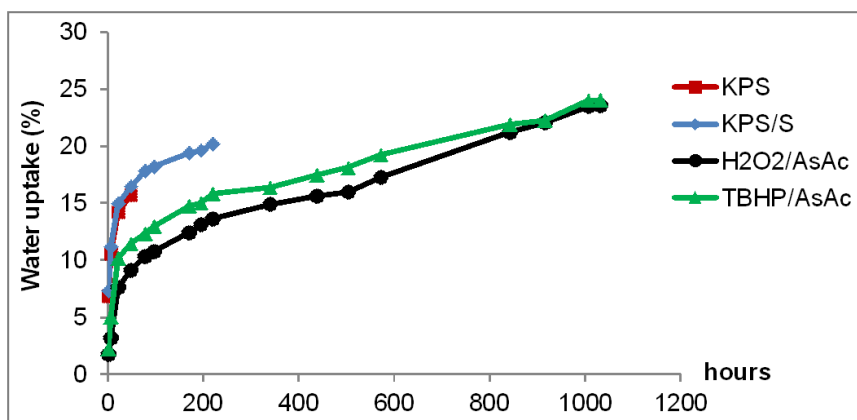


Figure 3.6. Water uptake of the films prepared by using different initiators

### Chapter 3

The mechanical properties of the films cast from the latexes are summarized in Table 3.7 and representative stress-strain curves are provided in Figure 3.7. Note that the films were dried at 23°C and 55% relative humidity and then annealed at 60°C for a day. The film with KPS/S had higher modulus and yield stress compared to the rest of the films due to the presence of S. No clear indication of the effect of NaSS incorporation on the mechanical properties could be seen.

**Table 3.7.** Mechanical properties of the films

	<b>Young's modulus x 10<sup>-2</sup> (MPa)</b>	<b>Yield stress (MPa)</b>	<b>Ultimate tensile strength (MPa)</b>	<b>Elongation at break (%)</b>
KPS	0.6 ± 0.1	2.4 ± 0.2	18.8 ± 1.2	365.7 ± 19.0
KPS/S	1.8 ± 0.3	6.5 ± 0.2	21.2 ± 1.1	282.3 ± 21.4
H <sub>2</sub> O <sub>2</sub> /AsAc	0.9 ± 0.2	3.2 ± 0.2	17.9 ± 1.2	281.4 ± 12.1
TBHP/AsAc	0.7 ± 0.1	2.7 ± 0.2	16.7 ± 0.7	340.3 ± 10.0

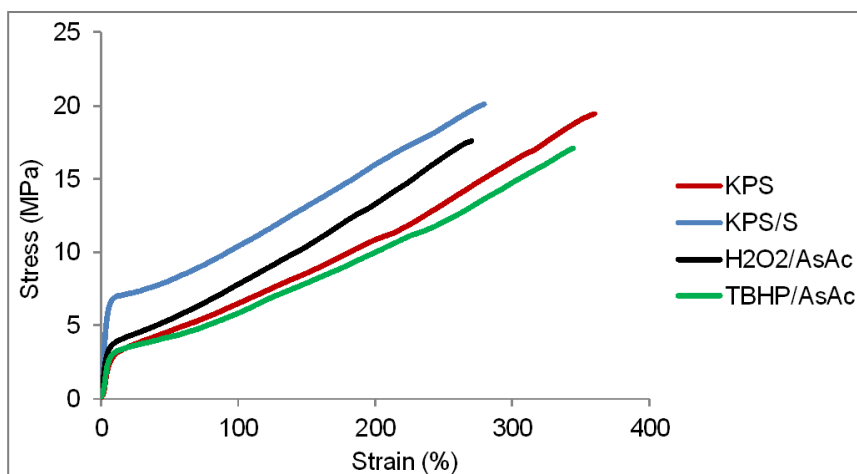


Figure 3.7. The stress-strain behavior of the films

### 3.4. Conclusions

In this chapter, effect of the nature of the initiator on the chemical incorporation of NaSS onto hydrophobic polymer particles was investigated. For that aim, four different initiators were compared, based on the type and hydrophobicity of the radicals formed. KPS, a water soluble thermal initiator that forms negatively charged hydrophilic radicals in the aqueous phase; KPS/S a small amount of styrene was added in an attempt to make the oligomers formed by the sulfate radicals more hydrophobic; AIBN is an oil soluble thermal initiator that mainly forms hydrophobic radicals in pairs in the organic phase; and two redox pair initiators, H<sub>2</sub>O<sub>2</sub>/AsAc water soluble system that forms neutral water soluble radicals, and TBHP/AsAc with one

### Chapter 3

component more hydrophobic (TBHP) that forms neutral hydrophobic radicals in aqueous phase.

Oil soluble initiator AIBN, was not efficient likely due to the fact that radicals were generated in the particles and the NaSS was in the aqueous phase, therefore they could not find each other. In this case, insufficient conversion of NaSS resulted in macroscopic coagulation.

Use of charged hydrophilic initiator (KPS) resulted in a low incorporation of NaSS due to the formation of water soluble polymer in the aqueous phase. As the hydrophobicity of the oligoradical increased by adding a small amount of a hydrophobic monomer (styrene) or by generation of nonionic radicals such as hydroxyl and tert-butoxy radicals, the incorporation of NaSS increased. The incorporation was highest for TBHP/AsAc initiator systems. These results indicated that polymerization of NaSS occurs in two loci: the aqueous phase that is a solution polymerization and the surface of the polymer particles that behaves as a radical compartmentalized system. On the surface of the particles these growing oligoradicals forms a water swollen shell, where monomers with different water solubility get in contact and most of the copolymerization occurs there.

The type of initiator also affected the characteristics of the latexes and the polymer films. Latexes with TBHP/AsAc for which the incorporation was high, presented good salt stability and excellent freeze-thaw stability. In the case of TBHP/AsAc the lack of migration of amphiphilic material was proven by the measurements of water

### Chapter 3

contact angles and AFM images of the surface before and after rinsing with water. Other latexes presented worse properties due to the presence of water soluble species. Regarding the polymer films, the ones containing charge fragments from initiators (with KPS and KPS/S) were highly water sensitive, presented high water uptake and even show to lost of the consistency in water after few days of immersion. Polymer films with redox pair initiators presented lower water-uptake, similar between them.

Generally speaking, use of TBHP/AsAc was found to be the most promising initiator in seeded semicontinuous copolymerization of MMA/BA/NaSS, due to the very high incorporation of NaSS achieved and good properties presented due to that.

## Chapter 3

### 3.5. References

- [1] Ilundain, P., Alvarez, D., Da Cunha, L., Salazar, R., Barandiaran, M.J. and Asua, J.M., Knowledge-based choice of the initiator type for monomer removal by postpolymerization. *Journal of Polymer Science Part A: Polymer Chemistry* **2002**, 40(23), 4245-4249.
- [2] Penboss, I.A., Napper, D.H. and Gilbert, R.G., Styrene emulsion polymerization. The effects of initiator charge. *Journal of the Chemical Society, Faraday Transactions 1: Physical Chemistry in Condensed Phases* **1983**, 79(5), 1257-1271.
- [3] Marestin, C., Guyot, A. and Claverie, J., Direct measurement of oligomers entry rate onto latex particles in an emulsion polymerization. *Macromolecules* **1998**, 31(5), 1686-1689.
- [4] van Berkel, K.Y., Russell, G.T. and Gilbert, R.G., Entry in emulsion polymerization: effects of initiator and particle surface charge. *Macromolecules* **2003**, 36(11), 3921-3931.
- [5] Aramendia, E., Barandiaran, M.J., de la Cal, J.C., Grade, J., Blease, T. and Asua, J.M., Incorporation of a new alkenyl-based nonionic surfmer into acrylic latexes. *Journal of Polymer Science Part A: Polymer Chemistry* **2004**, 42(17), 4202-4211.
- [6] Siadat, B., Oster, B. and Lenz, R.W., Preparation of ion-containing elastomers by emulsion copolymerization of dienes with olefinic sulfonic acid salts. *Journal of Applied Polymer Science* **1981**, 26(3), 1027-1037.
- [7] Weiss, R.A., Turner, S.R. and Lundberg, R.D., Sulfonated polystyrene ionomers prepared by emulsion copolymerization of styrene and sodium styrene sulfonate. *Journal of Polymer Science: Polymer Chemistry Edition* **1985**, 23(2), 525-533.

### Chapter 3

[8] Luo, Y. and Schork, F.J., Emulsion copolymerization of butyl acrylate with cationic monomer using interfacial redox initiator system. *Journal of Polymer Science Part A: Polymer Chemistry* **2001**, 39(16), 2696-2709.

[9] Cheong, I.W. and Kim, J.H., Simulation of secondary particle formation in seeded emulsion polymerization: The effect of surface charge density. *Macromolecular Theory and Simulations* **1998**, 7(1), 49-57.

[10] Autran, C., de la Cal, J.C. and Asua, J.M., (Mini) emulsion polymerization kinetics using oil-soluble initiators. *Macromolecules* **2007**, 40(17), 6233-6238.

[11] Deutsch, J.C., Ascorbic acid oxidation by hydrogen peroxide. *Analytical Biochemistry* **1998**, 255(1), 1-7.

[12] Boutti, S., Zafra, R.D., Graillat, C. and McKenna, T.F., Interaction of surfactant and initiator types in emulsion polymerisations: A comparison of ammonium persulfate and hydrogen peroxide. *Macromolecular Chemistry and Physics* **2005**, 206(14), 1355-1372.

[13] Da Cunha, L., Ilundain, P., Salazar, R., Alvarez, D., Barandiaran, M.J. and Asua, J.M., VOC formation during monomer removal by post-polymerization. *Polymer* **2001**, 42(2), 391-395.

[14] Dixon K.W. In *Polymer Handbook*, 4th ed.; Brandrup J., Immergut E.H., Grulke E.A., Eds.; John Wiley & Sons: USA, 1999; p II-5.

[15] Hiroki, A. and LaVerne, J.A., Decomposition of hydrogen peroxide at water-ceramic oxide interfaces. *The Journal of Physical Chemistry B* **2005**, 109(8), 3364-3370.

[16] Yadav, A.K., Barandiaran, M.J. and de la Cal, J.C., Effect of the polymerization technique and reactor type on the poly(n-butyl acrylate) microstructure. *Macromolecular Reaction Engineering* **2014**, 8(6), 467-475.

### Chapter 3

[17] González, I., Asua, J.M. and Leiza, J.R., The role of methyl methacrylate on branching and gel formation in the emulsion copolymerization of BA/MMA. *Polymer* **2007**, 48(9), 2542-2547.

[18] Ballard, N., Hamzehlou, S., Ruipérez, F. and Asua, J.M., On the termination mechanism in the radical polymerization of acrylates. *Macromolecular Rapid Communications* **2016**, 37(16), 1364-1368.

[19] Georgieff, K.K., Relative inhibitory effect of various compounds on the rate of polymerization of methyl methacrylate. *Journal of Applied Polymer Science* **1965**, 9(6), 2009-2018.

[20] Barton, S.C., Bird, R.A. and Russell, K.E., The effect of phenols and aromatic thiols on the polymerization of methyl methacrylate. *Canadian Journal of Chemistry* **1963**, 41(11), 2737-2742.

[21] Godsay, M.P., Harpell, G.A. and Russell, K.E., The effect of phenols on the polymerization of styrene. *Journal of Polymer Science* **1962**, 57(165), 641-650.

[22] Goicoechea, M., Barandiaran, M.J. and Asua, J.M., Entry of hydrophilic radicals into latex particles. *Macromolecules* **2006**, 39(15), 5165-5166.



## **Chapter 4. Effect of comonomer type on the chemical incorporation of sodium styrene sulfonate onto polymer colloids at high solids contents**

### **4.1 Introduction**

In Chapter 3, it was shown that 50 wt% solids content latexes can be produced in seeded semicontinuous emulsion polymerization using different initiator systems. The best results in terms of NaSS incorporation and application properties were achieved with TBHP/AsAc. On the other hand, in Chapter 2 it was found that the type of comonomer influences the incorporation of NaSS in the polymer particles. Specifically it was found that the incorporation of NaSS increased with the water solubility of the comonomer, whereas the functionality (methacrylate, acrylate, styrene) did not have a significant effect on NaSS incorporation. In Chapter 2, mainly pure comonomers and a low solids content formulation were used. These conditions are quite different from those used in commercial practice where multimonomer high solids formulations are used.

Therefore in this chapter, the effect of a wide range of mixtures of comonomers on the incorporation of NaSS to the polymer particles in high solids content formulations

## Chapter 4

(50 wt%) is studied using TBHP/AsAc as initiator. In addition, the possibility of reaching  $\geq 60$  wt% solids content is investigated.

### 4.2 Experimental

#### 4.2.1 Materials

The materials are given in Appendix II.

#### 4.2.2 Polymerizations

The details of the seed synthesis are presented in the experimental section of Chapter 3. The formulations used in the seeded semicontinuous emulsion polymerization are shown in Table 4.1. A 1 L reactor equipped with a stainless steel two-stage three-bladed Ekato MIG impeller, a reflux condenser, a N<sub>2</sub> inlet, a temperature probe, and feeding inlets, was first charged with the seed and purged with N<sub>2</sub> for 20 minutes under 200 rpm agitation. When the temperature reached 70°C, the reactants were added to the reactor in separate feeds. In runs 1-8, three feeds namely the comonomer mixture, the aqueous solution of TBHP and a NaSS/AsAc aqueous solution were applied for 210 minutes. In run 9, there were 4 feeds: the feeding of monomers and initiators were performed for 4.5 hours whereas the feed of NaSS was 4 hours. After the feedings, the systems were allowed to react batchwise

## Chapter 4

for 2 hours. The target solids content for most of the reactions was 50 wt% and the total amount of NaSS was varied in the range of 1.1 - 1.35 wt% based on monomers.

Table 4.1 shows the different monomer systems used. The base of the first three polymerizations was a typical coating formulation (MMA/BA = 1/1 wt/wt, run 1) to which a small fraction of water soluble monomers (4 wbm% of MAA in run 2 and 5 wbm% of 2HEA in run 3) was added. The rationale behind this choice is that in a low solids content system and for scarcely water soluble comonomers that formed the major part of the polymer, we demonstrated that the incorporation of NaSS onto the polymer particles increased with the water solubility of the comonomer (Chapter 2). Runs 1 - 3 try to find if similar effects can be achieved by using small amounts of water soluble comonomers, which have the additional advantage of enhancing the adhesion of the polymer on both polar and nonpolar substrates.<sup>1</sup> Taking run 1 as a reference, in runs 4 - 8, MMA was completely or partially substituted by either similar (EA, run 4) or less water soluble monomers (BMA or S, runs 5-8). These reactions were carried out to check the universality of the synthetic technique. In run 9, the possibility of reaching  $\geq 60$  wt% solids content was investigated.

Chapter 4

**Table 4.1.** The recipes for semicontinuous reactions

Run		1	2	3	4	5	6	7	8	9
Monomer (weight ratio)		MMA:BA (1:1)	MMA:BA:MAA (1:1:0.04)	MMA:BA:2HEA (1:1:0.05)	EA:BA (1:1)	BMA:BA (1:1)	BMA:BA (1.42:1)	S:BA (1:1)	MMA:S:BA (0.9:0.1:1)	MMA:BA* (1:1)
Initial charge	Seed (g)	225	225	225	225	225	225	225	225	200
Feed 1	MMA (g)	129.15	129.15	129.15	-	-	-	-	129.15	166.8
	BA (g)	129.15	129.15	129.15	129.15	129.15	129.15	129.15	129.15	166.8
	BMA (g)	-	-	-	-	129.15	183.40	-	-	-
	EA (g)	-	-	-	129.15	-	-	-	-	-
	S (g)	-	-	-	-	-	-	129.15	-	-
	MAA (g)	-	5.17	-	-	-	-	-	-	-
	2HEA	-	-	6.97	-	-	-	-	-	-
Feed rate	(g/min)	1.23	1.26	1.26	1.23	1.23	1.49	1.23	1.23	1.23
Feed 2	NaSS (g)	3.21	3.21	3.21	3.21	3.21	3.21	3.21	3.21	†
	AsAc (g)	0.69	0.69	0.69	0.69	0.69	0.69	0.69	0.69	0.91
	H <sub>2</sub> O (g)	54.5	54.5	54.5	54.5	54.5	54.5	54.5	54.5	13.8
Feed rate	(g/min)	0.28	0.28	0.28	0.28	0.28	0.28	0.28	0.28	0.054
Feed 3	TBHP (g)	0.7	0.7	0.7	0.7	0.7	0.7	0.7	0.7	0.91
	H <sub>2</sub> O (g)	29.3	33.65	35.4	29.3	29.3	83.3	29.3	29.3	22.2
Feed rate	(g/min)	0.143	0.163	0.172	0.143	0.143	0.400	0.143	0.143	0.085

\*Solids content: 60 wt%. †NaSS was fed as a separate stream with 0.122 g/min rate for 4 h (4.5 g NaSS in 24.7 g H<sub>2</sub>O).

The water solubility of the monomers used is given in Table 4.2. MAA and 2HEA are completely water soluble, but they partition between the monomer and aqueous phases. The values of the partitioning coefficients at 30°C in a MMA/water system are also given in Table 4.2. The value for MAA was determined at pH = 4.45. As the polymerizations were carried out at pH = 3, the partition coefficient is expected to be higher.

## Chapter 4

**Table 4.2.** Water solubilities of the comonomers

Comonomer	Solubility in water (mM) at 25°C
Styrene (S)	3.5 <sup>2</sup>
Butyl methacrylate (BMA)	4 <sup>2</sup>
Butyl acrylate (BA)	11 <sup>2</sup>
Ethyl acrylate (EA)	150 <sup>2</sup>
Methyl methacrylate (MMA)	150 <sup>2</sup>
Methacrylic Acid (MAA)	$\infty$ <sup>3</sup> ; $\Phi_{\text{MMA/water}}$ <sup>a</sup> = 7.04 <sup>4</sup>
2-hydroxy ethyl acrylate (2HEA)	$\infty$ <sup>3</sup> ; $\Phi_{\text{MMA/water}}$ <sup>a</sup> = 0.79 <sup>5</sup>

<sup>a</sup>  $\Phi = [\text{comonomer}]_{\text{organic phase}} / [\text{comonomer}]_{\text{water}}$

### 4.2.3 Characterizations

The characterization methods are given in Appendix II.

### 4.3 Results and Discussion

The characteristics of the seed presented in Table 4.3 were already discussed in Chapter 3. This seed was used in all of the seeded semicontinuous emulsion polymerization

## Chapter 4

**Table 4.3.** Characteristics of the seed

Particle size (Z-ave, nm)	Coag. (%)	Insoluble polymer (gel) wt%	M <sub>n</sub> (g/mol)	M <sub>w</sub> (g/mol)	Đ
115	0.3	54	169,500	362,300	2.1

The evolution of the conversion of comonomers in seeded semicontinuous reactions is presented in Figure 4.1. Most of the polymerizations were carried out under starved conditions and hence no significant difference between methacrylates and acrylates was observed. The slowest polymerization rate was for S/BA reaction, which can be explained by the low propagation rate constant of S<sup>6</sup> and the type of inhibitor included. The monomers used in this study were of technical grade. S contains tert-butyl catechol as inhibitor which has a stronger inhibition effect than the inhibitor monomethyl ether hydroquinone contained in the other monomers.<sup>7-9</sup> All reactions ended up with virtually complete conversion of the comonomers. The highest amount of residual comonomer was observed for S/BA reaction due to explained reasons. It is remarkable that stable 50 wt% solids content latexes for a wide range of monomer systems and 60 wt% solids content MMA/BA latex were synthesized under industrial-like semicontinuous conditions in the absence of surfactant.

## Chapter 4

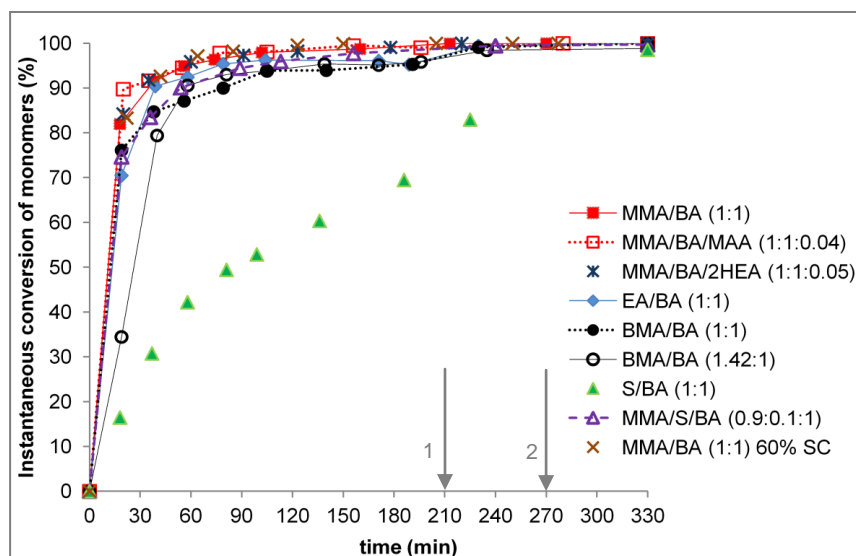


Figure 4.1. Evolution of the conversion of the monomers for the seeded semicontinuous emulsion polymerization. Arrow 1 indicates the end of feedings for runs 1-8 and arrow 2 indicates the end of feedings for run 9

The evolution of number of particles ( $N_p$ ) given in Figure 4.2, shows that  $N_p$  decreased slightly in all the reactions indicating some particle coagulation. It is interesting that the smaller number of particles corresponded to the reaction carried out with the formulations containing water soluble monomers.

Chapter 4

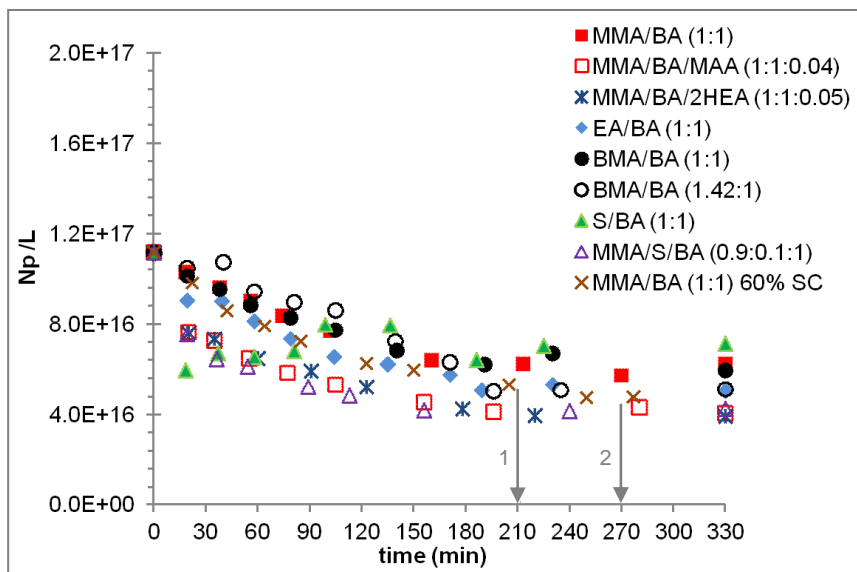


Figure 4.2. Evolution of the number of particles ( $N_p$ ) in the seeded semicontinuous emulsion polymerizations. Arrow 1 indicates the end of feedings for runs 1-8 and arrow 2 indicates the end of feedings for run 9

The characteristics of the latexes are given in Table 4.4. It can be seen that high conversion of the comonomers was achieved in all the polymerizations. Table 4.4 also shows that high conversions of NaSS were achieved at the end of the process. It is worth pointing out that post polymerization was not implemented to highlight the effect of the comonomer system on the NaSS conversion. With the exception of the polymerization carried out with MAA (run 2), the final conversion of NaSS in general increases with the hydrophilicity of the monomer system.

## Chapter 4

**Table 4.4.** Characteristics of the final latexes obtained by seeded semicontinuous emulsion polymerizations

Composition	Comonomer conv. (%)	NaSS conv. (%)	NaSS incorporation (%) (final latex)	NaSS incorporation (%) (semicont. step)	Z-ave diameter (nm)	Coag. (%)	Insoluble polymer (gel) (wt%)	M <sub>n</sub>	M <sub>w</sub>
MMA/BA	100	95.0	72.5	75.1	240	0.7	50.0	64,000	222,500
MMA/BA/MAA	100	92.7	66.9	68.7	280	0.2	50.9	83,400	234,300
MMA/BA/2HEA	100	96.8	76.8	80.0	280	0.6	53.5	43,100	163,800
EA/BA	99.9	94.8	74.9	77.8	260	0.6	56.8	51,200	138,600
BMA/BA (1:1)	100	80.5	58.7	59.4	245	1.4	54.8	65,000	172,600
BMA/BA (1.42:1)	98.8	86.2	61.2	62.3	255	1.7	54.3	85,300	246,000
S/BA	98.5	83.8	55.4	55.7	230	1.2	28.7	74,100	187,300
MMA/S/BA	99.9	90.3	62.8	64.1	275	0.4	40.9	59,600	155,600
MMA/BA (60% SC)	100	94.1	81.1	83.5	280	0.9 <sup>a</sup>	52.0	63,600	238,700

<sup>a</sup> represents the amount retained on the mesh during filtering of the latex

The fraction of the NaSS in the formulation that was incorporated in the particles is also presented in Table 4.4. The actual measurement is the incorporation in the final latex, namely including the contribution of the seed. The incorporation during the semicontinuous process was estimated considering that the NaSS incorporation in the seed was 54% and that the seed represented 12.5% of the final polymer. It can be seen that incorporation also increased with water solubility of the comonomer system (again with the exception of MAA). Obviously, as the incorporation was calculated based on the total amount of NaSS in the formulation, incorporation and conversion are coupled. However, the effect of the comonomer system on NaSS

## Chapter 4

incorporation was more accurate than on NaSS conversion and the differences in conversion did not justify the changes observed in incorporation.

The strong changes in incorporation can be linked to the composition of the oligoradicals formed in the aqueous phase. The higher the water solubility of the comonomer, the richer the oligoradicals in the relatively hydrophobic comonomer and hence the easier they become surface active and attached to the polymer particles.

However, the effect of the water solubility of the comonomer on NaSS conversion is not straightforward, because the processes discussed above remove radicals from the aqueous phase, where almost all of the NaSS is (the attempts carried out to measure the partitioning of NaSS between phases failed because virtually 100% of the NaSS was in the aqueous phase, Appendix I). At first sight, the increase in radical entry should lead to a lower NaSS conversion, which is not what was observed. A possible mechanism that accounts for these findings was already presented and discussed in Scheme 3.2 of Chapter 3. Namely, the surface active oligoradicals formed in aqueous phase attached to the polymer particles creating a water swollen shell around the hydrophobic core of the particle, where the radicals have access to both, NaSS and comonomers to copolymerize.

In this context, the results obtained in run 2 with MAA in the formulation are surprising. Considering only the hydrophilicity of the comonomer system, the NaSS conversion and incorporation should be between those of run 1 and 3, namely higher than for MMA/BA. However, this was not the case. Comparison between runs 1 and 2

## Chapter 4

shows that the addition of MAA to the MMA/BA mixture led to a decrease in both conversion and incorporation of NaSS.

Considering the mechanism in Scheme 3.2, this result suggests that MAA reduced the incorporation of oligoradicals to the particle shell. The consequence is an increase of the importance of solution (aqueous phase) polymerization with respect to the polymerization in the polymer particles, which resulted in lower polymerization rate and lower incorporation.

The incorporation of NaSS improved significantly as the solids content increased from 50 wt% to 60 wt% likely due to an enhanced probability for the oligoradical attachment and also because the feeding of NaSS was stopped before that of the monomers.

Stable 60 wt% solids content MMA/BA (1/1) latex was successfully synthesized with a viscosity of 200 mPa.s (at 100 s<sup>-1</sup>). It is worth to mention that the viscosity of the MMA/BA latex obtained in run 1 (50 wt% solids content) was 24 mPa.s and a viscosity lower than 500 mPa.s (at 100 s<sup>-1</sup>) can be considered acceptable from an industrial point of view. Moreover, by following the same procedure, it was possible to reach 62 wt% solids content with a viscosity of 450 mPa.s (at 100 s<sup>-1</sup>). To our knowledge, this is the highest solids content achieved for stable emulsifier-free MMA/BA latex produced by using sulfonate monomer. After 62 wt% solids content, the viscosity increased sharply. At 64 wt%, the latex was highly viscous (1770 mPa.s). At high volume fractions (>50%), dispersion viscosity exponentially increases

## Chapter 4

with the volume fraction. However, this increase depends of other factors such as the particle size distribution (PSD), surface charge density, presence of a hairy layer and ionic strength.<sup>11-17</sup> As a rule of thumb, for the same solids content, viscosity decreases with the broadness of the PSD, the maximum size of the dispersion and the ionic strength of the medium (for charged colloids); and increases with the surface charge density and the presence of a hairy layer. The current system has all the ingredients to show a high viscosity because as it is produced by seeded emulsion polymerization in the absence of secondary nucleation and almost negligible coagulation, it has a narrow PSD with a relatively small particle size (250 nm, Table 4.4). In addition, a high incorporation of NaSS was achieved (> 80% above 60wt% solids), which has two effects. On one part, increases the surface charge density and on the other, decreases the ionic strength of the medium, because NaSS is the main source of ions in the system. Finally, the formation of a shell made of a hydrophilic polymer (hairy layer, Scheme 3.2) lead to an increase of the apparent volume fraction of the system.

The comparison between the results obtained in Chapter 2 and in this chapter showed that the reactions at low solids contents worked well as the proof of concept in terms of the general trends for the extent of NaSS incorporation based on comonomer water solubility. Yet, there are some differences. In Chapter 2, seeded batch reactions of NaSS and a comonomer were performed at low solids contents (~15 wt%) and in this chapter, mixtures of comonomers were utilized with NaSS in high solids content seeded semicontinuous reactions. Here, NaSS conversions were

## Chapter 4

slightly higher which might be related with the synthesis method and also the increase in the total surface area of the particles at high solids contents.

The fraction of polymer insoluble in THF (gel) was the highest for acrylic system (EA/BA reaction). This is expected since acrylates suffer intermolecular chain transfer to polymer coupled with termination by combination, leading to gel formation.<sup>10</sup> On the other hand, since S is not prone to suffer transfer to polymer and hence to form gel, insoluble fractions were low in S containing systems. However, the gel contents were unusually high for all investigated systems, especially for methacrylates. A combination of factors could lead to such high gel contents. All reactions except S/BA were under monomer starved conditions increasing the possibility of chain transfer to polymer. In addition, it is very likely that sulfonate groups of NaSS induce ionic interactions between polymer chains and decrease their solubility in THF. Moreover, the oxygen centered tert-butoxy radicals that are hydrophobic enough to enter directly into the particles, are efficient in abstracting hydrogen from the polymer backbone. The contribution of the nature of the radical to the enhanced gel was supported by the fact that gel fraction in BMA/BA reactions was higher than that of MMA/BA. Since water solubility of MMA is significantly higher than BMA, the possibility for the oxygen centered radicals to react with the MMA comonomer before directly entering into the particles is higher. The carbon centered radicals are less effective in hydrogen abstraction; hence less gel was formed in the case of MMA.

## Chapter 4

To determine how incorporation of NaSS influences the latex and film properties, the freeze-thaw and salt stability tests were performed. The latexes containing NaSS were compared with a blank latex, in which stabilization was provided by a conventional emulsifier (sodium dodecyl sulfate, SDS). The results are given in Table 4.5. Both freeze-thaw and salt stability were significantly improved in almost all NaSS containing latexes. Comparison of NaSS containing latexes shows that softer polymers had poor freeze-thaw stability. It is known that the freeze-thaw stability of the low  $T_g$  polymers is typically low<sup>18, 19</sup> and more stabilizing moieties are required for soft polymer particles to achieve the same freeze-thaw stability than harder ones.<sup>20</sup> On the other hand, when harder polymers with similar  $T_g$ s namely MMA/BA, MMA/S/BA and S/BA were compared, it is seen that the higher the incorporation, the better the freeze-thaw stability.

The most significant difference in the stability of the latexes towards electrolyte addition was observed for the case of 0.5 M NaCl. The polymers with higher NaSS incorporations displayed better salt stability except the latex prepared with EA/BA. The fact that soft particles tend to aggregate faster and easier since they are more deformable<sup>21</sup> compared to high  $T_g$  particles may account for the inferior salt stability of EA/BA. The MMA/BA latex at 60 wt% solids content displayed superior performance in salt stability test likely due to high incorporation of NaSS.

Chapter 4

**Table 4.5.** Freeze-thaw and salt stability of the latexes prepared by using different comonomers (X means massive coagulation)

	Freeze-thaw stability			Salt stability				
	Cycle 1	Cycle 2	Cycle 3	0.02 M CaCl <sub>2</sub>	0.05 M CaCl <sub>2</sub>	0.5 M NaCl	0.75 M NaCl	1 M NaCl
MMA/BA	ok	ok	ok	ok	X	ok	X	X
MMA/BA/MAA	ok	ok	ok	ok	X	ok	size inc 300nm	X
MMA/BA/2HEA	ok	ok	ok	ok	X	ok	X	X
EA/BA	X			ok	X	X	X	X
BMA/BA (1:1)	X			ok	X	X	X	X
BMA/BA (1.42:1)	X			ok	X	size inc 530nm	X	X
S/BA	X			ok	X	size inc 380nm	X	X
MMA/S/BA	ok	ok	size inc 305nm	ok	X	size inc 310nm	X	X
MMA/BA (60% SC)	ok	ok	ok	ok	X	ok	ok	ok
MMA/BA (1:1) stabilized by SDS	X			%19 coag	X	size inc 450nm	X	X

In order to determine the influence of NaSS incorporation on polymer films, their water sensitivity were characterized by means of water uptake (Figure 4.3). The highest water uptake was observed in the case of film prepared from the latex EA/BA, perhaps because EA is the most hydrophilic of the major comonomers. In general, the more hydrophilic the monomer system and the higher the NaSS incorporation, the stronger the water sensitivity of the films. The weight loss of the polymer films after immersion in water for 10 days is inserted in Figure 4.3. The weight loss indicates diffusion of water-soluble species from the film into the water. The general trend is the

## Chapter 4

films that absorbed more water were the ones losing more weight and the amount lost was much lower than the amount of NaSS in the films. The films from hydrophobic polymers (BMA/BA, S/BA) did not display any detectable weight loss even though NaSS incorporation was lower. This may be because the diffusion of water into the film was hindered and hence free hydrophilic species were less accessible.

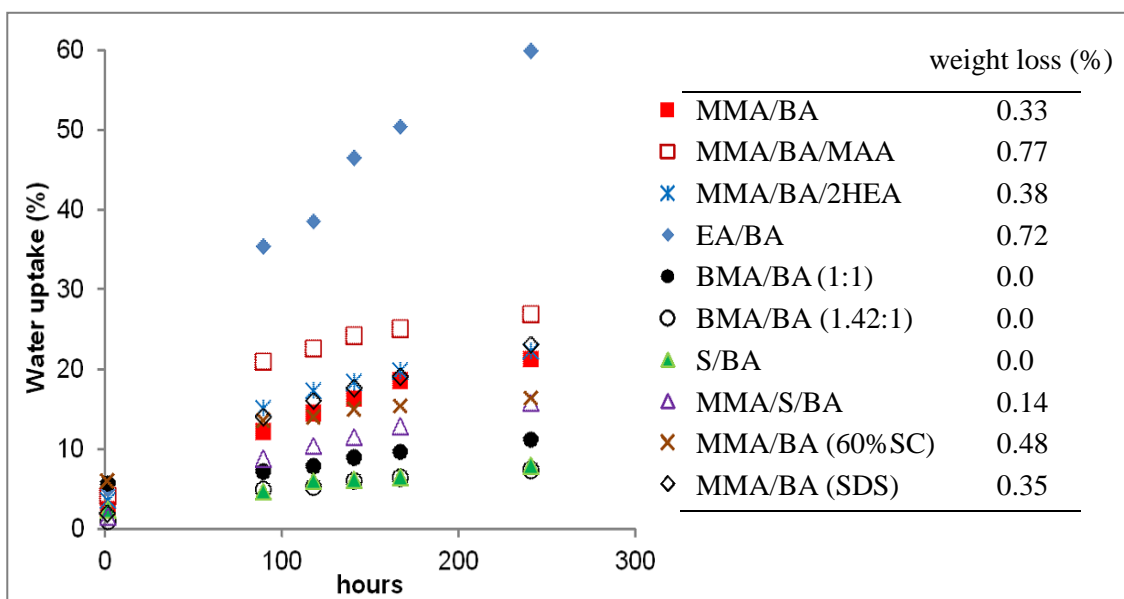


Figure 4.3. Water uptake of the polymer films

## Chapter 4

### 4.4. Conclusions

In this chapter, the effect of a wide range of mixtures of comonomers on the incorporation of NaSS to the polymer particles was studied using TBHP/AsAc as initiator and modest amounts of NaSS (1.1 – 1.35 wt% based on monomers).

Stable 50 wt% solids content latexes for a wide range of monomer systems and 60 wt% solids content MMA/BA latex were synthesized under industrial-like semicontinuous conditions in the absence of surfactant.

It was found that the chemical incorporation of NaSS on the polymer particles generally improved with the water solubility of the comonomers. Addition of small amounts of 2HEA in MMA/BA system increased the incorporation of NaSS. However, MAA reduced the incorporation indicating that the aqueous phase polymerization was more dominant than the polymerization in the polymer particles. The incorporation of NaSS also improved as the solids content of MMA/BA latex increased to 60 wt%.

NaSS containing latexes presented improved freeze-thaw and salt stability when compared with a similar latex in which stabilization was provided by SDS. For NaSS stabilized latexes freeze-thaw stability was low for soft copolymers, but for similarly hard polymers, freeze-thaw stability improved with NaSS incorporation.

Water uptake was mainly determined by the hydrophobicity of the comonomers, the higher the hydrophobicity the lower the water uptake.

## Chapter 4

### 4.5. References

- [1] Agirre, A., Nase, J., Degrandi, E., Creton, C. and Asua, J.M., Improving adhesion of acrylic waterborne PSAs to low surface energy materials: introduction of stearyl acrylate. *Journal of Polymer Science Part A: Polymer Chemistry* **2010**, 48(22), 5030-5039.
- [2] Chern, C-S. Principles and Applications of Emulsion Polymerization, John Wiley & Sons: USA, 2008.
- [3] Penzel, E., Polyacrylates. *Ullmann's Encyclopedia of Industrial Chemistry* **2000**, DOI:10.1002/14356007.a21\_157
- [4] Tripathi, A.K., Sundberg, D.C., Partitioning of functional monomers in emulsion polymerization: distribution of carboxylic acid monomers between water and monomer phases. *Industrial and Engineering Chemistry Research* **2013**, 52(48), 3306–3314.
- [5] Tripathi, A.K. and Sundberg, D.C., Partitioning of functional monomers in emulsion polymerization: distribution of hydroxy (meth) acrylate monomers between water and single and multimonomer systems. *Industrial and Engineering Chemistry Research* **2013**, 52(48), 17047-17056.
- [6] Buback, M., Gilbert, R.G., Hutchinson, R.A., Klumperman, B., Kuchta, F.D., Manders, B.G., O'Driscoll, K.F., Russell, G.T. and Schweer, J., Critically evaluated rate coefficients for free-radical polymerization, 1. Propagation rate coefficient for styrene. *Macromolecular Chemistry and Physics* **1995**, 196(10), 3267-3280.
- [7] Georgieff, K.K., Relative inhibitory effect of various compounds on the rate of polymerization of methyl methacrylate. *Journal of Applied Polymer Science* **1965**, 9(6), 2009-2018.

#### Chapter 4

[8] Barton, S.C., Bird, R.A. and Russell, K.E., The effect of phenols and aromatic thiols on the polymerization of methyl methacrylate. *Canadian Journal of Chemistry* **1963**, 41(11), 2737-2742.

[9] Godsay, M.P., Harpell, G.A. and Russell, K.E., The effect of phenols on the polymerization of styrene. *Journal of Polymer Science* **1962**, 57(165), 641-650.

[10] Ballard, N., Hamzehlou, S., Ruipérez, F. and Asua, J.M., On the termination mechanism in the radical polymerization of acrylates. *Macromolecular Rapid Communications* **2016**, 37(16), 1364-1368.

[11] Sudduth, R.D., A generalized model to predict the viscosity of solutions with suspended particles. I. *Journal of Applied Polymer Science* **1993**, 48(1), 25-36.

[12] Sudduth, R.D., A new method to predict the maximum packing fraction and the viscosity of solutions with a size distribution of suspended particles. II. *Journal of Applied Polymer Science* **1993**, 48(1), 37-55.

[13] Sudduth, R.D., A generalized model to predict the viscosity of solutions with suspended particles. III. Effects of particle interaction and particle size distribution. *Journal of Applied Polymer Science* **1993**, 50(1), 123-147.

[14] de FA Mariz, I., Leiza, J.R. and José, C., Competitive particle growth: A tool to control the particle size distribution for the synthesis of high solids content low viscosity latexes. *Chemical Engineering Journal* **2011**, 168(2), 938-946.

[15] Arevalillo, A., do Amaral, M. and Asua, J.M., Rheology of concentrated polymeric dispersions. *Industrial & Engineering Chemistry Research* **2006**, 45(9), 3280-3286.

[16] Guyot, A., Chu, F., Schneider, M., Graillat, C. and McKenna, T.F., High solid content latexes. *Progress in Polymer Science* **2002**, 27(8), 1573-1615.

## Chapter 4

[17] Schneider, M., Claverie, J., Graillat, C. and McKenna, T.F., High solids content emulsions. I. A study of the influence of the particle size distribution and polymer concentration on viscosity. *Journal of Applied Polymer Science* **2002**, 84(10), 1878-1896.

[18] Palmer Jr, C.F., Lester, A.H.I. and Wicker Jr, C.M., Ethox Chemicals, Llc, Additives to improve open-time and freeze-thaw characteristics of water-based paints and coatings, **2016**, U.S. Patent 9,309,376.

[19] Zong, Z., Li, Y.Z. and Ruiz, J., Rhodia Operations, Latex binders, aqueous coatings and paints having freeze-thaw stability and methods for using same, **2013**, U.S. Patent 8,580,883.

[20] King, A.P. and Naidus, H., The relationship between emulsion freeze-thaw stability and polymer glass transition temperature. I. A study of the polymers and copolymers of methyl methacrylate and ethyl acrylate. *Journal of Polymer Science Part C: Polymer Symposia* **1969**, 27(1), 311-319.

[21] Fernández-Barbero, A. and Vincent, B., Charge heteroaggregation between hard and soft particles. *Physical Review E* **2000**, 63(1), 0115091-7.

## **Chapter 5. Effect of sodium styrene sulfonate concentration on latex and film properties**

### **5.1. Introduction**

Literature review (Chapter 1) demonstrated that the concentration of NaSS in the formulation determines the number of particles created in the initial stage of the reaction, the ionic strength of the dispersion and the colloidal stability. As a result, the final particle size and particle size distribution, the reaction kinetics and the polymer properties highly depend on NaSS concentration.<sup>1-6</sup>

Although the effect of NaSS concentration on the reaction kinetics and polymer properties has been studied at low solids contents (10 - 25 wt%),<sup>1-6</sup> there are no data for high solids content emulsifier-free emulsion polymerization. As at high solids contents, the concentration of particles in dispersion will be much higher, it is extremely important to determine the behavior of such systems at different NaSS contents.

Therefore, in this chapter, the effect of NaSS concentration on reaction kinetics, NaSS conversion and incorporation in the polymer particles, particle size distribution, molecular weight, coagulum, surface tension, salt stability and freeze-thaw stability

## Chapter 5

were investigated. The effect of NaSS content on film properties such as water contact angle, water sensitivity, gloss, morphology and mechanical and thermal properties was also studied. All latex and film properties were compared with those of the control latex produced by using a conventional emulsifier (sodium dodecyl sulfate, SDS).

### **5.2. Experimental**

#### **5.2.1. Materials**

The materials are given in Appendix II.

#### **5.2.2. Polymerizations**

A 10 wt% solids content seed of composition MMA/BA/NaSS (50/50/2) was synthesized as detailed in Appendix III. The properties are given in Table 5.1. A NaSS-free control seed was synthesized using 1.3 wbm% SDS (Z-ave particle size: 117 nm).

Chapter 5

**Table 5.1.** Characteristics of the seed

Particle size (Z-ave, nm)	Coag. (%)	Insoluble polymer (gel) wt%	M <sub>n</sub> (g/mol)	M <sub>w</sub> (g/mol)	Đ
115	0.3	54	169,500	362,300	2.1

For seeded semicontinuous reactions, the set up presented in Chapter 4 was utilized. A typical coating formulation, MMA/BA (1/1 by weight) was used. The concentration of NaSS was varied from 0.175 to 3.6 weight based on monomer (wbm%) and the target solids content was 50 wt%. An initiator concentration of 0.54 wbm% and a feeding time of 3.5 hours were utilized in all the reactions. A representative recipe using 1.3 wbm% NaSS is given in Table 5.2.

**Table 5.2.** Basic recipe for the seeded semicontinuous reactions (50 wt% solids content)

	Initial charge	Feed 1	Feed 2 <sup>a</sup>	Feed 3
Seed (g)	225	-	-	-
MMA (g)	-	129.2	-	-
BA (g)	-	129.2	-	-
NaSS <sup>b</sup> (g)	-	-	3.21	-
AsAc (g)	-	-	0.69	-
TBHP (g)	-	-	-	0.7
H <sub>2</sub> O (g)	-	-	54.5	29.3

<sup>a</sup> For the latex 0.76% NaSS + NaCl, 0.4325 g NaCl was added within feed2

<sup>b</sup> 3.176 g SDS in the control latex

## Chapter 5

For the latex synthesized by using 0.175 wbm% NaSS, the only NaSS present was that of the seed, namely no NaSS was fed in the semicontinuous part. A reaction by using 0.76 wbm% NaSS and the amount of NaCl needed to have the same ionic strength as the latex with 1.3 wbm% NaSS (abbreviated as 0.76% NaSS + NaCl) was also performed. In the synthesis, NaCl was added into the reactor within Feed 2. The control latex stabilized with SDS was also synthesized by seeded semicontinuous polymerization using the seed prepared with SDS.

Post-polymerizations were performed to convert the residual NaSS. A water soluble redox initiator AsAc/H<sub>2</sub>O<sub>2</sub> was utilized at 70°C. The molar ratio used was 1/1/3 (unreacted NaSS/AsAc/H<sub>2</sub>O<sub>2</sub>). The aqueous solution of H<sub>2</sub>O<sub>2</sub> was added as a shot onto the latex in the reactor. After 45-60 seconds, the feeding of AsAc solution started and completed in 15 minutes. After 60 minutes, the conversion of NaSS was confirmed by the disappearance of the vinyl peaks in <sup>1</sup>H-NMR spectra.

### 5.2.3. Characterizations

The characterization methods are given in Appendix II.

### 5.3. Results and Discussion

#### 5.3.1. Latex properties

NaSS concentration used in the seeded semicontinuous reactions was varied from 0.175 to 3.6 wbm%. When the concentration of NaSS was  $\leq 0.25$  wbm%, a large amount of macroscopic coagulum was observed, and these reactions had to be stopped before completing the feedings. Thus, the concentration of 0.5 wbm% NaSS seems to be the minimum necessary to obtain stable latexes during synthesis.

Full gravimetric conversion of the main monomers was achieved for all the concentrations of NaSS  $\geq 0.5$  wbm% and no significant effect on the reaction kinetics in this NaSS concentration range was observed (Figure 5.1), likely because the reactions were performed under monomer starved conditions (Figure 5.2).

Figure 5.3 shows that the evolution of number of particles ( $N_p$ , calculated from DLS measurements) displayed a decreasing trend during the feeding process demonstrating some limited particle coagulation. No macroscopic coagulum was observed in these reactions. In general, ( $N_p$ ) increased with the NaSS concentration up to 1.3% NaSS. For 3.6% NaSS,  $N_p$  was lower probably due to the higher ionic strength.

Chapter 5

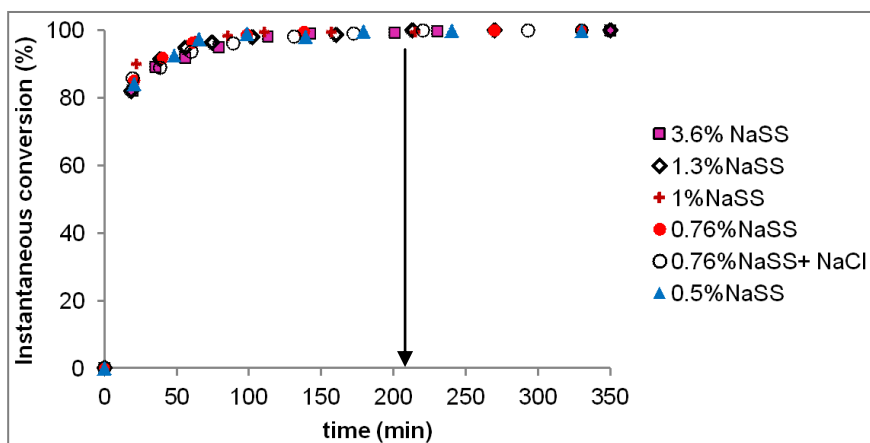


Figure 5.1. Time evolution of monomer conversion for seeded semicontinuous reactions by using different NaSS concentrations. The arrow indicates the end of feedings.

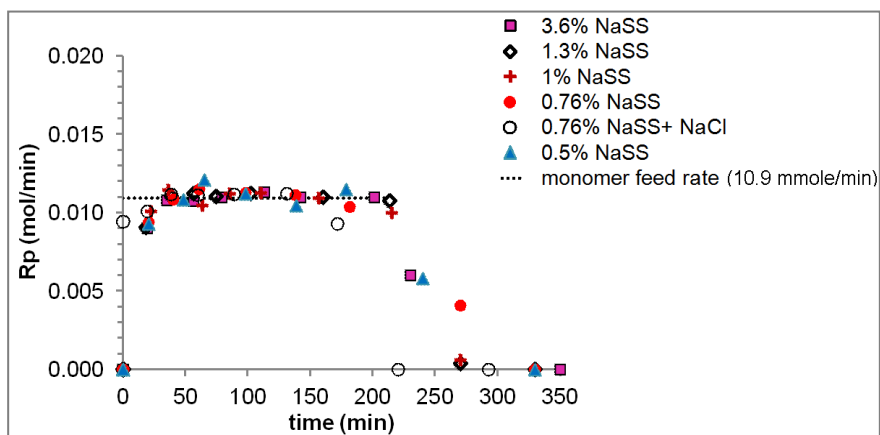


Figure 5.2. Rate of polymerization as a function of time for seeded semicontinuous reactions by using different NaSS concentrations.

## Chapter 5

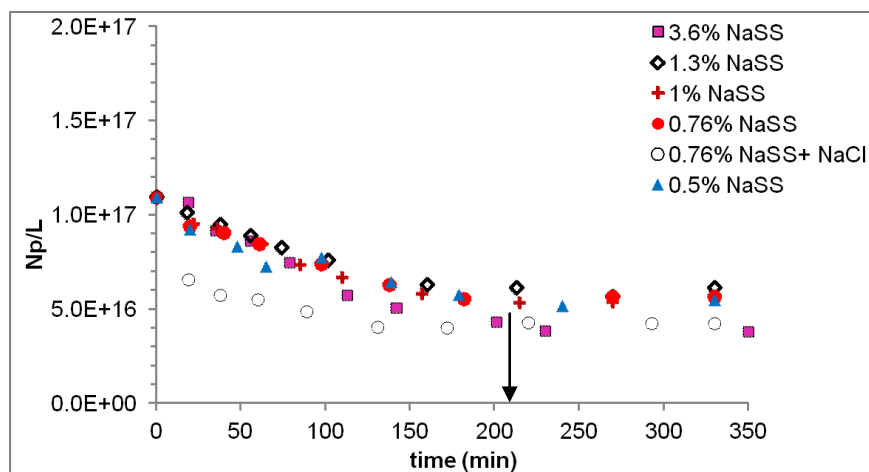


Figure 5.3. Number of particles (calculated from DLS measurements) as a function of time for seeded semicontinuous reactions by using different NaSS concentrations. The arrow indicates the end of feedings.

The analysis of the effect of the NaSS concentration on particle nucleation is complicated by the fact that NaSS affects both the concentration of in-situ surfactant formed and the ionic strength of the medium. In order to decouple these effects, in reaction 0.76% NaSS + NaCl, NaCl was added to achieve same ionic strength as the latex with 1.3% NaSS, which allowed to isolate the effect of NaSS concentration. A significant decrease in  $N_p$  was observed, especially in the first stages of the process due to the high ionic strength that shields the ionic groups on the particle surface decreasing the electrostatic repulsion between the particles and therefore particle stability. The final  $N_p$  in the reaction with NaCl is similar to that of 3.6 wbm% of NaSS,

## Chapter 5

indicating similar behavior induced by the presence of free electrolytes in the dispersions.

The particle size distributions are shown in Figure 5.4. All of the latexes present monomodal particle size distributions except 3.6% NaSS. In this reaction, a population of larger particles was observed. A monomodal latex of  $d_p = 275$  nm was found for 0.76% NaSS+NaCl latex. Figure 5.3 and 5.4 highlight the importance of the technique used to determine the particle size (see ref 7 for a discussion on the topic). Dynamic light scattering gives a higher size for 3.6% because the large particles of the second mode scatter more light than the smaller ones and biased the result.

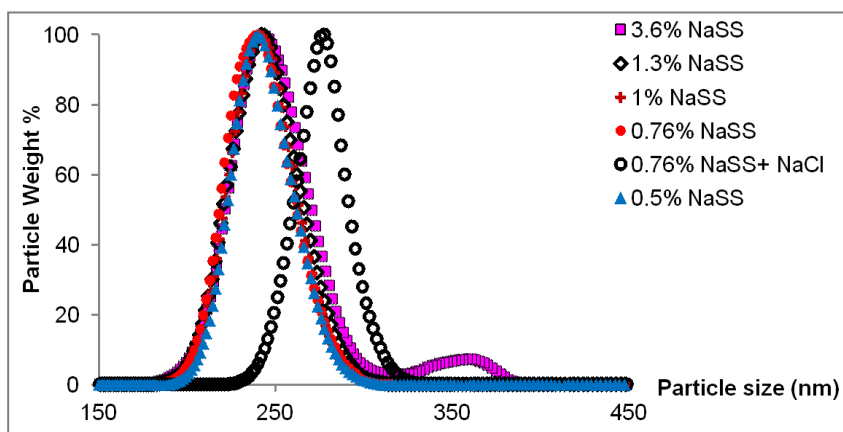


Figure 5.4. Particle size distribution (by CHDF) of the particles produced by using different NaSS concentrations

## Chapter 5

The characteristics of the latexes are displayed in Table 5.3. The conversion of NaSS decreased slightly, whereas its incorporation onto polymer particles increased significantly with NaSS concentration.

The surface tension values, which can be associated to the amount of free water soluble species in the aqueous phase, were more or less in line with NaSS incorporation. As the incorporation increased the drop in surface tension was noticed, so less free water soluble species were formed. The surface tension was the lowest for the control latex due to accumulation of free SDS in the latex-air interface. These results are surprising because increasing NaSS concentration is expected to yield a more hydrophilic polymer that tend to remain in the aqueous phase. Comparison between experiments carried out with 0.76%, 0.76% + NaCl and 1.3% of NaSS shed more light on this issue. It can be seen that for 0.76% the NaSS incorporation was only 63.3% whereas that of 1.3% was 72.5%, but when the ionic strength of the 0.76% latex was made similar to that of the 1.3% latex by adding NaCl, the incorporation of NaSS increased to 71.9%, namely to a value similar to that of the 1.3% latex. These results suggest that the higher incorporation observed for the latexes with higher NaSS concentration was due to the increasing ionic strength that shifted the adsorption equilibrium towards the polymer particles. This effect has been reported for a conventional anionic surfactant (SDS).<sup>8</sup>

The coagulum was the highest for the case of 3.6% NaSS due to high ionic strength of this system. The stability of the latexes during storage was very good.

## Chapter 5

After 2 years of storage, neither sedimentation nor change in particle size (measured by DLS) was observed.

The fraction of polymer insoluble in THF was generally high for all the latexes. As already explained in Chapter 3 and 4, a combination of factors could lead to such high gel contents. All reactions were carried out under monomer starved conditions increasing the possibility of chain transfer to polymer. Although no gel was reported for semicontinuous emulsion polymerization of MMA/BA =1/1 initiated with KPS,<sup>9</sup> the control latex was found to have an unexpectedly high gel (54.4 wt%). This indicates that the oxygen centered tert-butoxy radicals which are hydrophobic enough to enter directly into the particles, are efficient in abstracting hydrogen from the polymer backbone and therefore effective in the gel process. Moreover, the fact that gel content generally increased with the increase in NaSS concentration for NaSS containing latexes indicates that sulfonate groups of NaSS may induce ionic interactions between polymer chains and contribute to the decreased solubility in THF.

The sol molecular weights are presented in Table 5.3. The highest molecular weight was measured for 3.6% NaSS that has the highest gel fraction. This is surprising because in systems where gel is formed by intermolecular chain transfer to polymer followed by termination by combination, the sol MW decreases as the gel fraction increases due to the preferential incorporation of the longer polymer chains to the gel.<sup>9</sup> These results seem to support the hypothesis that the insolubility of the

Chapter 5

polymer was due to the high NaSS content, but this idea is in conflict with the high gel fraction measured for SDS.

**Table 5.3.** The characteristics of the latexes with different NaSS amounts

NaSS amount (wbm%)	NaSS conversion (%)	NaSS incorporation (%)	Surface tension (mN/m)	Size by CHDF (nm)	Coag. (%)	Gel content (wt%)	M <sub>w</sub>	Đ
3.6	95	84.7	51.8 ± 0.2	248.1 ± 30.7	1.8	56.5	332,000	4.7
1.3	95	72.5	54.8 ± 0.2	243.7 ± 19.2	0.7	50.8	251,800	4.5
1	93	64.7	58.1 ± 0.2	243.1 ± 18.3	1.2	51.6	260,400	3.6
0.76	94	63.3	60.7 ± 0.1	242.2 ± 18.4	0.8	49.5	253,700	3.6
0.76 <sup>a</sup>	99	71.9	58.1 ± 0.3	277.4 ± 15.4	1.4	46.9	261,200	3.9
0.5	98	64.4	63.3 ± 0.1	244.0 ± 17.4	0.7	47.6	262,600	3.7
0.25	-	-	65.7 ± 0.1 <sup>b</sup>	-	28	-	-	-
0.175	-	-	66.5 ± 0.1 <sup>c</sup>	-	30	-	-	-
0 <sup>d</sup>	-	-	40.9 ± 0.1	247.5 ± 16.0	0.5	54.4	256,100	4.8

a: NaCl was added to obtain the same ionic strength as 1.3% NaSS

b: measured at 46.4 wt% solids content

c: measured at 44.6 wt% solids content

d: NaSS-free control latex, 1.2 wbm% SDS was used.

The latexes were tested by determination of their sensitivity towards presence of salts by means of salt tolerance test and towards weather conditions changes by means of freeze-thaw cycling.

## Chapter 5

The results of the salt tolerance tests of the NaSS containing latexes and the control latex are presented in Table 5.4. It can be seen that salt stability increased with the NaSS concentration. For similar content of charges, NaSS containing latexes were more salt tolerant than the control latex prepared with SDS. The reason lies in the fact that the adsorption-desorption equilibrium of SDS was shifted towards the aqueous phase,<sup>10,11</sup> whereas most of the NaSS units are strongly bonded to the polymer particles. On the other hand, the latex with 0.76% NaSS + NaCl was less stable than the latex with 1.3% (with the same ionic strength) and less stable than the latex with 0.76 % NaSS (with the same NaSS content), probably due to the already existing salt in the system.

**Table 5.4.** Salt tolerances of the latexes produced by using different NaSS amounts (X means massive coagulation)

NaSS amount (%wbm)	mmole of sulfonate† groups / kg latex	0.02 M CaCl <sub>2</sub>	0.05 M CaCl <sub>2</sub>	0.5 M NaCl	0.75 M NaCl	1 M NaCl
3.6	86	ok	ok	ok	ok	ok
1.3	31	ok	X	ok	X	X
1	24	ok	X	ok	X	X
0.76	18	ok	X	ok	X	X
0.76 + NaCl	18	X	X	ok	X	X
0.5	12	ok	X	X	X	X
Control (SDS)	21*	%19 coag.	X	size inc 450nm	X	X

†in the recipe

\*Refers to sulfate groups (not sulfonate) in the control polymer

## Chapter 5

The results of the exposure of the latexes on the freeze-thaw cycles are presented in Table 5.5. The latexes with NaSS concentration higher than 1% withstood three freeze-thaw cycles. On the other hand, the control latex and the latexes with lower NaSS amounts failed in the first cycle. The latex with 0.76% NaSS + NaCl was also stable up to three cycles, likely due to the higher incorporated fraction of NaSS compared to the latex with 0.76% NaSS.

**Table 5.5.** Freeze thaw stability of the latexes produced by using different NaSS amounts (X means massive coagulation)

NaSS amount (%wbm)	1 <sup>st</sup> cycle	2 <sup>nd</sup> cycle	3 <sup>rd</sup> cycle
3.6	ok	ok	ok
1.3	ok	ok	ok
1	ok	ok	ok
0.76	X		
0.76 + NaCl	ok	ok	ok
0.5	X		
Control (SDS)	X		

### 5.3.2. Film Properties

Minimum film forming temperatures of all the latexes were determined to be very similar 17-18°C. The films were prepared at 23°C and 55% humidity.

**5.3.2.1. Water contact angle**

The surface of the polymer films were studied by measurements of water contact angle (CA) (Table 5.6), which can provide information about the surfactant migration to the film-air interface. The film with 3.6% NaSS was very hydrophilic and lost its integrity when rinsed with water. The films with NaSS content lower than 3.6% displayed very similar CAs, around 70°, and rinsing with water did not change these values, suggesting that there was no significant migration of free surfactant to the air-film interface because a high fraction of the in-situ formed emulsifier was chemically attached onto the particles. The CA of the control polymer (52°) increased significantly upon rinsing with water (68°), indicating that the SDS that migrated to the film-air interface was cleaned away.

**Table 5.6.** Contact Angles (CA) of the films

NaSS amount (% wbm)	CA before washing	CA after washing
3.6	32.5 ± 1.8	Integrity lost
1.3	68.4 ± 1.0	69.4 ± 0.4
1	71.1 ± 0.2	69.7 ± 0.3
0.76	69.5 ± 0.4	69.9 ± 0.2
0.76 + NaCl	69.3 ± 0.4	68.6 ± 0.6
0.5	69.8 ± 0.6	71.6 ± 1.0
Control	52.4 ± 4.8	68.3 ± 0.3

## Chapter 5

### 5.3.2.2. Gloss

The gloss can be additional indication for migration of surface active compounds to the film-air interface. The gloss of the films was first checked at 60° and the values higher than 70 gloss units revealed that the films were highly glossy, therefore the measurements were performed at 20° for differentiation. NaSS containing films displayed gloss values higher than the control film and the minimum difference with respect to the films cast from the NaSS latexes was 8 gloss units. Note that a trained observer can differentiate a gloss difference of minimum 5 gloss units by naked eye.<sup>12</sup>

These results confirm migration of free surfactant was minimum in NaSS containing films.

**Table 5.7.** Gloss of the films at 20°

NaSS amount (% wbm)	Gloss (gloss unit)
3.6	66.4 ± 0.5
1.3	64.3 ± 1.2
1	69.1 ± 1.1
0.76	71.4 ± 0.6
0.76 + NaCl	66.0 ± 1.4
0.5	66.1 ± 1.8
Control	56.3 ± 1.0

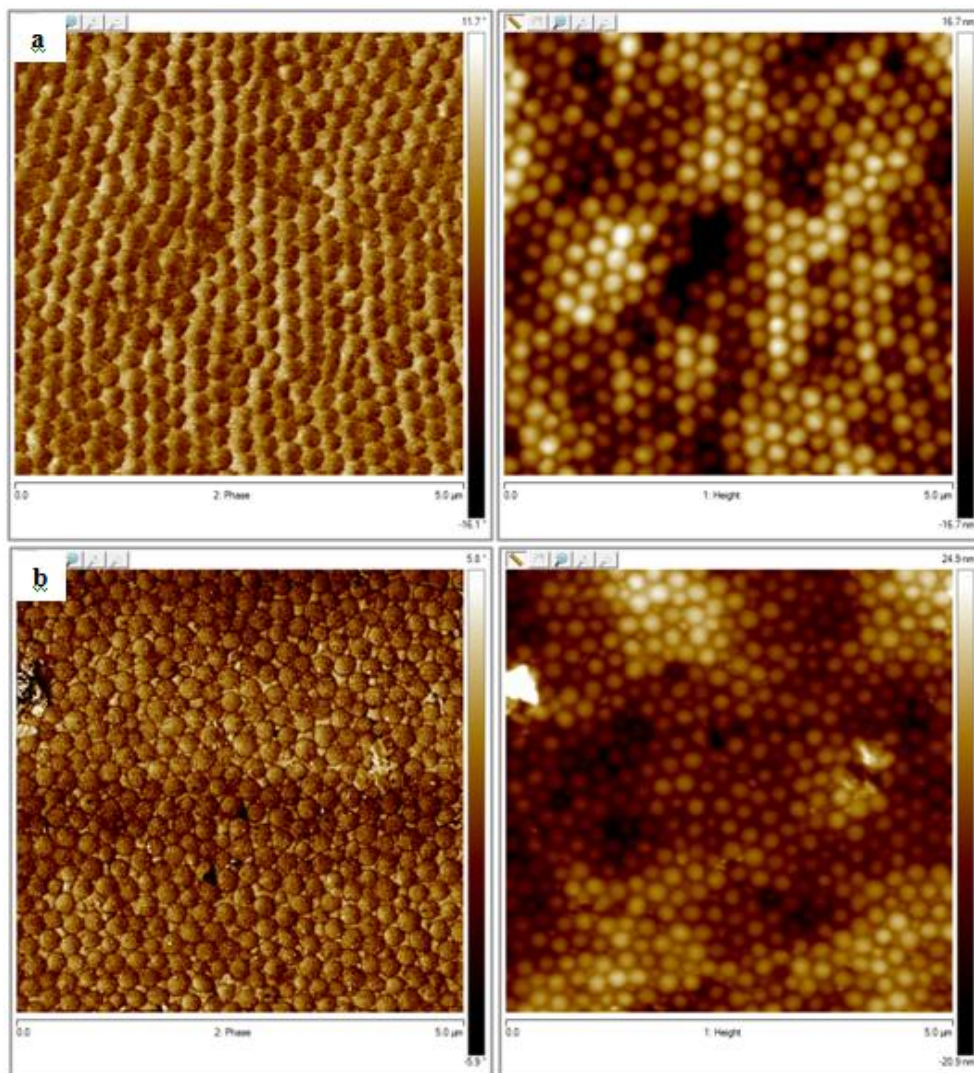
## Chapter 5

### 5.3.2.3. Film morphology

The morphology of the latex films was studied by AFM. Transparent films were prepared at 23°C (drying temperature was higher than the  $T_g$  of the polymers (18-19°C)).

AFM height and phase images for the film-air interfaces of the polymers with 1.3% NaSS and 0.76% NaSS, and the control polymer are presented in Figure 5.6. It can be observed the presence of slightly deformed particles in all films, but the borders of the particles are clearly seen. It can be seen that whereas the films cast with NaSS latexes almost did not present signals of migrated polymer, the control film was covered with an SDS layer (corresponds to areas in white color in the phase image). To check this, the films with 1.3% NaSS and control were immersed in deionized water for 24 hours, then dried and reanalyzed. The images are presented in Figure 5.7. Better contrast in the final image of the control polymer film (Figure 5.7b) showed that the water soluble SDS layer was washed away from the surface. In addition, rinsing with water led to more deformation of the particles with 1.3% NaSS (Figure 5.7a) probably because water acted as a plasticizer.

Chapter 5



Chapter 5

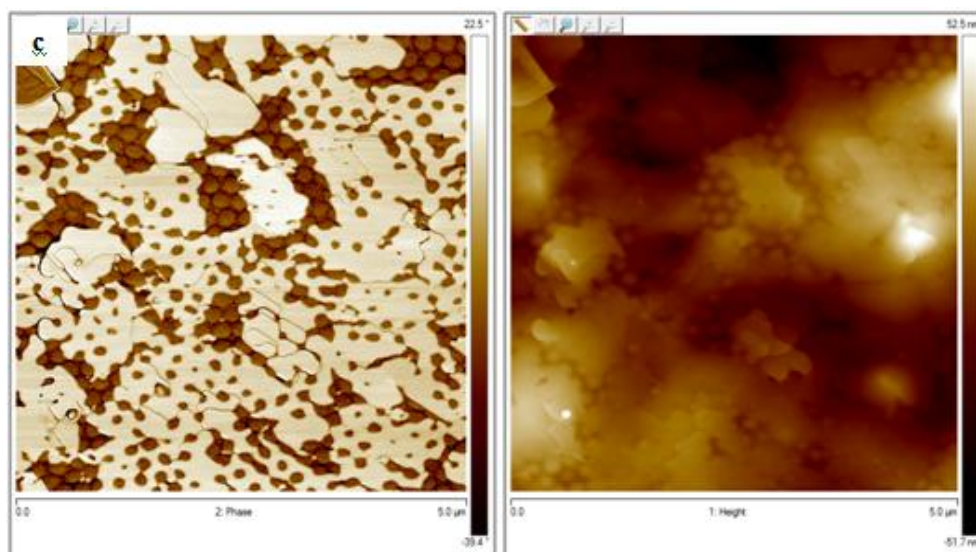


Figure 5.6. AFM phase and height images of film-air interfaces of polymers with a) 1.3% NaSS, b) 0.76% NaSS, c) SDS (control) (Scale: 5x5  $\mu\text{m}$ )

Chapter 5

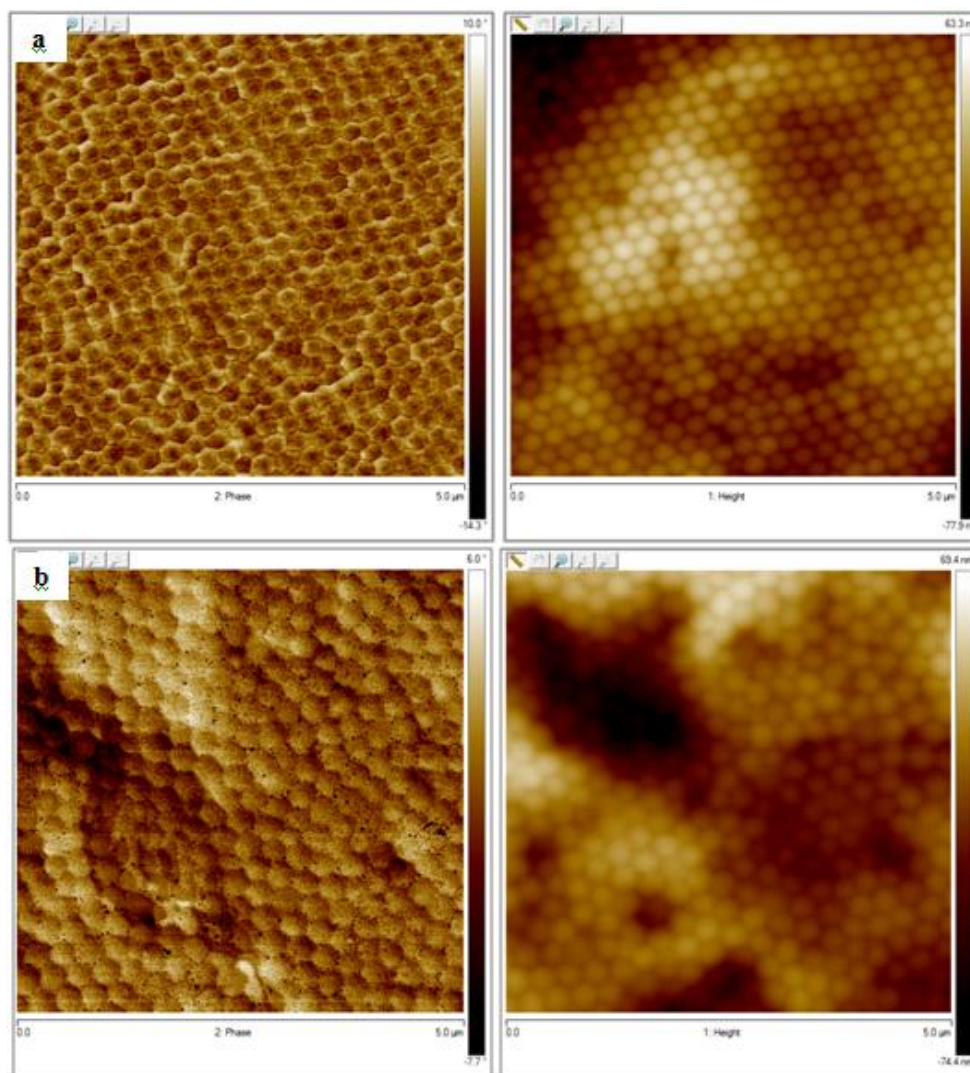


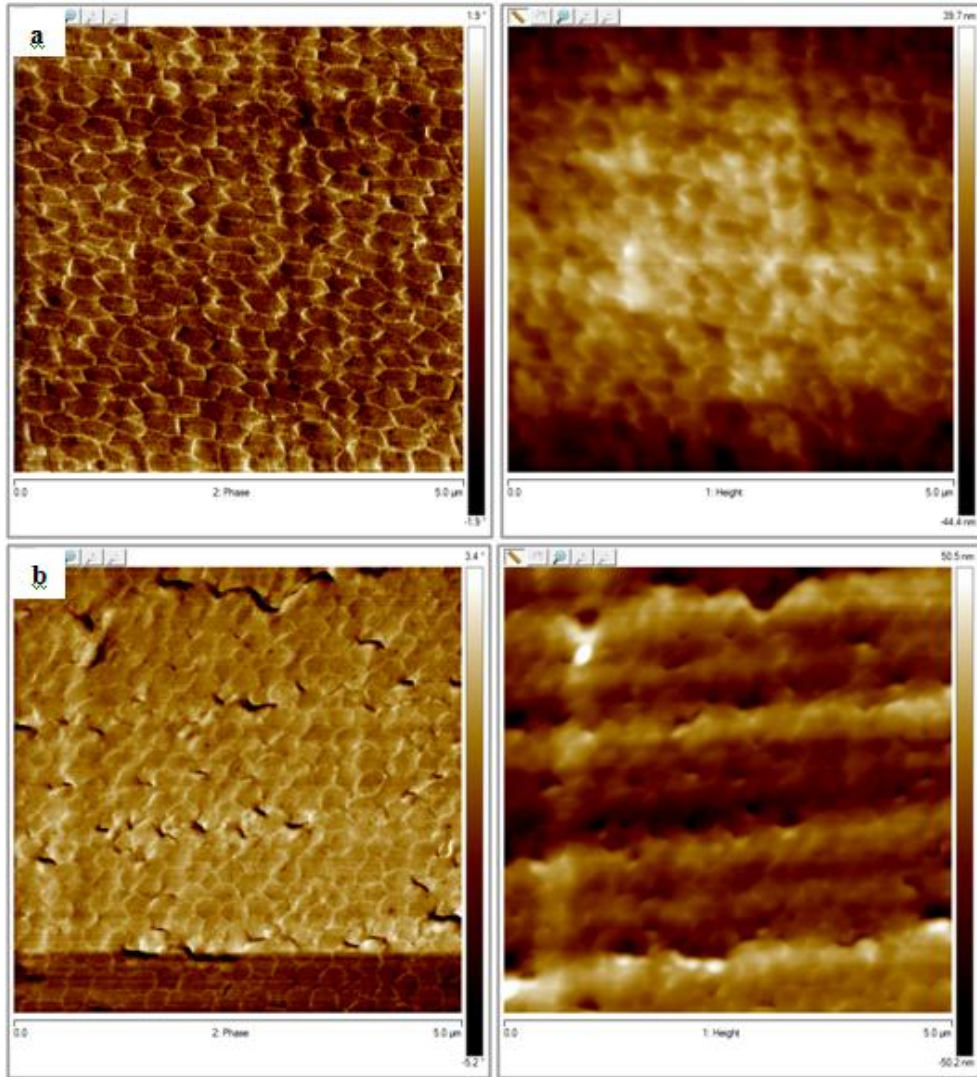
Figure 5.7. 5x5  $\mu\text{m}$  AFM phase and height images of film-air interfaces of polymers with a) 1.3% NaSS, and b) SDS (control) after washing with water (Scale: 5x5  $\mu\text{m}$ )

## Chapter 5

AFM images for the cross-section of the polymer films with 1.3% NaSS, 0.76% NaSS and SDS are presented in Figure 5.8. A honeycomb structure of deformed particles was evident for the NaSS films. Particle interpenetration was hindered by the hard white colored boundaries of the particles in phase contrast image. Likely this phase is NaSS rich polymer that formed a shell around the MMA/BA copolymer core and acted as a barrier against particle coalescence. The retardation effect of ionic groups on polymer diffusion has been reported for carboxylic acids.<sup>13,14</sup> On the other hand, the particle boundaries in the cross-section of the control film (Figure 5.8c) were not apparent and the particles coalesced significantly when compared to NaSS containing films. The structures in the interparticle void space can be due to the water pockets and the regions shown in white color are likely SDS aggregates.

In an attempt to favor interpenetration of polymer chains, the films were annealed at 60°C. AFM height and phase images for the cross-sections of the annealed films are presented in Figure 5.9. The particle boundaries in the cross-sections of the films with 1.3% NaSS and 0.76% NaSS were considerably less evident compared to those seen in Figure 5.8.

Chapter 5



Chapter 5

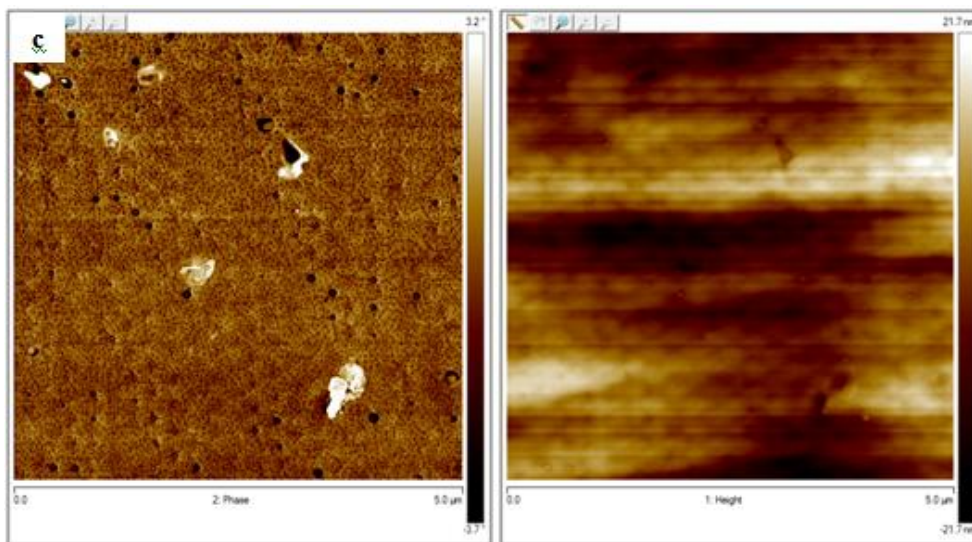
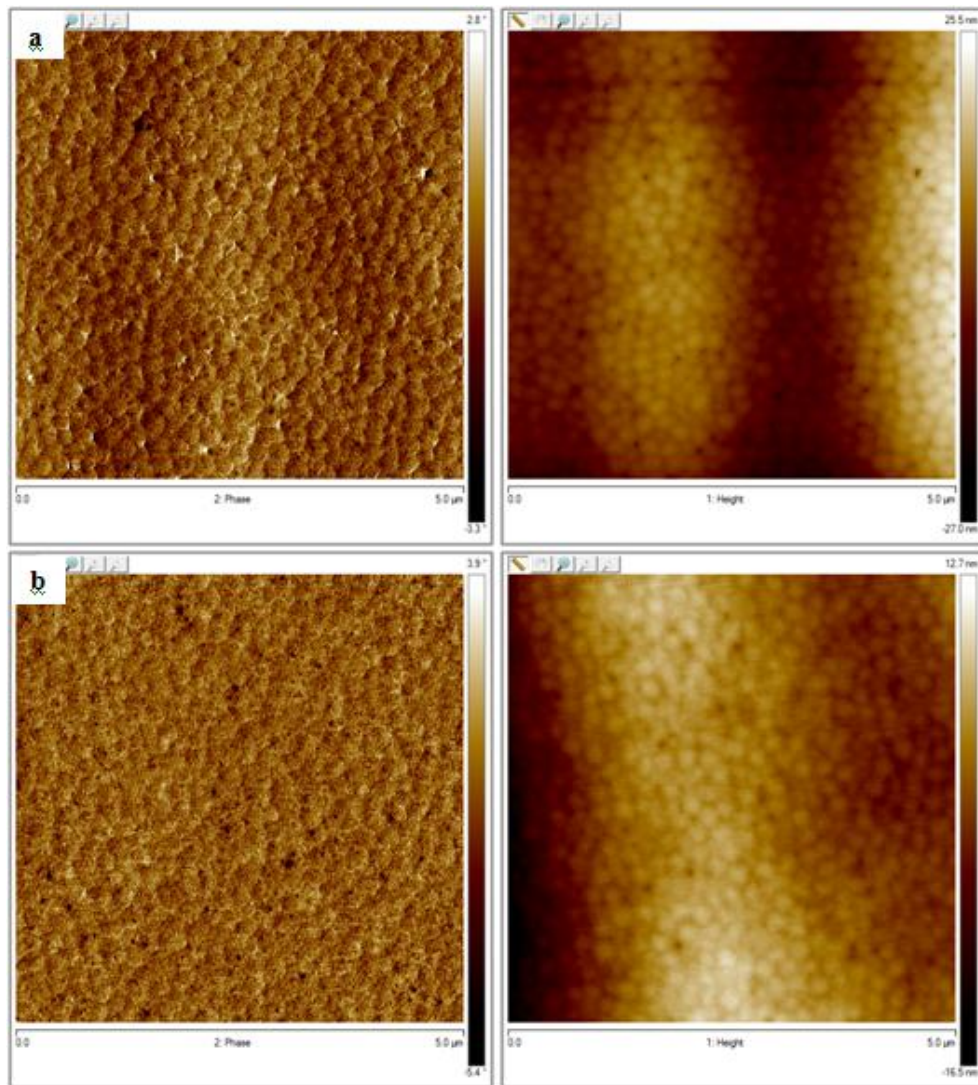


Figure 5.8. AFM phase and height images of film cross-section of polymers with a) 1.3% NaSS, b) 0.76% NaSS, c) SDS (control) (Scale: 5x5 μm)

Chapter 5



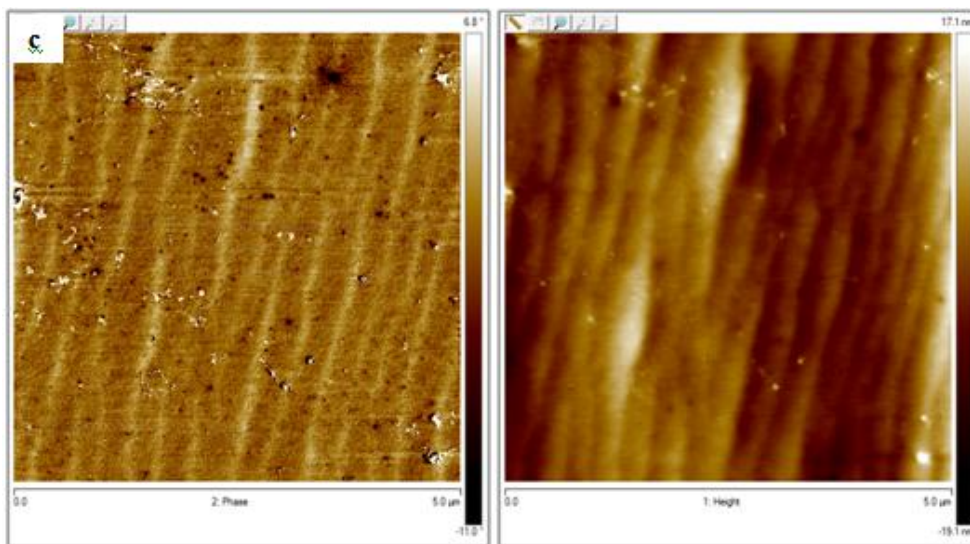


Figure 5.9. AFM phase and height images of film cross-section of the polymers annealed at 60°C, a) 1.3% NaSS, b) 0.76% NaSS, c) SDS (control) (Scale: 5x5 μm)

#### 5.3.2.4. Water sensitivity

The water uptake of the films prepared from the latexes with different NaSS amounts and the control film is given in Figure 5.10. The film with 3.6% NaSS that lost its integrity during the test is not included in the figure. The water uptake of the films increased with NaSS concentration because the ionic species increased the osmotic pressure which is the major driving force for water absorption.<sup>14</sup> Almost all of the films containing NaSS have similar profile of water uptake with tendency of saturation. The profile of 0.76%NaSS + NaCl is similar to that of the control film, showing continuous increase in the amount of absorbed water in the period

Chapter 5

investigated. This suggests that water diffused slowly to the hydrophilic regions created by SDS, but once they were reached, the aggregates absorbed large amounts of water. On the other hand, the NaSS formed a continuous percolating structure (see Figure 5.8 a and b) that might favor the relatively rapid penetration of water at the beginning. The weight loss after the tests was in line with the amount of free surfactant (Table 5.7).

Considering the total amount of charges, the control film corresponds between the films with 1% and 0.76% NaSS (see Table 5.4 for the amount of sulfate/sulfonate). Despite bearing less ionic groups than 1% NaSS, the control film displayed higher water uptake after 500 hours of immersion in water.

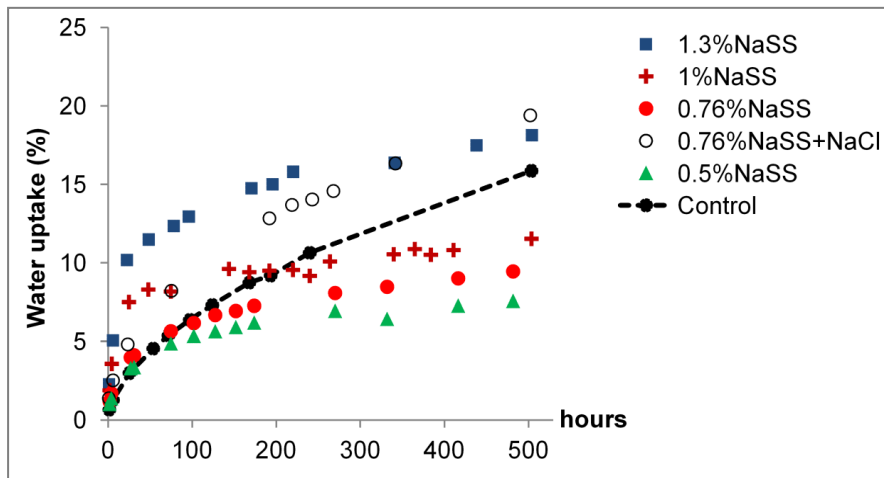


Figure 5.10. Water uptake behaviors of the polymer films with different NaSS amounts and SDS

**Table 5.7.** Weight loss after water uptake tests

NaSS amount (% wbm)	Weight loss (%)	Amount of free NaSS (% wt)
1.3	1.14 ± 0.15	0.358
1	0.80 ± 0.08	0.353
0.76	0.63 ± 0.02	0.279
0.76 + NaCl	0.61 ± 0.02	0.214
0.5	0.52 ± 0.03	0.178
Control	1.02 ± 0.13	-

#### 5.3.2.4. Moisture Permeability

The moisture permeability of the polymer films is presented on Table 5.8. As can be seen, the polymer films with NaSS < 1% have a low permeability that is similar to that of control film. However, a NaSS concentration of 1.3% increased more than fourfold the permeability.

For water to permeate through the polymer, three events need to take place: adsorption of moisture onto the polymer film, transport through the film and finally desorption (evaporation) to the atmosphere. The high permeability of the polymer with 1.3% NaSS can be explained by the presence of a continuous path for moisture penetration. It has a thicker percolating structure formed by NaSS-rich boundary layer between the particles (see Figure 5.8a). It has been known that chemically attached stabilizers such as surfmers adsorb in particle-particle boundaries and may form an ionic network for moisture penetration.<sup>14</sup> Better film formation and lack of a well-

## Chapter 5

connected hydrophilic network may slow down the process for the control film and the films with low concentrations of NaSS.

**Table 5.8.** Moisture permeability of the polymer films

NaSS amount (% wbm)	Moisture permeability (g.mm/m <sup>2</sup> .day)
1.3	59 ± 4
1	14 ± 2
0.76	11 ± 2
0.5	10 ± 0
Control	11 ± 0

### 5.3.2.5. Thermal properties

As measured by DSC, glass transition temperature of NaSS containing polymers is in the range 19-21°C and glass transition temperature of the control polymer is 18°C.

Thermal stabilities of some selected polymers were studied by thermo-gravimetric analysis (TGA) and no significant difference was observed between the films with different NaSS amounts and with the control film (Figure 5.10). They all show one-step degradation with onset temperatures of 345-350°C.

## Chapter 5

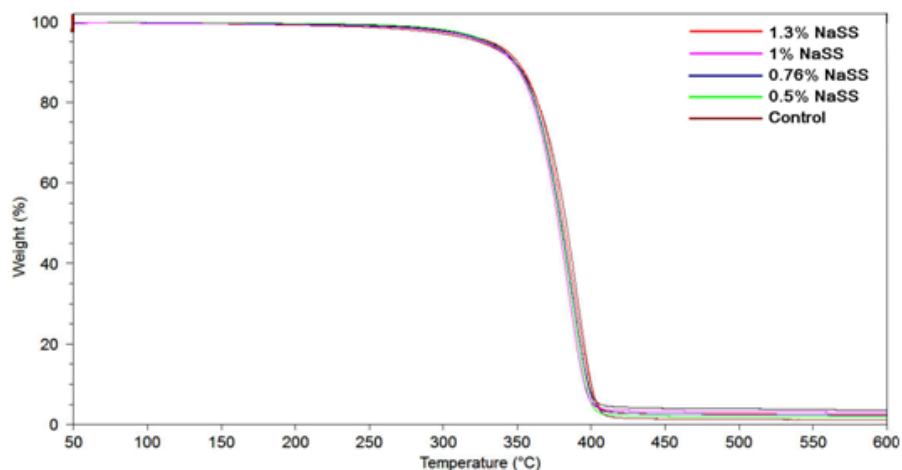


Figure 5.11. TGA plots of the polymer films

### 5.3.2.6. Tensile Properties

The stress-strain curves of the polymer films are displayed in Figure 5.12a. The ultimate tensile strength of the films containing NaSS were around 12-13 MPa, slightly higher than that of the control film. As the amount of NaSS in the film increased, the Young's modulus increased (Table 5.9) and the elongation at break decreased, namely the film becomes stiffer, likely due to the thicker percolating structure formed by the NaSS shell of the polymer particles. On the other hand, the control polymer displayed a slightly lower stress at break (~11 MPa) and much higher elongation. The yield stress increasing with the NaSS amount supports the reinforcing effect of NaSS.

Chapter 5

As the AFM images of the film cross-sections (Figure 5.8) show that no continuous film was formed from the NaSS containing latexes, in order to eliminate its effect to the mechanical properties, the films were annealed at 60°C for 3 days. The morphology of the annealed films is given in Figure 5.9. The annealing resulted in a significant improvement in the ultimate tensile strength and toughness (Table 5.9) for all the samples except for the control (Figure 5.12b). Possible explanation for this behavior is that particle coalescence and interdiffusion of the polymer chains throughout the film improved with annealing which led to a better integrity and hence better mechanical strength of the NaSS containing films. The control film as shown in Figure 5.8c showed continuous structure, thus, the annealing did not introduce a significant change in the morphology (Figure 5.9c), and hence in the tensile behavior.

**Table 5.9.** Young’s modulus and toughness of the films dried in ambient temperature before and after annealing at 60°C

NaSS amount (% wbm)	Dried at 23°C		Annealed at 60°C	
	Young’s modulus x 10 <sup>-2</sup> (MPa)	Toughness x 10 <sup>-6</sup> (J/m <sup>3</sup> )	Young’s modulus x 10 <sup>-2</sup> (MPa)	Toughness x 10 <sup>-6</sup> (J/m <sup>3</sup> )
3.6	0.70 ± 0.03	24.2	0.77 ± 0.07	42.7
1.3	0.47 ± 0.05	25.0	0.67 ± 0.07	37.6
1	0.50 ± 0.04	26.4	0.60 ± 0.06	36.7
0.76	0.38 ± 0.19	23.2	0.53 ± 0.08	38.5
0.76 + NaCl	0.38 ± 0.17	25.2	0.36 ± 0.08	25.4
0.5	0.38 ± 0.10	23.7	0.47 ± 0.01	35.1
Control	0.44 ± 0.11	32.0	0.43 ± 0.07	30.4

Chapter 5

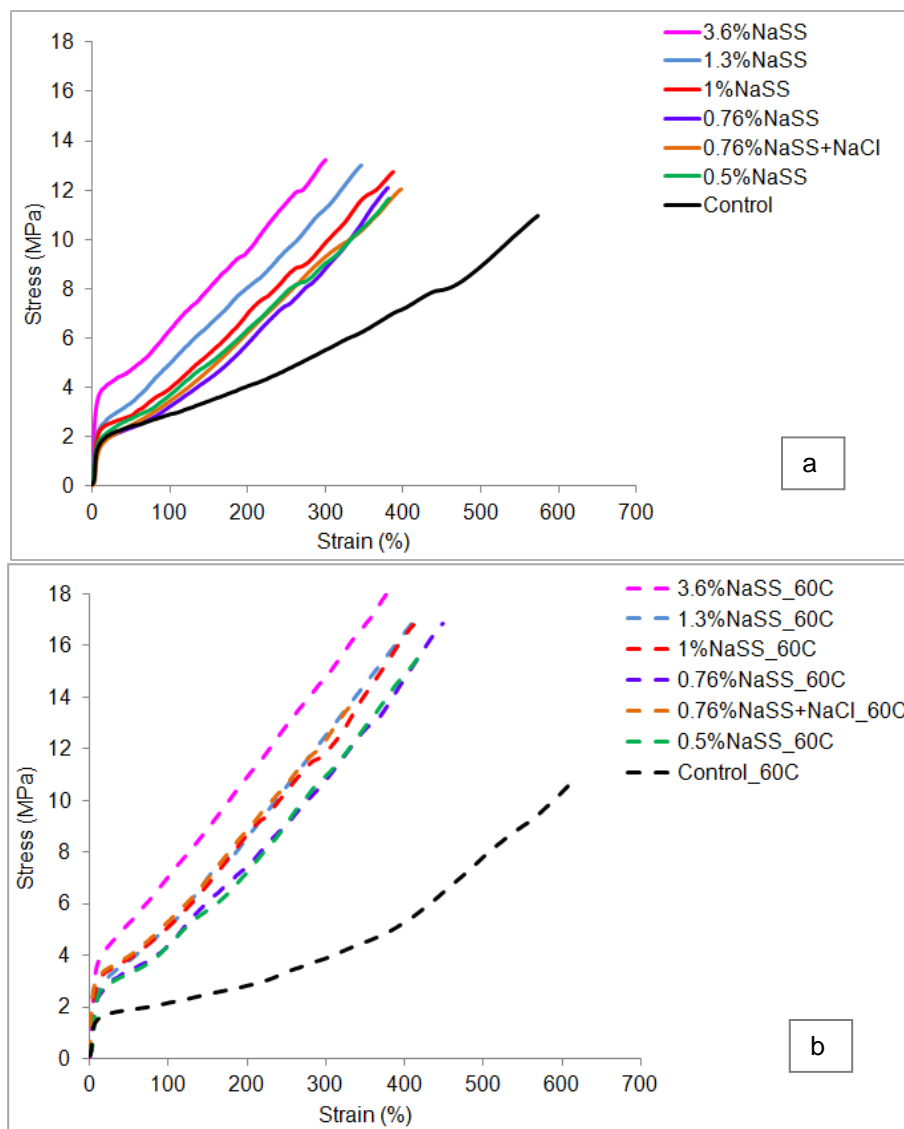


Figure 5.12. Stress-strain curves of the films with different NaSS amounts, a) dried in ambient temperature b) annealed at 60°C

#### 5.4. Conclusions

This chapter investigates the effect of NaSS concentration (0.175 – 3.6 wbm%) used in the high solids content emulsifier-free seeded semicontinuous emulsion polymerization of MMA/BA on the reaction kinetics, particle size and distribution, NaSS incorporation, stability of the latexes during synthesis and storage, and properties of the polymer films. With aim of comparison, a control latex stabilized with SDS was prepared under the same conditions.

Stable latexes were synthesized when NaSS concentration was  $\geq 0.5\%$ . No significant effect on kinetics was observed because the processes were carried out under monomer starved conditions. The number of particles ( $N_p$ ) increased with the NaSS concentration up to 1.3% NaSS. For 3.6% NaSS,  $N_p$  was lower because of the increase in ionic strength.

The extent of NaSS incorporation onto the polymer particles increased with the NaSS concentration, likely due to the increase of the ionic strength that caused a shift of the adsorption equilibrium of the NaSS containing oligoradicals towards the polymer particles.

NaSS containing latexes displayed excellent long-term storage, freeze-thaw and salt stability.

Water uptake of the polymer films increased with the NaSS concentration and, at long times, was smaller than that of the SDS film. The water contact angle of the films

## Chapter 5

containing up to 1.3% NaSS were found to be similar before and after rinsing with water, suggesting that there was no noticeable migration of in-situ formed surfactant in these films. This was confirmed by the improved gloss of the films containing NaSS when compared to control latex. AFM images showed that the film-air interfaces of NaSS containing films were cleaner than control film. The cross-section of the films observed with AFM showed that the polymer chains stabilized with NaSS maintained their identity, i.e. they did not interpenetrate and were separated by a hard honeycomb structure of NaSS rich polymer. Annealing of the films at 60°C resulted in a better film formation making particle boundaries less noticeable.

The films cast from NaSS containing latexes displayed higher tensile strength and lower elongation at break compared to the control film. As the amount of NaSS increased, the Young's modulus and the yield stress increased, and the elongation at break decreased likely due to the thicker percolating structure formed by the NaSS shell of the polymer particles. Annealing enhanced the ultimate tensile strength and toughness of the films due to better film formation and better integrity gained.

## Chapter 5

### 5.5. References

- [1] Juang, M.S.D. and Krieger, I.M., Emulsifier-free emulsion polymerization with ionic comonomer. *Journal of Polymer Science: Polymer Chemistry Edition* **1976**, *14*(9), 2089-2107.
- [2] Kim, J.H., Chainey, M., El-Aasser, M.S. and Vanderhoff, J.W., Preparation of highly sulfonated polystyrene model colloids. *Journal of Polymer Science Part A: Polymer Chemistry* **1989**, *27*(10), 3187-3199.
- [3] Kim, J.H., Chainey, M., El-Aasser, M.S. and Vanderhoff, J.W., Emulsifier-free emulsion copolymerization of styrene and sodium styrene sulfonate. *Journal of Polymer Science Part A: Polymer Chemistry* **1992**, *30*(2), 171-183.
- [4] Cheong, I.W. and Kim, J.H., Effects of surface charge density on emulsion kinetics and secondary particle formation in emulsifier-free seeded emulsion polymerization of methyl methacrylate. *Colloid and Polymer Science* **1997**, *275*(8), 736-743.
- [5] Wutzel, H. and Samhaber, W.M., Synthesis and characterization of sulphonated core-shell latices in the size range between 30 and 80nm. *Colloids and Surfaces A: Physicochemical and Engineering Aspects* **2008**, *319*(1), 84-89.
- [6] Farias-Cepeda, L., Herrera-Ordonez, J., Estevez, M., Luna-Barcenas, G. and Rosales-Marines, L., New Insights on surfactant-free styrene emulsion polymerization in the presence of sodium styrene sulfonate. *Colloid and Polymer Science* **2016**, *294*(10), 1571-1576.
- [7] Elizalde, O., Leal, G.P. and Leiza, J.R., Particle size distribution measurements of polymeric dispersions: a comparative study. *Particle and Particle Systems Characterization* **2000**, *17*(5-6), 236-243.

## Chapter 5

[8] Brown, W. and Zhao, J., Adsorption of sodium dodecyl sulfate on polystyrene latex particles using dynamic light scattering and zeta potential measurements. *Macromolecules* **1993**, 26(11), 2711-2715.

[9] González, I., Asua, J.M. and Leiza, J.R., The role of methyl methacrylate on branching and gel formation in the emulsion copolymerization of BA/MMA. *Polymer* **2007**, 48(9), 2542-2547.

[10] Ballard, N., Urrutia, J., Eizagirre, S., Schafer, T., Diaconu, G., de la Cal, J.C. and Asua, J.M., Surfactant kinetics and their importance in nucleation events in (mini) emulsion polymerization revealed by quartz crystal microbalance with dissipation monitoring. *Langmuir* **2014**, 30(30), 9053-9062.

[11] Meconi, G.M., Ballard, N., Asua, J.M. and Zangi, R., Adsorption and desorption behavior of ionic and nonionic surfactants on polymer surfaces. *Soft Matter* **2016**, 12(48), 9692-9704.

[12] BYK Gardner GmbH, Gloss Introduction, Retrieved from: <http://www.glossmeters.com/GlossIntro.html#2>

[13] Park, Y.J., Lee, D.Y. and Kim, J.H., Atomic force microscopy study of PBMA latex film formation: effects of carboxylated random copolymer. *Colloids and Surfaces A: Physicochemical and Engineering Aspects* **1998**, 139(1), 49-54.

[14] Keddie, J., Routh A.F. *Fundamentals of Latex Film Formation: Processes and Properties*. Springer: Dordrecht, 2010.

## **Chapter 6. Use of other sulfonate monomers in emulsifier-free emulsion polymerization**

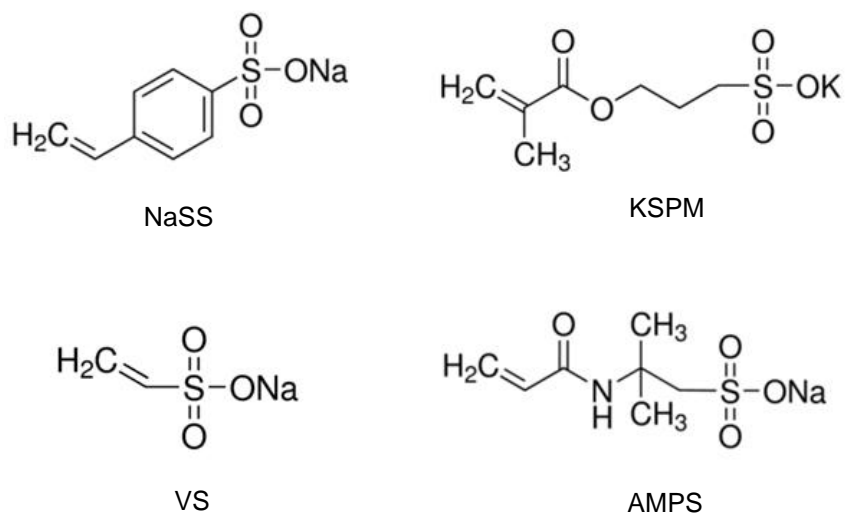
### **6.1. Introduction**

In the previous chapters, NaSS was used to synthesize emulsifier-free high solids content stable MMA/BA latexes. In this chapter, other sulfonate monomers were studied in order to compare their potential for stabilization of MMA/BA emulsifier-free latexes with that of NaSS. The studies were performed under conditions in which the reaction with NaSS resulted in high incorporations and low amount of coagulum.

Three different monomers were investigated: 3-sulfopropyl methacrylate potassium salt (KSPM), vinyl sulfonic acid sodium salt (VS) and 2-acrylamido-2-methylpropanesulfonic acid sodium salt (AMPS), bearing different reactive groups than NaSS (Scheme 6.1).

The same seed was utilized in all the seeded semicontinuous reactions to eliminate the effect of particle size (total surface area) and total number of particles on the incorporation of the sulfonate monomer.

## Chapter 6



Scheme 6.1. The chemical structures of the sulfonate monomers used

As it was shown in Chapter 1, various sulfonate monomers have been already used in emulsifier-free emulsion polymerization, however in these studies either the reactions were performed at low to moderate solids contents (up to 30 wt%)<sup>1-3</sup> or at higher solids contents (40-60 wt%) the incorporation of the sulfonate monomer onto polymer particles was not studied.<sup>4-7</sup>

## 6.2. Experimental

### 6.2.1. Materials

The materials are given in Appendix II.

## Chapter 6

### 6.2.2. Polymerizations

#### 6.2.2.1. Seed synthesis

The details of the seed synthesis are presented in the experimental section of Chapter 3 (Section 3.2.2.1).

#### 6.2.2.2. Seeded semicontinuous reactions

A 1 L reactor equipped with a stainless steel two-stage three-bladed Ekato MIG impeller, a reflux condenser, a N<sub>2</sub> inlet, a temperature probe, and three feeding inlets, was first charged with the seed and purged with N<sub>2</sub> for 20 minutes at 200 rpm. The feedings started when the temperature reached 70°C. One feed was composed of the comonomer mixture (MMA/BA or VAc/VeoVa10), the second feed was the aqueous solution of TBHP and the third feed was the aqueous solution of sulfonate monomer and AsAc. After the feedings (3.5 hours), the system was allowed to react batchwise for 2 hours. A representative recipe to synthesize the latexes is given in Table 6.1 for the reaction with NaSS in which MMA/BA (50/50) was used. The sulfonate monomer content was fixed at 14 mmole in the semicontinuous part for all the runs. This corresponds to 1.3 wbm% (weight based on monomer) for NaSS. Note that the concentration of NaSS in Chapter 5 was in the range 0.175 - 3.6 wbm% and the minimum concentration required for stable latex was determined as  $\geq 0.5$  wbm%. The target solids content was 50 wt%.

## Chapter 6

**Table 6.1.** Representative recipe for seeded semicontinuous reactions

	Initial charge	Feed 1	Feed 2	Feed 3
Seed (g)	225	-	-	-
MMA <sup>a</sup> (g)	-	129.2	-	-
BA <sup>a</sup> (g)	-	129.2	-	-
NaSS <sup>b</sup> (g)	-	-	3.21	-
AsAc (g)	-	-	0.69	-
TBHP (g)	-	-	-	0.7
H <sub>2</sub> O (g)	-	-	54.5	29.3

<sup>a</sup> For the reaction with VAc/ VeoVa10, 180.8 g VAc and 77.5 g VeoVa10 was used.

<sup>b</sup> For other sulfonate monomers; KSPM: 3.52 g, AMPS: 3.21 g (6.42 g from 50 wt% aq. solution), VS: 1.82 g (7.29 g from 25 wt% aq. solution) was used.

### 6.2.3. Characterizations

The characterization methods are given in Appendix II.

### 6.3. Results and Discussion

The characteristics of the seed are presented in Table 6.2. This seed was used in all of the seeded semicontinuous emulsion polymerizations.

## Chapter 6

**Table 6.2.** Characteristics of the seed

Particle size (Z-ave, nm)	Coag. (%)	Insoluble polymer (gel) wt%	M <sub>n</sub> (g/mol)	M <sub>w</sub> (g/mol)	Đ
115	0.3	54	169,500	362,300	2.1

The details of the seeded semicontinuous reactions by using different sulfonate monomers are presented in Table 6.3. The polymerization reactions of MMA/BA with either NaSS or KSPM yielded stable latexes with negligible amount of coagulum during the syntheses. However, 26.3 wt% coagulum was obtained in the reaction carried out with AMPS. It is worth pointing out that stable high solids content latexes (40-50 wt%) with less than 1 wt% coagulum were obtained using AMPS in the emulsion copolymerization of S and BA using KPS as initiator.<sup>4-5</sup> The difference with the current case may be in the contribution of the initiator sulfate groups to the stability. The worse performance of AMPS as compared with NaSS may be due to the higher hydrophilicity of AMPS that make more difficult the attachment of the oligoradicals to the polymer particles.

The reaction with VS had to be stopped after 135 min. of feeding due to a massive coagulation (87.2 wt%) that blocked the mechanical stirrer in the reactor. In order to check if this was due to the low reactivity of the vinyl functional group of the VS with MMA/BA, VAc/VeoVa10 that have a similar reactivity than VS was utilized. Although significantly less amount of coagulum was formed in this reaction (21.5 wt%), still it was too high and the process was stopped after 175 minutes of feeding. As in the

## Chapter 6

case of AMPS, the likely reason for this high amount of coagulum was the hydrophilicity of VS.

**Table 6.3.** Seeded semicontinuous reactions by using different sulfonate monomers

Sulfonate monomer	Monomer system (wt/wt)	Coagulation (wt%) and remarks
NaSS	MMA/BA (50/50)	0.7
KSPM	MMA/BA (50/50)	0.5
AMPS	MMA/BA (50/50)	26.3
VS	MMA/BA (50/50)	87.2, feed stopped at 135 min
	VAc/ VeoVa10 (70/30)	21.5, feed stopped at 175 min

The conversion of MMA/BA in the seeded semicontinuous reactions with NaSS and KSPM is displayed in Figure 6.1. Full conversion of MMA/BA was observed at the end of both reactions and there was no significant difference in the conversion profiles perhaps because the reactions were carried out under monomer starved conditions (Figure 6.2). The evolution of number of particles displayed almost the same profile in both reactions with a decrease during the feed period due to limited particle coagulation (Figure 6.3).

Chapter 6

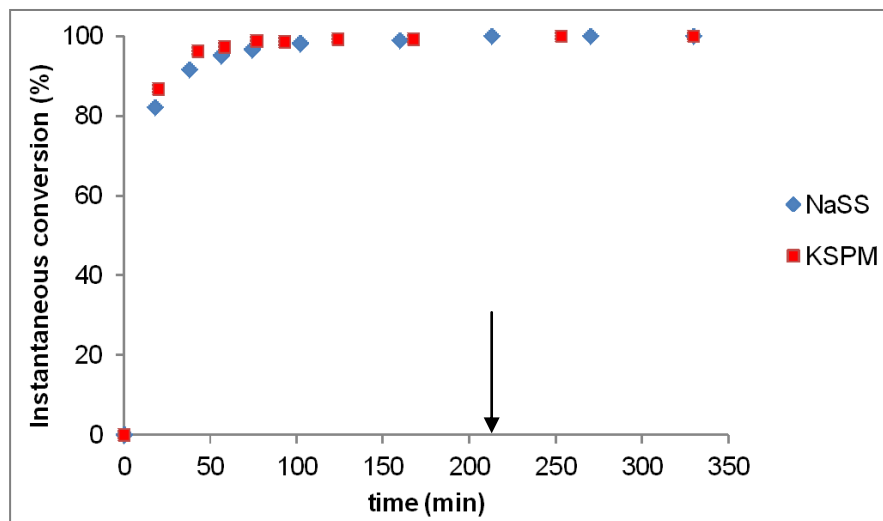


Figure 6.1. Evolution of the conversion of MMA/BA for seeded semicontinuous reactions with NaSS and KSPM. The arrow indicates the end of feedings.

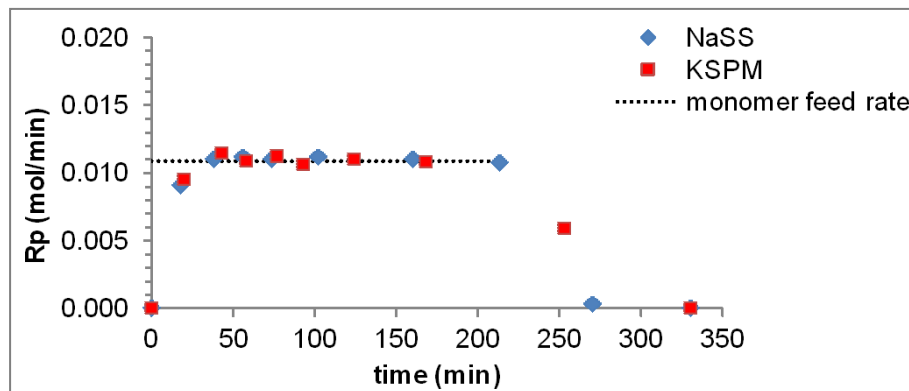


Figure 6.2. Rate of polymerization as a function of time for seeded semicontinuous reactions with NaSS and KSPM.

Chapter 6

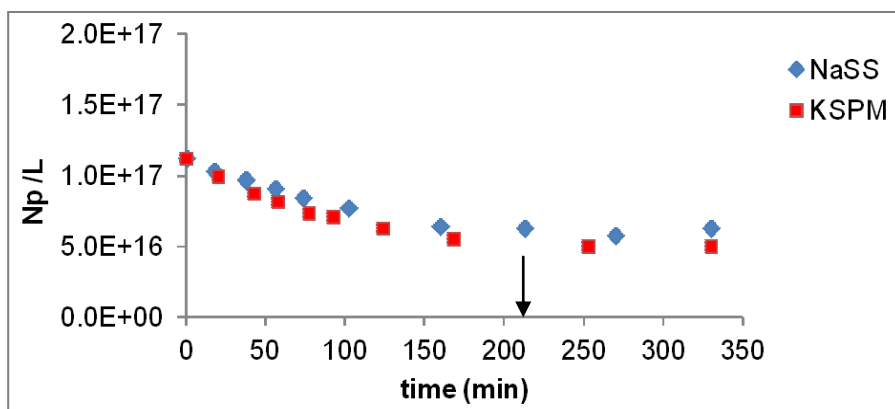


Figure 6.3. Number of particles as a function of time for seeded semicontinuous reactions with NaSS and KSPM. The arrow indicates the end of feedings.

The characteristics of the latexes prepared by using NaSS and KSPM are presented in Table 6.4. The final conversion of NaSS was 95% and that of KSPM was 91.4%. There was no significant difference in the incorporation of the sulfonate groups onto MMA/BA particles. The gel fractions and molecular weights of the polymers were similar for functional monomers.

## Chapter 6

**Table 6.4.** The characteristics of the latexes synthesized by using NaSS and KSPM

Sulfonate monomer	Sulfonate monomer amount (% wbm)	$d_{\text{particle}}$ (nm) CHDF	Sulfonate monomer conversion (%)	Incorporation of sulfonate groups (%)	Insoluble polymer (gel) (wt%)	$M_w$ (sol)	PDI
NaSS	1.3	243.7 ± 19.2	95.0	72.5	50.0	222,500	3.5
KSPM	1.4	234.1 ± 18.9	91.4	71.8	52.6	248,400	2.8

The latex with NaSS displayed better salt and freeze-thaw stability than KSPM (Table 6.5). Taking into account that both monomers led to a similar incorporation of sulfonate groups onto polymer particles, the differences in stability should be due to Hofmeister effects.<sup>8</sup> Although these effects have been known for more than a century, the molecular mechanisms governing them are not well understood. In any case, for the present discussion, it is enough to say that the type of monovalent cation has a strong influence on the destabilization of anionically stabilized latexes, and that  $K^+$  has a higher destabilization power than  $Na^+$ ,<sup>9</sup> which justifies the data in Table 6.5.

Chapter 6

**Table 6.5.** Freeze-thaw and salt stability of the latexes prepared by using different sulfonate monomers (X means massive coagulation)

Sulfonate monomer	Salt stability				Freeze-thaw stability		
	0.02 M CaCl <sub>2</sub>	0.05 M CaCl <sub>2</sub>	0.5 M NaCl	0.75 M NaCl	Cycle 1	Cycle 2	Cycle 3
NaSS	ok	X	ok	X	ok	ok	ok
KSPM	ok	X	size inc 330nm	X	X		

The surface properties of the films were also studied by water contact angle and gloss measurements (Table 6.6). The water contact angles of the both films have similar values, indicating that they have similar hydrophilic character. In addition, no variation of the contact angles after rinsing with water was observed, which indicates that no hydrophilic species migrated to the film surface. Moreover, there was no significant difference in the gloss of the film surfaces.

**Table 6.6.** Contact Angles (CA) and gloss of the film surfaces

Sulfonate monomer	CA (°) before washing	CA (°) after washing	Gloss* (gloss unit)
NaSS	68.4 ± 1.0	69.4 ± 0.4	64.3 ± 1.2
KSPM	68.9 ± 0.4	68.0 ± 0.7	59.8 ± 2.5

\*at 20° incident angle

## Chapter 6

Figure 6.4 presents the water uptake of polymer films upon immersion in water. The film containing KSPM has a slightly lower water uptake than that containing NaSS. The weight loss after the tests was also very similar. Considering the similar amount of incorporated ionic monomers onto the polymer particles and similar weight loss, it is difficult to explain this difference without further characterization of the films.

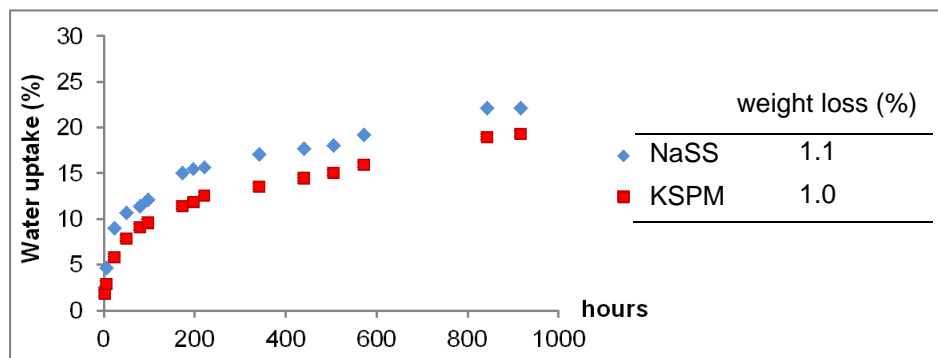


Figure 6.4. Water uptake behaviors of the polymer films

### 6.4. Conclusions

This chapter explores the possibility of using different functional monomers to in-situ generate surfactant moieties in high solids emulsifier-free semicontinuous emulsion polymerization. It was found that 3-sulfopropyl methacrylate potassium salt performed in a similar way than NaSS, but the salt and freeze-thaw stability was lower because of Hofmeister effects (higher destabilization power of  $K^+$  as compared

## Chapter 6

to Na<sup>+</sup>). 2-acrylamido-2-methylpropanesulfonic acid sodium salt and vinyl sulfonic acid sodium salt led to massive coagulation likely because they are too hydrophilic and the oligomers formed in the aqueous phase did not adsorb on the polymer particles.

## Chapter 6

### 6.5. References

- [1] Guillaume, J.L., Pichot, C. and Guillot, J., Emulsifier-free emulsion copolymerization of styrene and butyl acrylate. II. Kinetic studies in the presence of ionogenic comonomers. *Journal of Polymer Science Part A: Polymer Chemistry* **1988**, 26(7), 1937-1959.
- [2] Juang, M.S.D. and Krieger, I.M., Emulsifier-free emulsion polymerization with ionic comonomer. *Journal of Polymer Science: Polymer Chemistry Edition* **1976**, 14(9), 2089-2107.
- [3] Chang, H.S. and Chen, S.A., Kinetics and mechanism of emulsifier-free emulsion polymerization. II. Styrene/water soluble comonomer (sodium methallyl sulfonate) system. *Journal of Polymer Science Part A: Polymer Chemistry* **1988**, 26(4), 1207-1229.
- [4] Chang, W., Liu, L., Zhang, J., Pan, Q. and Pei, M., Preparation and characterization of styrene/butyl acrylate emulsifier-free latex with 2-acrylamido-2-methyl propane sulfonic acid as a reactive emulsifier. *Journal of Dispersion Science and Technology* **2009**, 30(5), 639-642.
- [5] Dai, M., Zhang, Y. and He, P., Preparation and characterization of stable and high solid content St/BA emulsifier-free latexes in the presence of AMPS. *Polymer Bulletin* **2011**, 67(1), 91-100.
- [6] Tang, G.L., Song, M.D., Hao, G.J., Guo, T.Y. and Zhang, B.H., Studies on the preparation of stable and high solid content emulsifier-free latexes and characterization of the obtained copolymers for MMA/BA system with the addition of AHPS. *Journal of Applied Polymer Science* **2001**, 79(1), 21-28.
- [7] Guo, T.Y., Tang, G.L., Hao, G.J., Song, M.D. and Zhang, B.H., Morphologies and dynamic mechanical properties of core-shell emulsifier-free latexes and their

## Chapter 6

copolymers for P (BA/MMA)/P (MMA/BA) and P (BA/MMA)/PSt systems in the presence of AHPS. *Journal of Applied Polymer Science* **2002**, 86(12), 3078-3084.

[8] Hofmeister, F., On the understanding of the effects of salts. *Archiv for Experimentelle Pathologie und Pharmakologie* **1888**, 24, 247-260.

[9] Oncsik, T., Trefalt, G., Borkovec, M. and Szilagyi, I., Specific ion effects on particle aggregation induced by monovalent salts within the Hofmeister series. *Langmuir* **2015**, 31(13), 3799-3807.

## **Chapter 7. Evaluation of emulsifier-free MMA/BA latexes as binders in paint applications**

### **7.1. Introduction**

The synthesis and characterization of emulsifier-free MMA/BA latexes have been explained in Chapter 5. In this chapter, the results obtained during three months internship in Synthomer, Malaysia are presented. There, emulsifier free MMA/BA/NaSS latexes were synthesized and incorporated in exterior paint formulation. The aim was to evaluate the performance of these latexes as binders in paints and investigate the influence of the presence of NaSS and its amount on the final properties. Considering the fact that pure acrylics are widely used in exterior paints, exterior application was selected for the synthesized NaSS containing latexes. The performances of the novel NaSS containing paints were compared with one reference and one control paint. The reference paint was prepared by using a binder provided by Synthomer and the control paint was prepared by using a binder based on a conventional emulsifier, namely sodium dodecyl sulfate (SDS).

## Chapter 7

### 7.1.1. Definitions

There are two important concepts regarding the quality of the paint: volume solid and pigment-volume concentration. They are given in percentages and it is not possible to estimate one from the other.

**Volume solid** is a measure of the volume of the dry film left after evaporation of water and volatile components from the paint. Since the contribution of the thickeners and nonvolatile additives are negligible, only the volumes of binder, pigment and fillers are counted. Volume solid is calculated by the formula:

$$\text{Volume Solid} = \frac{V_P + V_F + V_B}{V_{\text{wet paint}}} \times 100 \quad (7.1)$$

where  $V_P$ ,  $V_F$  and  $V_B$  refer to the volumes of the pigment (such as  $\text{TiO}_2$ ), filler (such as  $\text{CaCO}_3$ ) and binder, respectively.

The amount of pigment is expressed as the **pigment-volume concentration** (PVC) by the formula:

$$\text{PVC} = \frac{V_P + V_F}{V_P + V_F + V_B} \times 100 \quad (7.2)$$

PVC allows us to know the ratio of pigments to binders in a paint which determines many resultant characteristics. As PVC increases, typically gloss, durability, scrubability decreases whereas hiding power and density increases.

## Chapter 7

### **7.2. Experimental**

#### **7.2.1. Materials**

Technical grade methyl methacrylate (MMA, Evonik Germany), n-butyl acrylate (BA, BASF Petronas), tert-butyl hydroperoxide (TBHP, 70 wt% aqueous solution, Arkema), hydrogen peroxide (HPO, 30 wt% aqueous solution, May Chemical) and potassium persulfate (KPS, Evonik), sodium p-styrene sulfonate (NaSS, purity  $\geq 90\%$ , Sigma Aldrich), ascorbic acid (AsAc, reagent grade, Sigma Aldrich), sodium dodecyl sulfate (SDS, Sigma Aldrich) were used as received. In all reactions, distilled water was utilized.

For the paint formulation, thickener Natrosol 250 HBR (Ashland), dispersant Dispex N40 (BASF), wetting agent Hydropalat 1080 (BASF), antifoam Foamaster 111 (BASF), pH adjuster AMP95 (Dow Chemical), in-can preservative Acticide MV (Thor), co-solvent Propylene Glycol, pigment Tioxide TR 92 (Huntsman), filler calcium carbonate  $\text{CaCO}_3$  600 mesh, thickener Rheolate 644 (Elementis), coalescing solvent Optifilm Enhancer 300 (Eastman), dry film preservative Acticide EPW (Thor) was utilized.

#### **7.2.2. Polymerizations**

The abbreviation for emulsifier free latexes with different NaSS amounts is based on NaSS content. A control latex with sodium dodecyl sulfate was also produced and

## Chapter 7

named as SDS. The latex provided by Synthomer which is referred as Syn-A was selected based on the similarity of glass transition temperatures of the NaSS containing latexes and Syn-A. In order to make an adequate comparison with Syn-A, a reaction with a smaller final particle size was produced by using a charged initiator (KPS) in the seed synthesis. This latex is referred as Smallsize. Moreover, a reaction by using a hydrophilic redox initiator couple hydrogen peroxide/ascorbic acid was carried out and named as HPO. The details of the reactions are given below.

### **7.2.2.1. Reaction Set up**

A jacketed 1L reactor equipped with a stainless steel pitched blade impeller, a reflux condenser, a Nitrogen inlet and three feeding inlets, was used in semi-automated mode by controlling three pumps manually. Nitrogen was only utilized for ca. 20 minutes before the feedings to flush out oxygen and to form a blanket on top of the reaction mixture.

### **7.2.2.2. Seed Synthesis**

The recipe used to synthesize the seed is given in Table 7.1. The reactor was first charged with an aqueous solution of NaSS and MMA/BA mixture. The content was stirred at 200 rpm under N<sub>2</sub> for 20 minutes. As the temperature reached 70°C, the aqueous solutions of reductant and oxidant TBHP/AsAc (0.54% wbm / 0.53% wbm)

## Chapter 7

were fed separately at a rate of 0.615 g/min for 90 minutes. After that, the reaction mixture was allowed to react batchwise for 2 hours. A control seed was also synthesized by using 1.21 g SDS instead of NaSS by using the same recipe.

**Table 7.1.** The recipe for seed production (10wt% solids content, particle size: 120nm)

	Initial charge	Feed 2	Feed 3
MMA (g)	46.1	-	-
BA (g)	46.1	-	-
NaSS <sup>a</sup> (g)	1.84	-	-
AsAc (g)	-	0.49	-
TBHP (g)	-	-	0.50
H <sub>2</sub> O (g)	745.6	54.8	54.8

<sup>a</sup> 1.21 g SDS in control seed

Since the seed produced had a relatively large size (Z-ave: 120 nm), a smaller size seed was produced by using the recipe in Table 7.2. The reactor was charged with MMA, BA, NaSS and water. When the temperature reached to 70°C, an aqueous solution of potassium persulfate was added as a shot. The reaction mixture was allowed to react batchwise for 3.5 hours. The reason to utilize KPS was that KPS can yield smaller particle sizes due to contribution of the sulfate groups to colloidal stability. The size of this seed was 70 nm.

## Chapter 7

**Table 7.2.** The recipe for seed production using KPS (15wt% solids content, particle size: 70nm)

	Initial charge	Shot
MMA (g)	69	-
BA (g)	69	-
NaSS (g)	2.76	-
KPS (g)	-	1.104
H <sub>2</sub> O (g)	773.5	30.4

### 7.2.2.3. Seeded semicontinuous reactions

A representative recipe for typical seeded semicontinuous reaction is given for the latex with 1.3 wbm% NaSS in Table 7.3. The reactor was first charged with the seed and purged with N<sub>2</sub> for 20 minutes under 200 rpm agitation. The feedings started when the temperature reached 70°C. One feed composed of MMA/BA mixture, the second feed was the aqueous solution of TBHP and the third feed was NaSS/AsAc aqueous solution. After 3.5 hours of feeding, the system was allowed to react batchwise for 2 hours. The control latex was synthesized following a similar seeded semicontinuous polymerization recipe by using 5.56 g SDS instead of NaSS (1.23 wbm% SDS).

In the reaction where HPO/AsAc was used, the same seed was utilized. However, the semicontinuous step included HPO instead of TBHP as oxidant in the recipe (Table 7.4).

Chapter 7

**Table 7.3.** The recipe of seeded semicontinuous reaction with 1.3 wbm% NaSS by using TBHP/AsAc as initiator (50 wt% solids content, abbr. as 1.3%)

	Initial charge	Feed 1	Feed 2	Feed 3
Seed_120nm (g)	394	-	-	-
MMA (g)	-	226.15	-	-
BA (g)	-	226.15	-	-
NaSS <sup>a</sup> (g)	-	-	5.62	-
AsAc (g)	-	-	1.21	-
TBHP (g)	-	-	-	1.23
H <sub>2</sub> O (g)	-	-	95.43	51.3

<sup>a</sup> 5.56 g SDS in control latex

**Table 7.4.** The recipe of seeded semicontinuous reaction with 1.3 wbm% NaSS by using HPO/AsAc as initiator (50 wt% solids content, abbr. as HPO)

	Initial charge	Feed 1	Feed 2	Feed 3
Seed_120nm (g)	394	-	-	-
MMA (g)	-	226.15	-	-
BA (g)	-	226.15	-	-
NaSS <sup>a</sup> (g)	-	-	5.62	-
AsAc (g)	-	-	0.80	-
HPO (g)	-	-	-	0.46
H <sub>2</sub> O (g)	-	-	92.5	52.1

In the reaction where smaller particle size was targeted, the seed produced by using KPS at a solids content of 15 wt% was utilized (Table 7.2). The recipe in which

## Chapter 7

the target final solids contents was 45 wt% is displayed in Table 7.5. The total charge in the reaction was adjusted so that the total charge contribution of KPS and NaSS is equal to the charge of the latex with 1.3% NaSS (Table 7.3).

**Table 7.5.** The recipe of seeded semicontinuous reaction with 1.23 wbm% NaSS (45 wt% solids content, abbr. as Smallsize)

	Initial charge	Feed 1	Feed 2	Feed 3
Seed_70nm (g)	394	-	-	-
MMA (g)	-	206	-	-
BA (g)	-	206	-	-
NaSS <sup>a</sup> (g)	-	-	4.62	-
AsAc (g)	-	-	1.10	-
TBHP (g)	-	-	-	1.12
H <sub>2</sub> O (g)	-	-	124.6	125.1

### 7.2.2.4. Post-polymerizations

Post-polymerizations were performed to remove residual NaSS in the latexes, except for the control latex (SDS) and the latex with smaller particle size (Smallsize) since no NaSS was utilized in the former and the latter included a water soluble initiator (KPS). In the post-polymerization reactions, HPO/AsAc redox couple was used since they form noncharged hydrophilic radicals. The molar ratio used was 1/1/3 (NaSS/AsAc/H<sub>2</sub>O<sub>2</sub>). After the semicontinuous part (3.5 hours feeding + 2 hours batch), the aqueous solution of H<sub>2</sub>O<sub>2</sub> was added as one shot. After 45-60 seconds, the AsAc

## Chapter 7

solution (7.4% in water) was fed manually in 10 minutes. After 1 hour, the reaction temperature was decreased. The latexes were filtered by using a metal mesh of 120  $\mu\text{m}$  size.

### 7.2.3. Preparation of Paints

The waterborne paints were prepared by using an exterior formulation with 45% PVC (pigment-volume concentration). The recipe of the millbase is given in Table 7.6 together with the specific function of each constituent. Water (85% of the total amount), dispersant, wetting agent, antifoam, buffer, co-solvent and in-can preservative was weighed into a 10L cylindrical tank with a cooling jacket and stirred by using a high speed dispersant at 500 RPM for 20 minutes. Then titanium dioxide (pigment) and  $\text{CaCO}_3$  (filler) was added slowly and the stirring rate increased to 2000 RPM. After mixing for 20 minutes, thickener was added slowly and the rest of the water (15%). Whole dispersion was mixed for another 30 minutes to ensure homogeneity of the system. The final quality check was made by using a Hegman gauge to determine the fineness of the grind. The minimum requirement is to be below 40  $\mu\text{m}$ , which was the case for the prepared millbase.

## Chapter 7

**Table 7.6.** Millbase formulation

<b>Ingredient</b>	<b>Commercial name</b>	<b>Amount (g)</b>	<b>wt%</b>
Water		1496	29.41
Dispersant	Dispex N40	30.8	0.61
Wetting agent	Hydropalat 1080	17.6	0.35
Defoamer	Foamaster 111	17.6	0.35
pH modifier	AMP95	17.6	0.35
Cosolvent	Propylene Glycol	132	2.60
In-can preservative	Acticide MV	13.2	0.26
Pigment	Tioxide TR 92	1874.4	36.85
Filler	CaCO <sub>3</sub> 600 mesh	1460.8	28.72
Thickener	Natrosol 250 HBR	26.4	0.52

The next stage in paint preparation is letdown. This stage includes blending of the millbase with the binder (latex) and other ingredients as shown in Table 7.7 with the corresponding function and amounts in the formulations. Note that the amount of binder, coalescing solvent and water was different for the latexes Syn-A and Smallsize than the rest of the paint formulations.

Before blending of the millbase with the binder (latex), the pHs of the binders were adjusted to 9-9.5 by using pH modifier to prevent coagulation in further steps. Under continuous mixing of the millbase, the binder, coalescing solvent, dry film preservative, antifoam and 90% of the water was added, respectively. First pH was rechecked to ensure a pH of 9-9.5. Then viscosities of the paints were measured. In order to satisfy a viscosity of 89-99 kU (Krebs unit), thickener was added. When less

## Chapter 7

rheology/pH modifier than that in the recipe was used, the difference was compensated by adding water.

**Table 7.7.** Letdown stage

<b>Ingredient</b>	<b>Commercial name</b>	<b>Amount (g)</b>	<b>Amount (g) Smallsize</b>	<b>Amount (g) Syn-A</b>
Millbase		410		
Binder*		226	250.26	224.86
Coalescing solvent*	Optifilm Enhancer 300	2.84	2.84	5.67
Dry film preservative	Acticide EPW	10.64		
Antifoam	Foamaster 111	0.71		
pH modifier	AMP95	1.42		
Thickener	Rheolate 644	3.55		
Water*		54.19	29.93	52.49
Paint weight solid		54.0	54.0	54.2
Paint volume solids		35.4	35.4	35.5
Pigment volume content (PVC) %		45		

\* The amount of binder, coalescing solvent and water was varied for the latexes Syn-A and Smallsize.

Paint volume solids and PVC of the paints were held constant since the former determines the dry film thickness (in turn durability, permeability, etc.) and the latter

## Chapter 7

affects opacity (hiding power), durability, scrub resistance, gloss, etc.<sup>1</sup> Since the latexes Syn-A and Smallsize have different solids contents than the rest of the latexes, the amount of latex and water in the formulation was varied. In addition, the latexes have different MFFT's so the amount of coalescing solvent added to achieve the common industry standard of 5°C MFFT, was also different. For instance, while 2.5% (wb binder solid) was enough for NaSS containing latexes, 5% (wb binder solid) was utilized for Syn-A.

### **7.2.4. Characterization methods**

#### **7.2.4.1. Latex characterization methods**

##### **Particle size**

Z-average particle diameter was measured at 25°C by using dynamic light scattering (DLS) Malvern Zetasizer Nano ZS90 instrument. The latex sample was diluted with deionized water to prevent multiple scattering.

##### **Solids content (SC) by weight**

The solids contents of the latexes/paints were determined gravimetrically. The sample was weighed in an aluminum pan and put into oven at 140°C for 1 hour to dry. The ratio of weight of solid to that of wet latex/paint gave the SC.

## Chapter 7

### **Viscosity**

Brookfield Dial Reading LVT model viscometer was utilized to measure the viscosity of the as-produced latexes. The measurements were performed by using LV-1, LV-2 or LV-3 spindle at a speed of 60 RPM (or 30 RPM) at room temperature.

### **Specific gravity (SG)**

An aluminum specific gravity cup of 100 cc/mL capacity was used to calculate SG of the as-produced latexes/paints.

### **Minimum film forming temperature (MFFT)**

MFFT of the latexes were measured in MFFT-60 instrument (Rhopoint) at a temperature range of 5-23°C. Films with a thickness of 75  $\mu\text{m}$  and a width of 1.9 cm were cast on the MFFT bar.

### **Water blanching test**

Films of 150  $\mu\text{m}$  thicknesses were cast on glass substrates, dried at 50°C for 30 min, and then cooled down to 23°C in a temperature controlled room. The edges of the films were covered with the masking type and the substrates were immersed up to half of their height in a tap water tank at 23°C. The observations such as blistering, wrinkling and discoloration were recorded in certain time intervals (30 min, 1 h, 3 h, 4 h, 24 h).

## Chapter 7

### **Thermal analysis**

Glass transition temperatures ( $T_g$ ) of the polymers were measured in a TA instruments Q2000 differential scanning calorimeter (DSC). Samples in aluminum pans, were first heated to 100°C with a heating rate of 10°C/min then cooled down to -80°C with a cooling rate of 5°C/min and reheated to 100°C with a heating rate of 10°C/min. The second heating run was used to determine  $T_g$ .

### **Volatile organic compounds (VOCs)**

Agilent 7890B gas chromatography coupled with a 5977A mass-selective detector was utilized to quantify the amount of VOCs in the latexes, such as unreacted monomers (MMA, BA) and side products (tert-butanol, n-butanol, butyl acetate).

#### **7.2.4.2. Paint characterization methods**

Before any measurement, coating and characterization, the paints were slightly mixed with a spatula to obtain a smooth and homogeneous mixture.

#### **Krebs unit (kU) viscosity by Stormer-type viscometer**

Sheen 480 Krebs viscometer was used to measure the Stormer viscosity (consistency) of the paints. It resembles to pouring the paint.

## Chapter 7

### **Cone & plate viscosity**

ICI type cone & plate analogue viscometer was used to measure viscosity of the paints under high shear ( $12,000 \text{ sec}^{-1}$ ) to mimic the shear conditions applied during brushing, rolling or spraying

### **Storage stability**

This test is an accelerated test for the storage stability of the paints. In addition, it gives an idea about the resistance of the paint to high temperatures encountered during transport and storage especially in hot climates.

300 g of paints were taken into containers and put into oven at  $50^{\circ}\text{C}$ . The changes in the appearance and condition of the paints (such as yellowing, phase separation, coagulation, and odor) were checked at certain intervals (2 weeks, 1 month, etc). pH, Stormer viscosity, yellowing index and gloss of the paints were also measured and compared with the initial values.

### **Efflorescence resistance**

Water soluble compounds in the highly alkaline masonry substrate are often carried by the effect of humidity, hence leach out to the wall surface and form white deposits on the wall. This phenomenon is called efflorescence<sup>2</sup> and it is important especially in exterior coatings. The extent of efflorescence depends on the nature of the soluble compounds in the concrete and atmospheric conditions such as temperature, wind, rain and snow (exposure to water and its rate of evaporation is

## Chapter 7

important).<sup>3</sup>  $\text{Na}_2\text{SO}_4$  and  $\text{K}_2\text{SO}_4$  are the main efflorescence salts.<sup>4</sup>  $\text{CaCO}_3$ , which is formed from the reaction of leached  $\text{CaOH}$  with carbon dioxide on the surface, can also be seen.<sup>5</sup> Enough time should be given for concrete to cure and dry before the application of sealer followed by two coats of paint. However, due to time and cost limitations, paints can be directly applied on still wet concrete making the efflorescence occur earlier. Solid deposits on the paint surface is an esthetical problem, in addition crystallization of the water soluble compounds at the masonry-paint interface can push the paint/coating off the wall.

First layer of paints were applied onto the smooth side of cement fiber boards by using a brush and they were allowed to dry for 2 hours before the application of the second layer. The paints were dried in temperature controlled room ( $23^\circ\text{C}$ ) overnight. The test tray was filled with the efflorescence test solution ( $0.25\text{ M NaOH} + 0.07\text{ M Na}_2\text{SO}_4$  in water) until 1 cm height, the filter wool was put as the absorbent material, and then the substrates were horizontally placed onto the wool. The reason to use an alkaline solution in the test is to mimic the alkalinity of the masonry. The changes in the appearance of the paints such as yellowing and salt formation (graded as mild, moderate and severe) and also the extents of peel off from the substrate (if applicable) were recorded at days 1, 3 and 7. For illustrative purposes, a paint before and after the efflorescence resistance test is displayed in Figure 7.1.

## Chapter 7

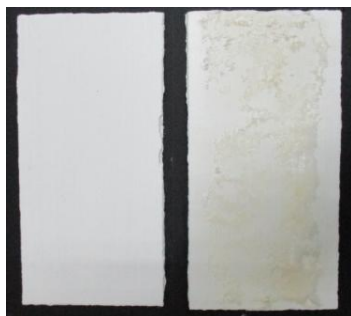


**Figure 7.1.** Paint before and after efflorescence resistance test

### **Contrast ratio, yellowness index and whiteness index**

These properties were determined on 150  $\mu\text{m}$  thickness paint films, cast onto standard white and black paper charts and dried at temperature controlled room (23°C) for 1 day.

The contrast ratio, yellowing index, whitening index are calculated from 3D color space numerical data representing the color of the paint. X,Y,Z tristimulus values and L, a, b values of the specimens were obtained by using Minolta CR-300 Chroma meter with a circular measuring area of 8 mm and 0° measuring angle. The instrument was calibrated against a standard calibration plate (Minolta), before each set of measurements.

**The contrast ratio (CR)** is a measure of the opacity of the paint, calculated by taking the ratio of Y tristimulus value of the specimen on black background to that on white background:

## Chapter 7

$$CR = \frac{Y_{\text{black}}}{Y_{\text{white}}} * 100 \quad (7.3)$$

Yellowness of the paints is usually seen as a quality flaw since it is generally associated with dirtiness, aging and degradation. **The yellowness index (YI)** was calculated according to ASTM D1925 by the formula:

$$YI = \frac{[(1.28 * X) - (1.06 * Z)] * 100}{Y} \quad (7.4)$$

White color gives an impression of being clean and fresh. Whiteness of the paints is aimed to accomplish perfect white, but typically shifted in blue-yellow dimension. When the value is lower than 100%, it means the paint is slightly yellower than perfect white. **The whiteness index (WI)** was calculated according to ASTM E313 by the formula:

$$WI = (3.388 * Z) - (3 * Y) \quad (7.5)$$

### **Hiding power (by appearance)**

100  $\mu\text{m}$  thickness films from the paints were cast onto standard contrast cards (Figure 7.2) and dried for 1 day at 23°C. The hiding power was evaluated on 1-5 scale, where 1 indicates weak hiding power and 5 means that the card is completely covered.

## Chapter 7



**Figure 7.2.** Uncoated and coated contrast cards used to evaluate hiding power

### **Gloss**

150  $\mu\text{m}$  thickness films from the paints were cast onto standard white substrates and dried for 1 day at 23°C. Gloss measurements were carried out by using Sheen Tri-glossmaster at three angles (20°, 60° and 85°). The average of three measurements is reported.

### **Alkali resistance**

Two layers of the paints were applied on both sides of the cement fiber boards by using a paint brush. 2 hours was given for drying of the first layer before the application of the second one. The paints were then dried for 1 day at 23°C. 1/8<sup>th</sup> of the substrates were soaked vertically into the alkaline solution (10% NaOH in water). At day 1, 3 and 7, the substrates were rubbed with a fabric and the amount of chalking was evaluated based on a scale 0-5, where 0 means no chalking and 5 indicates severe chalking.

## Chapter 7

### **Scrub resistance**

100  $\mu\text{m}$  thickness films were cast from the paints onto Leneta black scrub test panels (vinyl chloride/acetate copolymer). One set of the films was kept at 23°C for 6 days and then at 50°C for 1 day. The second set was kept for 7 days at 50°C. The panels were scrubbed by using Leneta standardized scrub medium (diluted in 2:1 ratio) in Sheen wet abrasion scrub tester machine. The number of cycles at which one continuous line along the shim observed was taken as maximum.

### **Color development & Color Rub**

If the paint and colorant are not compatible, the colorant may not disperse well in the paint and poor color development is observed. This results in the loss of colorant value and unexpected final color. Moreover, paint with poor color development can display color differences when subjected to different shear forces during application.<sup>6</sup>

35.0 g paint, 0.50 g colorant (a mixture of blue, red, green, yellow, black, red oxide tints) and 14.5 g paint is weighed into plastic centrifuge cup, respectively. The content is mixed at 2000 RPM for 3 minutes by using Thinky ARE-310 model centrifugal mixer. After 2 hours of rest at 23°C, a film of 100  $\mu\text{m}$  thickness was cast onto standard white substrate, and immediately a small area of the partially dry film was subjected to shear stress by finger-rubbing. The paint was allowed to dry for 1 day at 23°C and the next day colorimetric measurements were performed on both unrubbed and rubbed areas of the film.

## Chapter 7

Lightness (L) of the colorant added paints were compared to assess the extent of color development. L is given in the range of 0-100 where 100 represents white and 0 represents black (Figure 7.3). The color rub was evaluated by  $\Delta E_{ab}$  which is the average sum of the differences in colorimetric values L, a and b of the rubbed and unrubbed regions of the paint film.  $\Delta E_{ab}$  is calculated by the formula

$$\Delta E_{ab} = \sqrt{(\Delta L^2 + \Delta a^2 + \Delta b^2)} \quad (7.6)$$

where L is lightness and a and b are red-green and blue-yellow chromatic coordinates in color space, respectively (Figure 7.3). The smaller the difference ( $\Delta E_{ab}$ ) the better the color rub.

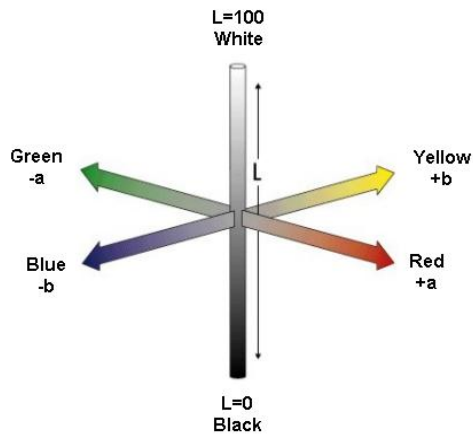


Figure 7.3. L\*a\*b\* color space

## Chapter 7

### **X-cut adhesion test**

A paint is expected to adhere well to the substrate, such as exterior walls of buildings.<sup>7</sup> This test gives an idea of the adhesion of the paint to the cement fiber board.

First layer of paints were applied onto the smooth side of cement fiber boards by using a brush and allowed to dry for 2 hours before the application of the second layer. The paints were then dried at 23°C for 1 day. An X-cut was made on the film by using a blade, a pressure-sensitive tape was applied and then pulled back according to the standard ASTM D 3359 – 97. The amount of peel off along the incision (and of the coating) was evaluated on a scale of 0-5, where 5 indicates no removal (for details of the scale, refer to the standard). The test was performed at minimum 2 points on days 1, 5 and 7.

### **Blocking resistance**

The paint can be applied on surfaces in contact such as door and jam.<sup>8</sup> When freshly painted door is closed, it may stick shut if blocking resistance is poor.

150  $\mu\text{m}$  paints were cast on Leneta paper and left at room temperature for 1 day. Substrates with dimensions 3cmx7cm were cut, left face-to-face under 0.5 kg force for 1 day and then peeled apart. The blocking resistance was evaluated on a scale of 0-10 by taking into account the extent of tack/ seal of the substrates according to the ASTM D 4946 – 89.

## Chapter 7

### **Natural Weathering**

First layer of paints were applied onto the smooth side of cement fiber boards by using a brush and they were allowed to dry for 2 hours before the application of the second layer. The paints were left at temperature controlled room (23°C) for 7 days. Colorimetric measurements were performed and ¼ of the panels were covered for protection. The panels were left in natural weathering area and changes in the physical appearance (such as color fading, blistering, chalking, cracking), gloss and colorimetric values were recorded. The conditions to which the paints were exposed were 24-40°C average temperatures, humidity changes of 40-95% and heavy rains. The follow up normally takes for a minimum of 1 year. The artificial weathering was not applied because it may not be representative in some cases.<sup>9</sup>

### **Mechanical Tests**

Mechanical tests are performed on paints in order to account for some end-use properties such as scrub resistance<sup>10</sup> and also fulfill some specific needs of the market. For instance, in new buildings, plaster cracks in the first 2-3 years hence as well the paints applied onto (map cracking). Therefore, it is demanded that the paint be flexible enough to bridge cracks but at the same time with minimum dirt pick up and good waterproofing and breathability.<sup>11</sup> Singaporean Standards for Elastomeric Wall Coating (SS500) lists the minimum requirements for such paint as 1.5 MPa tensile strength and 100% elongation at break.

## Chapter 7

The paints were cast on polyethylene sheets by using a 4-sided bird type applicator with 500  $\mu\text{m}$  gap depth. Two samples of each paint were prepared and dried either at 23°C or 50°C for 6 days. Dog-bone shaped specimens were punched out of the films. The stress-strain tests were performed in a LR10K plus instrument (Lloyd Inst) by applying a cross-head speed of 50 mm/min. For each paint, at least six specimens were tested.

### **7.3. Results and Discussion**

#### **7.3.1. Latex (binder) properties**

The characteristics of the synthesized latexes are displayed in Table 7.8. The latexes synthesized by using NaSS yielded particles with particle sizes 145-310 nm depending on the amount of NaSS and the particle size of the seed used. The latex produced by using a smaller seed yielded particles of 145 nm size. The latex with 3.6% NaSS displayed the highest average particle size. This may be due to the high amount of NaSS yielding excessive amount of water soluble polymer destabilizing the particles. The pHs of the latexes were 2.5-3 since no buffer was utilized in the syntheses. The viscosities of the latexes were low however, the viscosity response of the latexes, which will be discussed later, is more important. The  $T_g$  of the latexes with NaSS were in the range 15-18°C. Minimum film forming temperatures (MFFT) of the latexes stabilized with NaSS were higher than that of SDS (8.5°C). The MFFT of

Chapter 7

the latex with 3.6% NaSS was the highest likely due to the fact that ionic groups (either chemically attached or physically adsorbed on the particles) may retard particle deformation so MFFT is seen at slightly higher temperatures.<sup>12</sup> MFFT of Syn-A was higher than the rest.

**Table 7.8.** Characteristics of the latexes

Code	Z-ave (nm)	Solids Content (%)	pH	Specific gravity (g/cm <sup>3</sup> )	Viscosity* (cP)	T <sub>g</sub> (°C)	MFFT (°C)
<b>3.6%</b>	310	49.0	2.85	1.0553	82 (1/60)	16.7	11.6
<b>1.3%</b>	250	49.2	2.74	1.0551	24.5 (1/60)	16.9	9.9
<b>1.0%</b>	240	49.6	2.63	1.0561	32 (1/60)	16.3	10
<b>0.76%</b>	270	48.7	2.61	1.0551	24 (1/60)	15.9	9.9
<b>0.5%</b>	280	49.6	2.56	1.0552	50 (1/60)	17.6	10.5
<b>HPO</b>	280	48.2	2.97	1.0543	14.5 (1/60)	18.3	9.9
<b>Smallsize</b>	145	44.5	2.46	1.0506	41 (1/60)	15.2	9.0
<b>SDS</b>	225	49.4	2.61	1.0534	173 (1/30)	14.0	8.5
<b>Syn-A</b>	150	50	8.20	1.0630	130 (3/60)	17.0	17.0

\*The first number in parenthesis refers to the code of the spindle used and the second number is the spinning rate

VOC contents of the latexes used as binders in the paints are important since the amount of VOCs in coatings is restricted by environmental regulations worldwide. For instance, starting from 2010, the permissible VOC limit for the waterborne paints used

## Chapter 7

on exterior walls of mineral substrate has been decreased to 40 g/L (in ready-to-use form) by European Directive 2004/42/CE.

The amounts of residual monomers (MMA, BA) and by products such as tert-butanol, n-butanol and butyl acetate in the latexes are displayed in Table 7.9. Tert-butanol is produced by hydrogen abstraction of tert-butoxy radical. Hydrolysis of butyl acrylate yields acetic acid and n-butanol which can further react to form butyl acetate.<sup>13</sup> Acetone is also a by-product however it is not quantified due to being exempt in VOCs.

**Table 7.9.** Volatile organic compound content (VOC) of the latexes

Code	VOCs (ppm)				
	MMA	BA	tert-butanol	n-butanol	butyl acetate
<b>3.6%</b>	26	-	34	119	53
<b>1.3%</b>	27	-	40	127	55
<b>1.0%</b>	26	-	30	114	53
<b>0.76%</b>	27	-	37	120	58
<b>0.5%</b>	26	-	38	101	60
<b>HPO</b>	30	1204	18	94	57
<b>Smallsize</b>	33	36	29	127	54
<b>SDS</b>	147	226	43	221	42

## Chapter 7

In the reactions 3.6%-0.5% NaSS where TBHP/AsAc was used, MMA content was below 30 ppm and no BA was detected. However, in the case of HPO/AsAc, the residual BA was 1200 ppm although post-polymerization was performed. The reason can be that HPO/AsAc producing hydrophilic radicals may be less efficient for the conversion of BA. The amount of residual MMA is the same regardless of the initiator system. In the production of the latexes Smallsize and SDS, no post-polymerization was performed. The residual MMA content of SDS was higher than the rest.

### **7.3.2. Water Blanching of Latex Films**

Water blanching of latex films after 24 hours is displayed in Figure 7.4. The visual inspection showed that the films SDS, Syn-A, HPO and 3.6% were not resistant to water. For SDS and Syn-A, the reason is that emulsifiers aggregate as hydrophilic pockets and increase water sensitivity. The poor resistance in the case of 3.6% can be due to the presence of higher amount of water soluble polymer. Most of the NaSS containing films were better than SDS and Syn-A. The best performance was displayed by 1.3% and Smallsize. When NaSS content is lowered to 0.76% or 0.5% more whitening than 1.3% was observed. It can be due to the fact that weaker repulsive interactions between the particles may ease the plasticization effect of water leading to more whitening. The detailed observations made at certain intervals are given in Appendix IV.

## Chapter 7

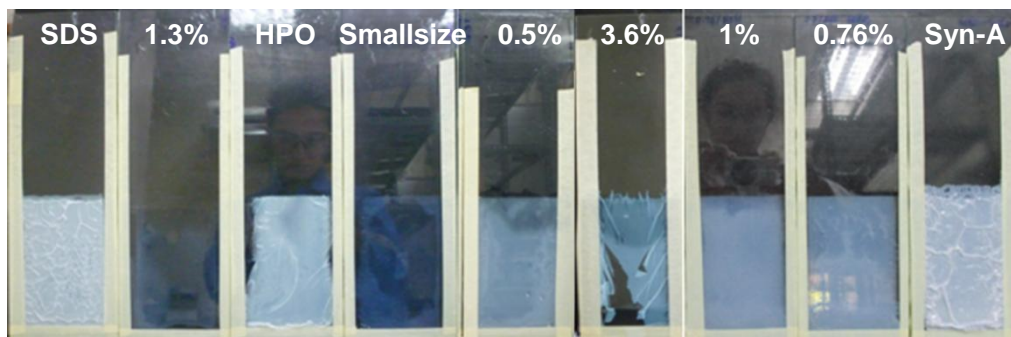


Figure 7.4. Water blanching of latex films after 24 hours

### 7.3.3. Properties of liquid paints

The theoretical amounts of components used in letdown stage were given in Table 7.7. However, since the viscosities of the paints were adjusted in the range of 89-99 kU, the paints required either more or less thickener than the theoretical amount depending on the thickening response of the binder as shown in Figure 7.5. The theoretical amount in the formulation 0.5wt% is shown as red line. Thickening response can be defined as the ability of the binder to respond to an added thickening agent. Higher the thickening response, less the thickener added and hence the cost is reduced.

Thickening response of Smallsize was the highest due to its small particle size. Since the paints contain the same solids content, as particle size was smaller (Smallsize), the number of particles increased, hence particle-particle interactions increased. Therefore resistance to flow could be enhanced by using a lower

Chapter 7

concentration of thickener. 3.6% required more thickener than the theoretical amount, which indicates an insufficient thickening response. This can be explained by the bigger particles in the latex. All of the other binders reached the viscosity of Syn-A with lower amount of thickener. Considering the fact that more coalescing solvent was used for Syn-A (coalescing solvents enhance the thickening response), it can be concluded that most of the NaSS containing binders displayed very good thickening response.

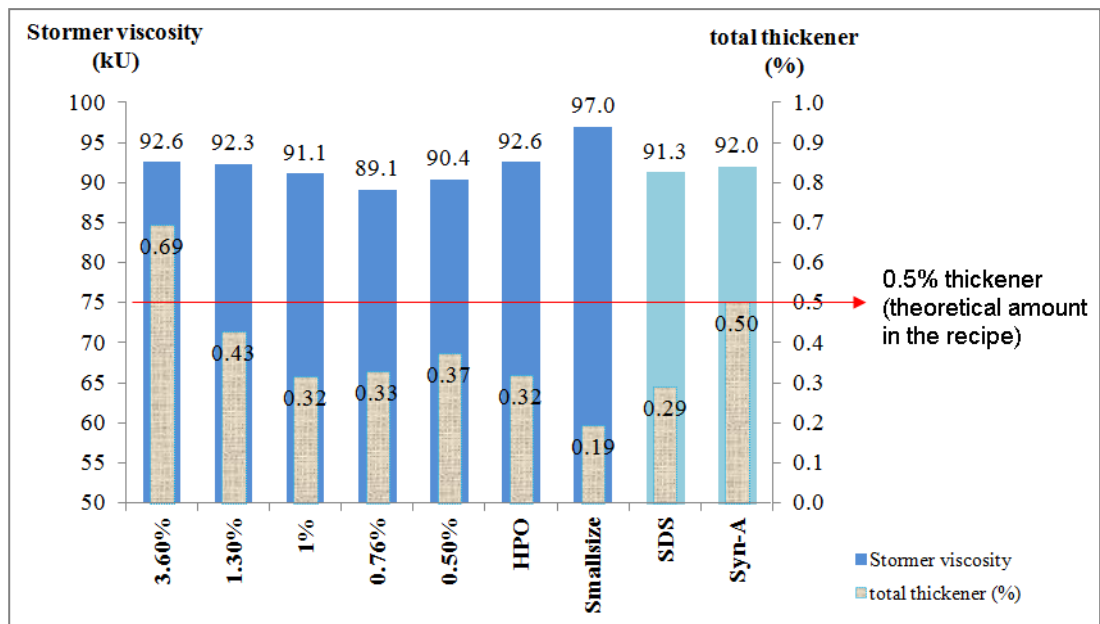


Figure 7.5. Thickening response of the binders upon addition of thickener

## Chapter 7

The characteristics of the paints are summarized in Table 7.10. Total solids content (TSC) and specific gravity (SG) were measured as a quality control for the paints. They were within the expected values indicating that the paint preparation step was good. Stormer viscosities were adjusted in the range of 89-99 kU. Brushability was good as indicated by low cone & plate viscosity. % coalescing solvents used to prepare the paints were also provided to see the difference.

**Table 7.10.** Characteristics of the paints

	<b>3.6%</b>	<b>1.3%</b>	<b>1%</b>	<b>0.76%</b>	<b>0.5%</b>	<b>HPO</b>	<b>Smallsize</b>	<b>SDS</b>	<b>Syn-A</b>
<b>TSC (%)</b>	55.0	54.9	54.6	54.5	54.8	54.6	54.8	55.0	55.3
<b>pH</b>	9.7	9.8	9.8	9.8	9.8	9.8	9.7	9.7	9.5
<b>SG (g/cm<sup>3</sup>)</b>	1.407	1.405	1.399	1.401	1.403	1.399	1.399	1.403	1.406
<b>Stormer viscosity (kU)</b>	92.6	92.3	91.1	89.1	90.4	92.6	97.0	91.3	92.0
<b>Cone &amp; plate viscosity (Poises)</b>	0.40	0.45	0.50	0.35	0.30	0.15	0.45	0.55	0.35
<b>%coalescing solvent (wb binder)</b>	2.5	2.5	2.5	2.5	2.5	2.5	2.5	2.5	5

## Chapter 7

### 7.3.3.1. Storage stability at 50°C

The changes in paint appearances upon storage for 2 and 4 weeks at 50°C are given in Figure 7.6. It is worth to mention that all paints were white in the beginning. Upon storage, all paints displayed phase separation. Syn-A displayed less yellowing in comparison to SDS and NaSS containing paints. The yellowing can be explained by the presence of AsAc in the formulations. AsAc can be a problem in terms of yellowing of paints but can be prevented by replacing it with alternative reductants such as sodium salt of sulfinic acid.<sup>14</sup> The details of all measurements performed at certain intervals are provided in Appendix IV. No significant change in pH was observed. Drop in viscosity was the highest for SDS. The yellowing in the paints was reflected as a drop in whiteness index and a rise in yellowness index. The changes in these values were low for Syn-A. Contrast ratio retention was lowest for SDS, whereas it was good for NaSS containing latexes except HPO. Since gloss values were small, it was not possible to make a solid conclusion for gloss retention.

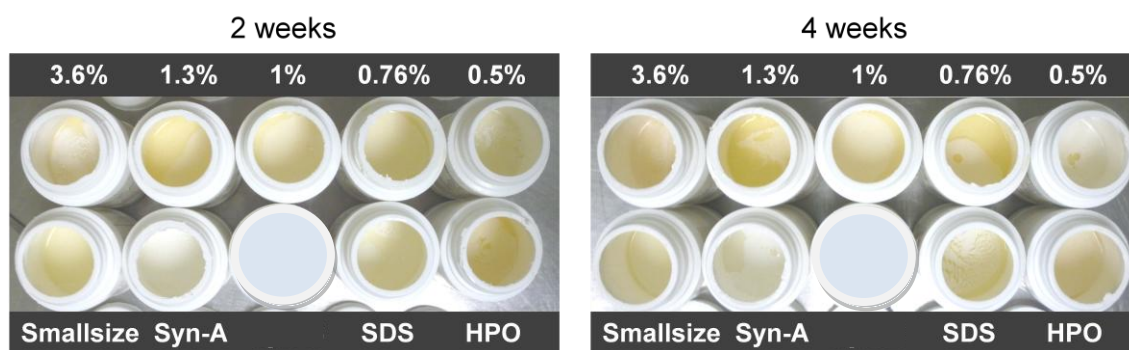


Figure 7.6. The appearance of the paints upon storage for 2 and 4 weeks at 50°C

## Chapter 7

### 7.3.3.2. Freeze-thaw stability

Freeze thaw stability is an important feature of the paint especially in some climates. During freezing, water forms ice crystals therefore concentration of particles in the fluid phase increases. If the particles are not well stabilized, irreversible coagulation takes place. The results are given in Table 7.11 with the inset photos of the failed paints. It can be seen that paints containing latexes stabilized with more than 0.76% NaSS resisted 6 cycles. Reference paint Syn-A was stable up to 4<sup>th</sup> cycle. The paint with conventional emulsifier (SDS) turned into gel since ionic emulsifiers tend to leach out from the particle surface during freeze-thaw cycles. Smallsized failed in the first cycle. This can be due to the fact that particles with small sizes tend to fail more in freeze-thaw cycles due to resistance to redispersion.<sup>15</sup> Here, it can be also due to insufficient particle stabilization since smaller particles had more surface area, thus, the number of NaSS groups per particle was decreased. Stability after 3-5 freeze-thaw cycles is accepted as good enough for most commercially available paints.<sup>16</sup>

Chapter 7

**Table 7.11.** Freeze-thaw stability of the paints

	3.60%	1.30%	1%	0.76%	0.50%	HPO	Smallsize	SDS	Syn-A
1 <sup>st</sup>	✓	✓	✓	✓	viscosity inc. consistency lost	viscosity inc. consistency lost	X Gel	X Gel	✓
2 <sup>nd</sup>	✓	✓	✓	✓					✓
3 <sup>rd</sup>	✓	✓	✓	✓					✓
4 <sup>th</sup>	✓	✓	✓	✓					viscosity inc.
5 <sup>th</sup>	✓	✓	✓	✓					X Gel
6 <sup>th</sup>	✓	✓	✓	✓					

**7.3.4. Properties of the paint films**

**7.3.4.1. Surface properties**

The gloss is important for the visual appearance of the paints. The previous gloss measurements on the films cast from the latexes with NaSS showed that they had highly glossy surfaces with ca. 10 gloss unit (GU) difference from the control film with SDS. However, the paints prepared displayed matt surfaces (Table 7.12) and there was no difference in gloss to the naked eye. This is due to the high PVC (45%) of the formulation. Since the paints have low gloss (below 10 GU) at 60°, the gloss values at 85° should be considered. No significant difference either in gloss or gloss retention values was observed. In order to see a significant difference in gloss, paint formulation should be modified to low PVC (such as 15-25%).

Chapter 7

**Table 7.12.** Gloss of the paint films

	°	3.6%	1.3%	1%	0.76%	0.5%	HPO	Smallsize	SDS	Syn-A
<b>initial</b>	20	1.4±0.0	1.4±0.0	1.4±0.0	1.4±0.0	1.4±0.0	1.4±0.0	1.4±0.0	1.4±0.0	1.4±0.0
	60	4.2±0.0	4.6±0.1	4.5±0.0	4.4±0.0	4.5±0.0	4.3±0.1	4.8±0.0	4.2±0.0	4.4±0.0
	85	2.7±0.0	3.2±0.1	3.1±0.1	3.2±0.0	3.2±0.0	3.1±0.1	3.1±0.1	2.7±0.0	2.5±0.0
<b>2 weeks</b>	20	1.4±0.0	1.5±0.0	1.4±0.0	1.4±0.0	1.5±0.0	1.4±0.0	1.5±0.0	1.4±0.0	1.4±0.0
	60	4.2±0.0	4.7±0.1	4.4±0.0	4.4±0.0	4.5±0.1	4.3±0.1	4.8±0.1	4.2±0.0	4.2±0.0
	85	2.6±0.0	3.0±0.0	2.8±0.0	3.1±0.0	3.0±0.1	3.0±0.1	3.0±0.1	2.6±0.1	2.3±0.1
<b>4 weeks</b>	20	1.5±0.1	1.5±0.0	1.4±0.0	1.4±0.1	1.5±0.0	1.6±0.1	1.6±0.1	1.4±0.1	1.5±0.1
	60	4.0±0.0	4.4±0.1	4.2±0.1	4.3±0.0	4.3±0.1	4.2±0.1	4.7±0.1	4.1±0.0	4.1±0.0
	85	2.7±0.1	2.8±0.2	2.9±0.1	2.9±0.0	3.0±0.2	2.7±0.1	2.8±0.2	2.6±0.0	2.4±0.1

The opacity of the paints was evaluated based on the hiding power by appearance and the contrast ratio (Table 7.13). The contrast ratio values did not differ significantly except for 0.5% NaSS. The hiding power of SDS was the worst and opacity of NaSS containing paints was comparable to Syn-A.

**Table 7.13.** Opacity of the paint films

	3.6%	1.3%	1%	0.76%	0.5%	HPO	Smallsize	SDS	Syn-A
<b>Contrast ratio (%)</b>	90.7	88.4	90.5	89.1	85.7	88.6	87.8	90.7	87.5
<b>Hiding power by appearance*</b>	2	2	2	2	2	2	2	1	2

\*Visually evaluated on a scale 0-5; where 0 is poor and 5 is good coverage

Chapter 7

**7.3.4.2. Color Development and color rub**

The colorimetric values (L, a, b) of the paints were determined after addition of colorant to the paints and are given in Table 7.14. The charts for color tests are displayed in Figure 7.7.  $\Delta E_{ab}$  gives the difference between unrubbed and rubbed areas of the paint and the smaller the difference the better the color rub. Although  $\Delta E_{ab}$  values are within tolerance of  $\pm 0.5$ , good color rub was observed for most of the NaSS containing paints.

**Table 7.14.** Colorimetric values for color development and color rub tests for the colorant added paints

	3.6%	1.3%	1%	0.76%	0.5%	HPO	Smallsize	SDS	Syn-A
<b>L</b>	62.9	63.0	63.2	62.8	62.8	62.7	63.3	62.8	63.1
<b>a</b>	0.9	1.1	1.1	1.1	1.0	1.0	0.7	1.0	0.9
<b>b</b>	-12.8	-12.7	-12.6	-12.6	-12.6	-12.9	-13.2	-12.6	-13.3
<b><math>\Delta E_{ab}</math></b>	0.1	0.1	0.1	0.1	0.1	0.3	0.2	0.1	0.2

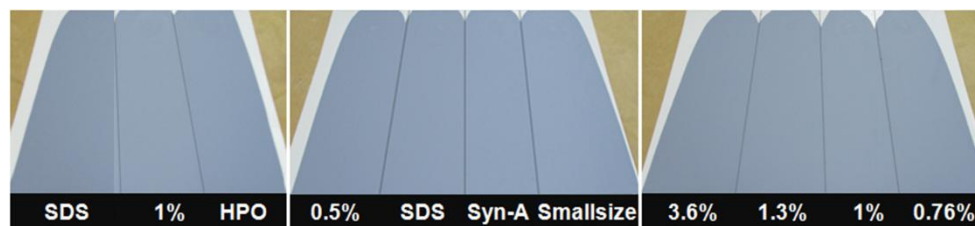


Figure 7.7. Appearance of colorant added paints

## Chapter 7

### 7.3.4.3. Efflorescence resistance

The observations made during efflorescence resistance test are provided in Table 7.15. Severe salting was observed in most of the NaSS containing paints. Blistering was also seen in some of the paints. Interestingly, efflorescence resistance of the paints SDS and Syn-A was good.

**Table 7.15.** Observations\* made during efflorescence resistance tests for the paints

	Initial	Day 1	Day 3	Day 7
3.6%	Clear white	Slight yellowing	Salting moderate (3)	Salting severe (5), blistering
1.3%	Clear white	More yellowing	Salting mild	Salting severe (5), yellowing, blistering
1%	Clear white	Slight yellowing	Salting mild	Salting severe (4)
0.76%	Clear white	Slight yellowing	Salting mild	Salting severe (5), blistering
0.5%	Clear white	Slight yellowing	Salting moderate (3)	Salting severe (5), yellowing, blistering
HPO	Clear white	Slight yellowing	Salting mild	Salting severe (5), yellowing
Smallsize	Clear white	Slight yellowing	Salting mild	Salting severe (4)
SDS	Clear white	Slight yellowing	Salting mild	Salting moderate (2)
Syn-A	Clear white	More yellowing	Salting mild	Salting mild (1)

\*Salting was evaluated in the range 0-5; where 0 is no salt and 5 is severe salting

For efflorescence to take place, there must be moisture and alkalinity in the masonry and also a path for moisture penetration throughout the paint film.<sup>4</sup> The test solution fulfills the first two requirements. Moisture passes from the film-substrate interface, migrates through the paint film cross-section and reach paint-air interface.

## Chapter 7

As water evaporates, it leaves a dry solid behind, what is seen as solid deposits. The reason for bad efflorescence resistance observed in NaSS containing paints can be the presence of path for moisture penetration.

It has been known that chemically attached stabilizers (such as surfmers) can be adsorbed in particle-particle boundaries, forming a continuous path through the film for moisture penetration.<sup>17</sup> Although coalescent agents are added in the paints, the ionic network can be preserved up to a certain level in paint films. This could explain insufficient efflorescence resistance of NaSS containing paints.

For the case of SDS and Syn-A, most of the emulsifier molecules were expected to migrate to the film-air interface. Therefore film-substrate interface and particle-particle boundaries are expected to be almost free of ionic moieties. This could lead to improved film formation in film-substrate interface and absence of an ionic network throughout the film cross-section, both could delay efflorescence. Good efflorescence resistance and high water blanching may seem contradictory. In efflorescence tests, the absorption of moisture is from film-substrate interface while in water blanching tests the samples are completely immersed in water. Film-air interface is always richer in SDS than film-substrate interface and the bulk. This makes SDS less reachable by water in efflorescence tests. On the other hand, in water blanching, SDS molecules in the film-air surface are cleaned away easily and as soon as hydrophilic SDS aggregates are reached, they can absorb large amounts of water

## Chapter 7

and result in discoloration and delamination and the total amount of water adsorbed is far more than that absorbed by NaSS containing films.

### 7.3.4.4. Mechanical properties

The mechanical properties of the paints kept at 23°C and 50°C for 6 days are given in Table 7.16. It can be seen that the tensile strength improved in films dried at higher temperature, indicating better film formation with temperature. Paints based on NaSS containing binders had higher tensile strength but less elongation at break compared to SDS and Syn-A. Binders with carboxylic acid monomers are known to have high pigment binding capacity due to ionic charges.<sup>18</sup> Similar behavior can be expected for NaSS containing binders. Strong adhesion of the pigment and the binder can result in less deformable paints with higher tensile strength.<sup>19</sup> Moreover,  $\text{SO}_3^- \text{Na}^+$  groups may form ionic aggregates which act as physical crosslinks in the film, hence increase the tensile strength.

Chapter 7

**Table 7.16.** Mechanical properties of the paint films prepared at different drying conditions (23°C and 50°C)

	<b>Tensile stress 23°C (MPa)</b>	<b>Elongation at break 23°C (%)</b>		<b>Tensile stress 50°C (MPa)</b>	<b>Elongation at break 50°C (%)</b>
<b>3.6%</b>	3.10 ± 0.13	24 ± 4		4.74 ± 0.23	72 ± 6
<b>1.3%</b>	2.43 ± 0.20	88 ± 10		3.59 ± 0.10	126 ± 18
<b>1%</b>	1.74 ± 0.05	66 ± 4		3.00 ± 0.22	79 ± 21
<b>0.76%</b>	2.81 ± 0.11	61 ± 10		3.93 ± 0.24	96 ± 18
<b>0.5%</b>	2.16 ± 0.05	43 ± 12		3.11 ± 0.17	165 ± 35
<b>Smallsize</b>	2.50 ± 0.08	65 ± 20		4.54 ± 0.30	117 ± 19
<b>SDS</b>	1.23 ± 0.03	169 ± 35		1.91 ± 0.06	145 ± 26
<b>Syn-A</b>	1.43 ± 0.07	280 ± 30		2.97 ± 0.27	311 ± 69

**7.3.4.5. Scrub Resistance**

Scrub resistance is affected by many parameters such as hydrophilicity of the paint (formulation ingredients), flexibility (mechanical properties), pigment binding ability and extent of coalescence (drying time and conditions).

The scrub resistance of the paints cast at 23°C and 50°C are given in the order of maximum scrub cycle that the paints can withstand (Table 7.17). It is seen that scrub resistances of the paints cast at 50°C were significantly higher than those cast at 23°C, likely due to better coalescence of polymer particles and film quality.

Poor scrub resistance of the paint with high NaSS content (3.6%) can be explained by the hydrophilicity of the binder. As NaSS content decreased, scrub

## Chapter 7

resistance improved. This can be a result of both decreased hydrophilicity and enhanced film formation with the decrease in coalescence retardant ionic groups. When particle size was smaller, scrub resistance was better, most probably due to better coalescence of particles by enhanced capillary pressure. Interestingly, although water sensitivity of SDS was not good, scrub resistance was the best. This can be explained by higher flexibility of the paint (Table 7.16).

**Table 7.17.** Scrub resistance of the paint films cast at 23 °C and 50°C

	<b>3.6%</b>	<b>1.3%</b>	<b>1%</b>	<b>0.76%</b>	<b>0.5%</b>	<b>HPO</b>	<b>Smallsize</b>	<b>SDS</b>	<b>Syn-A</b>
Max cycles 23°C	260	610	950	1450	1400	950	1190	>2400	1260
Max cycles 50°C	480	1300	1800	2400	2770	2040	2330	>3200	2400

### 7.3.4.6. Block Resistance

There is no significant difference in the block resistance of the paints (Table 7.18).

**Table 7.18.** Block resistance\* of the paints

<b>3.6%</b>	<b>1.3%</b>	<b>1%</b>	<b>0.76%</b>	<b>0.5%</b>	<b>HPO</b>	<b>Smallsize</b>	<b>SDS</b>	<b>Syn-A</b>
9	9	9	9	10	9	10	9	8

\*Evaluation: 10: no tack, 9: trace tack, 8: slight tack

Chapter 7

**7.3.4.7. Alkali Resistance**

Alkali resistances of the paints (Table 7.19) were comparable.

**Table 7.19.** Alkali resistance\* of the paints

	3.6%	1.3%	1%	0.76%	0.5%	HPO	Smallsize	SDS	Syn-A
<b>Day1</b>	1	1	1	2	1	1	2	2	2
<b>Day7</b>	3	3	3	3	4	4	3	3	3

\*Evaluation: 0: good resistance, 5: poor resistance

**7.3.4.8. X-cut adhesion test**

X-cut adhesion test results of the paints are given in Table 7.20. Except 0.76%, NaSS containing paints were slightly better than SDS and Syn-A, however the difference was not significant.

**Table 7.20.** X-cut adhesion\* test results for the paints

	3.6%	1.3%	1%	0.76%	0.5%	HPO	Smallsize	SDS	Syn-A
<b>Day1</b>	4A	4A	4A	3A	4A	4A	5A	4A	4A
	4A	4A	4A	4A	3A	4A	4A	4A	4A
<b>Day 5</b>	4A	5A	4A	3A	4A	4A	5A	4A	3A
	4A	4A	4A	4A	4A	4A	4A	3A	4A
<b>Day 7</b>	4A	4A	4A	3A	4A	4A	3A	4A	4A
	4A	3A	5A	3A	4A	3A	3A	4A	3A
	4A	4A	4A	4A	4A	3A	4A	4A	4A

\*Evaluation: 5A: no removal, 4A: trace peeling along the incision, 3A: jagged removal (flakes)

## Chapter 7

### 7.3.4.9. Natural Weathering

The paints exposed to natural weathering were inspected after 2 and 4 weeks. All data obtained is provided in Appendix IV. Table 7.21 summarizes the results of 4 weeks. Noticeable darkening to naked eye occurred in the reference paints and SDS (Figure 7.8). They displayed higher loss in lightness ( $\Delta L$ ) and higher dirt retention ( $\Delta E_{ab}$ ) than the paints with NaSS. In addition, the reference paint Syn-A had more decline in whiteness index and higher increase in yellowness index. In conclusion, paints prepared from latexes with NaSS were more stable towards 4 weeks of natural weathering.

**Table 7.21.** Natural weathering of the paints after 4 weeks

	<b>3.6%</b>	<b>1.3%</b>	<b>1%</b>	<b>0.76%</b>	<b>0.5%</b>	<b>HPO</b>	<b>Smallsize</b>	<b>SDS</b>	<b>Syn-A</b>
<b><math>\Delta L</math></b>	-0.89	-0.62	-0.97	-0.65	-0.75	-1.72	-1.38	-2.01	-2.46
<b><math>\Delta WI</math></b>	-2.32	-4.16	-3.49	-3.72	-4.59	-6.96	-5.20	-6.13	-9.91
<b><math>\Delta YI</math></b>	0.35	1.01	0.56	0.83	1.23	1.21	0.76	0.77	1.71
<b><math>\Delta E_{ab}</math></b>	0.94	0.81	1.00	0.77	0.96	1.82	1.43	2.03	2.60

## Chapter 7

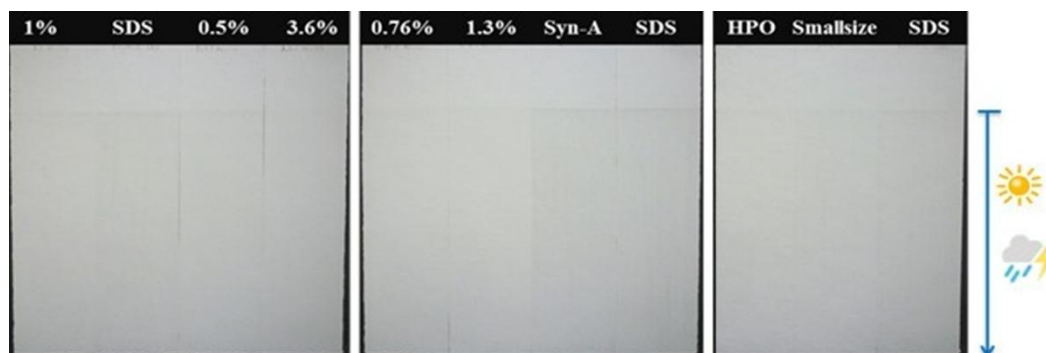


Figure 7.8. Paints exposed to natural weathering for 4 weeks

### 7.4. Conclusions

Emulsifier-free MMA/BA latexes stabilized by different amounts of NaSS were incorporated into exterior paint formulation. The performances of these binders in paints were compared with two paints: the reference paint was prepared by using a binder provided by Synthomer and the control paint was prepared by using a binder stabilized by SDS.

Paints prepared by using NaSS containing binders had good color development/rub. They also displayed superior thickening response, excellent stability towards natural weathering and similar gloss than the control and reference paint.

Efflorescence resistances were inferior to emulsifier based paints, most probably due to formation of a continuous ionic network that allow moisture migration.

## Chapter 7

Excellent freeze-thaw stability (6 cycles) was found for paints containing latexes with more than 0.76% NaSS.

Scrub resistance decreased with the NaSS concentration and only for a concentration of 0.76% met the performance of the reference paint.

The other tests such as block resistance, alkali resistance and X-cut adhesion yielded comparable results with reference paint.

## Chapter 7

### 7.5. References

- [1] Resene Paints. (2005). Volume solids, PVC, hiding power. <[http://www.resene.co.nz/archspec/cpd\\_earn\\_points/pdfs/CPD\\_volumesolidspvchiding\\_oct2003.pdf](http://www.resene.co.nz/archspec/cpd_earn_points/pdfs/CPD_volumesolidspvchiding_oct2003.pdf)>
- [2] Scholz, W. (2004). Paints and coatings – how surfactants can advance new developments, CD Proceedings 6<sup>th</sup> World Surfactant Congress, Germany.
- [3] Portland Cement Association. (2004). Trowel tips information efflorescence. <[http://www.cement.org/docs/default-source/fc\\_mat-app\\_pdfs/masonry/is239-pca-efflorescence.pdf](http://www.cement.org/docs/default-source/fc_mat-app_pdfs/masonry/is239-pca-efflorescence.pdf)>
- [4] Merrigan, M.W., Efflorescence: cause and control. *Masonry Society Journal* **1986**, 5(1).
- [5] Bensted, J. (2000). Efflorescence - Prevention is Better than Cure. <<http://www.pavezone.com/sealing/pdf/efflorescence.pdf>>
- [6] ASTM D5326 – 94a, Standard Test Method for Color Development in Tinted Latex Paints.
- [7] ASTM D3359 – 97, Standard Test Methods for Measuring Adhesion by Tape Test.
- [8] ASTM D4946 – 89, Standard Test Method for Blocking Resistance of Architectural Paints.
- [9] Merlatti, C., Perrin, F.X., Aragon, E. and Margailan, A., Natural and artificial weathering characteristics of stabilized acrylic–urethane paints. *Polymer Degradation and Stability* **2008**, 93(5), 896-903.
- [10] Koleske, J.V., Mechanical properties of solid coatings. *Encyclopedia of Analytical Chemistry* **2006**. DOI: 10.1002/9780470027318.a0608

## Chapter 7

- [11] Kuek, G. (2005). Ensuring good paint performance, *Roof & Facade Asia*, 13.
- [12] Keddie, J. (2013). Emulsion Polymerization Processes Course 2013, Film Formation of Waterborne Coatings lecture notes, University of the Basque Country, Spain.
- [13] Da Cunha, L., Ilundain, P., Salazar, R., Alvarez, D., Barandiaran, M.J. and Asua, J.M., VOC formation during monomer removal by post-polymerization. *Polymer* **2001**, 42(2), 391-395.
- [14] Paulis, M. (2013). Emulsion Polymerization Processes Course 2013, Emulsion Polymerization Reactors lecture notes, University of the Basque Country, Spain.
- [15] Nakamura, A. and Okada, R., The coagulation of particles in suspension by freezing-thawing. *Colloid and Polymer Science* **1976**, 254(8), 718-725.
- [16] Chern, C-S. Principles and Applications of Emulsion Polymerization, John Wiley & Sons: USA, 2008.
- [17] Keddie, J., Routh A.F. Fundamentals of Latex Film Formation: Processes and Properties. Springer: Dordrecht, 2010.
- [18] Khorassani, M., Afshar-Taromi, F., Mohseni, M. and Pourmahdian, S., The role of auxiliary monomers and emulsifiers on wet scrub resistance of various latex paints at different pigment volume concentrations. *Journal of Applied Polymer Science* **2009**, 113(5), 3264-3268.
- [19] Kirsch, S., Pfau, A., Frechen, T., Schrof, W., Pföhler, P. and Francke, D., Scrub resistance of highly pigmented paints: A study on abrasion mechanisms of different scrub techniques. *Progress in Organic Coatings* **2001**, 43(1), 99-110.

## Chapter 8. Conclusions

This PhD thesis aims at producing colloidally stable, high solids content and film forming emulsifier-free latexes, in which the colloidal stability is solely provided by chemically incorporated and pH insensitive ionic moieties onto the polymer particles. The main reason for avoiding surfactants is that they reduce desirable properties of the films cast from the dispersions such as gloss, adhesion and water resistance. As major comonomers, a typical coating formulation MMA/BA (50/50 by weight) and the pH and temperature insensitive sodium styrene sulfonate (NaSS) was selected as ionic monomer.

The implementation of this idea was not straightforward because MMA and BA are sparingly water soluble monomers mainly located in polymer particles (and monomer droplets) and NaSS is a water soluble monomer that is virtually located in the aqueous phase. In order to provide stability to the polymer dispersions during synthesis and storage, and to avoid the negative effects of the migratory hydrophilic species on the application properties, NaSS should be chemically incorporated onto the polymer particles and the fraction that remains in the aqueous phase as water-soluble polymer should be minimized. Moreover, for the practical use, the dispersions needed to be at high solids contents ( $\geq 50$  wt%) and film-forming. Seeded semicontinuous method, which is typically used in industry for consistent product

## Chapter 8

quality and better control of nucleation and heat removal, was selected as the process strategy.

The colloidal stability could be achieved by shifting the locus of polymerization from the aqueous phase to the particle phase by altering the hydrophobicity of the oligoradicals growing in the aqueous phase. This can be accomplished by varying the nature of initiator and comonomers with which NaSS reacts.

The effect of the comonomer on the chemical incorporation of NaSS onto polymer particles was studied by model reactions at low solids contents (Chapter 2). Using monomers of different functionality (styrene, acrylates, methacrylates) and different water solubilities, it was found that the key factor controlling the chemical incorporation of NaSS was the concentration of the comonomer in the aqueous phase, whereas the functionality did not play any significant role. Of practical importance is the finding that chemical incorporation of NaSS to a rather hydrophobic dispersion can be boosted using small amounts of a relatively water soluble monomer in the formulation.

The effect of the initiator on the chemical incorporation of NaSS onto polymer particles was investigated by using four different initiators, namely potassium persulfate (water soluble) and azobisisobutyronitrile (oil soluble) as thermal, and tert-butyl hydroperoxide/ ascorbic acid (yielding hydrophobic radicals in the aqueous phase) and hydrogen peroxide/ ascorbic acid (yielding hydrophilic radicals in the aqueous phase) as redox initiators (Chapter 3). The results indicated that

## Chapter 8

polymerization of NaSS occurs in two loci: the aqueous phase that is a solution polymerization and the surface of the polymer particles that behaves as a radical compartmentalized system. On the surface of the particles the growing oligoradicals form a water swollen shell, where monomers with different water solubility get in contact and most of the copolymerization occurs. TBHP/AsAc was found to be the most promising initiator in seeded semicontinuous copolymerization of MMA/BA/NaSS. Thanks to the high incorporation of NaSS achieved by this redox initiator system, good latex stability (salt and freeze-thaw) and film properties (water sensitivity) were observed.

Stable, emulsifier-free 50 wt% solids content latexes for a wide range of monomer systems and 62 wt% solids content for MMA/BA latex with an acceptable viscosity were produced by seeded semicontinuous emulsion polymerization using NaSS (Chapter 4). It was found that the chemical incorporation of NaSS generally improved with the water solubility of the comonomers. Addition of small amounts of 2HEA in MMA/BA system increased the incorporation, however, MAA reduced the incorporation indicating that the aqueous phase polymerization was more dominant than the polymerization in the polymer particles. The incorporation of NaSS also improved with the solids content. NaSS containing latexes presented improved freeze-thaw and salt stability when compared with a control latex in which stabilization was provided by conventional surfactant SDS. For NaSS stabilized latexes freeze-thaw stability was low for soft copolymers, but for similarly hard polymers, it improved with NaSS incorporation. Water uptake was mainly determined

## Chapter 8

by the hydrophobicity of the comonomers, the higher the hydrophobicity the lower the water uptake.

The effect of NaSS concentration was studied from 0.175 to 3.6 wbm% for emulsifier-free seeded semicontinuous emulsion polymerization of MMA/BA at 50 wt% solids content (Chapter 5). The minimum concentration of NaSS to obtain stable latexes was determined as  $\geq 0.5\%$ . The extent of NaSS incorporation onto the polymer particles increased with the NaSS concentration, likely due to the increase of the ionic strength that caused a shift of the adsorption equilibrium of the NaSS containing oligoradicals towards the polymer particles. NaSS containing latexes displayed excellent long-term storage, freeze-thaw and salt stability compared to the control latex stabilized by SDS. Water uptake of the polymer films increased with the NaSS concentration and, for long times, was lower than that of the SDS film. The water contact angle of the films containing up to 1.3% NaSS was found to be similar before and after rinsing with water, suggesting that there was no noticeable migration of NaSS based in-situ formed surfactant. This was confirmed by the improved gloss of the films containing NaSS when compared to control latex. AFM images showed that the film-air interfaces of NaSS containing films were cleaner than control film. The cross-section of the films observed with AFM showed that the particles formed a honeycomb structure and the particle boundaries were made of the hard NaSS rich polymer. Annealing of the films at 60°C resulted in a better film formation making particle boundaries less noticeable. The films cast with NaSS containing latexes displayed higher tensile strength and lower elongation at break compared to the

## Chapter 8

control film. As the amount of NaSS increased, the Young's modulus and the yield stress increased, and the elongation at break decreased likely due to the thicker percolating structure formed by the NaSS shell of the polymer particles. Annealing enhanced the ultimate tensile strength and toughness of the films due to better film formation and better integrity gained.

The possibility of using different sulfonate monomers was also explored (Chapter 6). 3-sulfopropyl methacrylate potassium salt performed in a similar way to NaSS, however the salt and freeze-thaw stability was lower because of Hofmeister effects. 2-acrylamido-2-methylpropane sulfonic acid sodium salt and vinyl sulfonic acid sodium salt led to massive coagulation likely because they were too hydrophilic and the oligomers formed in the aqueous phase did not adsorb on the polymer particles.

The performance of emulsifier-free MMA/BA/NaSS latexes as binders in exterior paint formulation was evaluated and compared with one reference binder (provided by Synthomer) and one control binder based on a conventional emulsifier SDS. Paints prepared by using NaSS containing binders had good color development/rub, superior thickening response, excellent stability towards natural weathering and similar gloss than the control and reference paint. Efflorescence resistances were inferior to emulsifier based paints, most probably due to formation of a continuous ionic network that allow moisture migration. Excellent freeze-thaw stability (6 cycles) was found for paints containing latexes with more than 0.76% NaSS. Scrub resistance decreased with the NaSS concentration and only for a concentration of

## Chapter 8

0.76% met the performance of the reference paint. The other tests such as block resistance, alkali resistance and X-cut adhesion yielded comparable results with reference paint.

### ***Future perspectives***

A PhD Thesis has a limited time span and hence there are aspects that remain to be investigated. Some suggestions for the next PhD are as follows.

The polymer particles synthesized in this thesis generally displayed monomodal particle size distributions. It has been known that monomodal particle size distributions show a steeper increase in viscosity than bimodal or wide particle size distributions. By using these distributions, it could be possible to push the solids content even up to 70 wt%.

The mechanism of particle nucleation was not studied in the thesis. Therefore, this can be investigated in the future.

Chapter 7 scratches the surface of the application area, but broader and deeper studies are needed to take advantage of the potential of the NaSS stabilized dispersions.

## List of publications and conference presentations

Parts of this thesis have been published or will be published soon. The list of papers and conference presentations is as follows:

- S. Bilgin, R. Tomovska, J. M. Asua, "Fundamentals of chemical incorporation of ionic monomers onto polymer colloids: paving the way for surfactant-free waterborne dispersions" *RSC Advances* (6) 2016, 63754-63760.
- S. Bilgin, R. Tomovska, J. M. Asua, "Surfactant-free high solids content polymer dispersions" *Submitted to Polymer*
- S. Bilgin, R. Tomovska, J. M. Asua, "Effect of sodium styrene sulfonate concentration on latex and film properties" *In preparation*

### Poster presentations:

- Dependence of final polymer properties on the polymerization conditions in emulsions stabilized by ionic monomers, European Polymer Congress, 2015, Dresden, Germany
- Development of a process strategy for production of emulsifier-free industrial-like waterborne polymers, European Symposium on Chemical Reaction Engineering (ESCRE), 2015, Fürstenfeldbruck, Germany

**Oral presentations:**

- Synthesis and characterization of emulsifier-free high solids content waterborne polymers, 4th PhD Workshop on Polymer Reaction Engineering, 2015, Fürstenfeldbruck, Germany
- Stabilization of emulsions by using ionic monomers, 3rd PhD Workshop on Polymer Reaction Engineering, 2014, San Sebastián, Spain

## Conclusiones

El objetivo de esta tesis doctoral es producir látex libres de emulsificantes, formadores de película, con alto contenido en sólidos y coloidalmente estables, en el que la estabilidad coloidal se logra mediante restos iónicos insensibles al pH e incorporados químicamente sobre las partículas de polímero. La principal razón para evitar los tensioactivos es que reducen las propiedades deseables de las películas como el brillo, la adhesión y la resistencia al agua. Como comonómeros principales, se seleccionó una formulación de revestimiento típica MMA / BA (50/50 en peso) y el estireno sulfonato de sodio (NaSS), insensible al pH y a la temperatura, como monómero iónico.

La implementación de esta idea no fue sencilla porque tanto el MMA y BA son monómeros insolubles en agua y por lo tanto, se encuentran localizados principalmente en las partículas de polímero (y gotitas de monómero). Al contrario, NaSS es un monómero soluble en agua que está prácticamente localizado en la fase acuosa. Para obtener estabilidad en las dispersiones poliméricas durante la síntesis y almacenamiento, y para evitar los efectos negativos de las especies hidrófilas migratorias sobre las propiedades de películas en aplicación, el NaSS debe estar incorporado químicamente sobre las partículas de polímero y hay que minimizar la fracción que permanece en la fase acuosa. Además, para el uso práctico, las dispersiones deben tener un alto contenido en sólidos ( $\geq 50\%$  en peso) y formar

## Conclusiones

películas. En este trabajo se seleccionó el método de semicontinuo con siembra como estrategia del proceso porque es el método que se utiliza normalmente en la industria para obtener una calidad consistente del producto y un mejor control de la nucleación y la eliminación del calor.

La estabilidad coloidal podría lograrse desplazando el lugar de polimerización de la fase acuosa a la fase de partícula, alterando la hidrofobicidad de los oligoradicales que crecen en la fase acuosa. Esto puede lograrse variando la naturaleza del iniciador y los comonómeros con los que NaSS reacciona.

El efecto del comonómero sobre la incorporación química de NaSS sobre las partículas de polímero se estudió mediante reacciones del modelo a bajos contenidos de sólidos (Capítulo 2). Usando monómeros de diferentes funcionalidades (estireno, acrilatos, metacrilatos) y diferentes solubilidades en agua, se encontró que el factor clave que controlaba la incorporación química de NaSS era la concentración del comonómero en la fase acuosa, pero la funcionalidad no tuvo ningún papel significativo. La importancia práctica es que la incorporación química de NaSS en una dispersión hidrófoba se puede aumentar usando pequeñas cantidades de un monómero relativamente soluble en agua en la formulación.

El efecto del iniciador en la incorporación química de NaSS sobre partículas de polímero se investigó utilizando cuatro iniciadores diferentes: persulfato de potasio (soluble en agua) y azobisisobutironitrilo (soluble en la fase orgánica) como iniciadores térmicos, e hidroperóxido de terc-butilo / ácido ascórbico (generando

## Conclusiones

radicales hidrófobos en la fase acuosa) y peróxido de hidrógeno / ácido ascórbico (produciendo radicales hidrófilos en la fase acuosa) como iniciadores redox (Capítulo 3). Los resultados indicaron que la polimerización de NaSS se produce en dos lugares: en la fase acuosa, que es una polimerización en solución y en la superficie de las partículas de polímero, que se comporta como un sistema de compartimentación de radicales. En la superficie de las partículas los oligoradicales en crecimiento forman una coraza hinchada con agua, en la que se ponen en contacto monómeros con diferentes solubilidades en agua y se produce la mayor parte de la copolimerización. Se encontró que TBHP / AsAc era el iniciador más prometedor en la copolimerización semicontinua sembrada de MMA / BA / NaSS. Gracias a la alta incorporación de NaSS lograda por este sistema iniciador redox, se observaron buenas propiedades de estabilidad del látex (sal y congelación-descongelación) y de la película (sensibilidad al agua).

Se produjeron látex estables y sin emulsionantes con un 50% en peso de sólidos para una gama de monómeros. Además se produjo látex MMA / BA con un contenido en sólidos del 62% en peso y con una viscosidad aceptable utilizando NaSS (Capítulo 4). Se encontró que la incorporación química de NaSS mejoraba generalmente con la solubilidad en agua de los comonómeros. La adición de pequeñas cantidades de 2HEA en el sistema MMA / BA aumentó la incorporación de NaSS, sin embargo el MAA redujo su incorporación, indicando que la polimerización en fase acuosa era más dominante que la polimerización en las partículas de polímero. La incorporación de NaSS también mejoró con el contenido en sólidos. Los

## Conclusiones

látex que contenían NaSS presentaban mejoras en la congelación-descongelación y la estabilidad de la sal cuando se comparaban con un látex de control en el que la estabilización la proporcionaba el SDS (tensioactivo convencional). Para los látex estabilizados con NaSS, la estabilidad de congelación-descongelación fue baja para copolímeros blandos, pero para polímeros duros similares mejoró con la incorporación de NaSS. La absorción de agua se determinó principalmente por la hidrofobicidad de los comonómeros. La captación de agua era menor cuando la hidrofobicidad era mayor.

El efecto de la concentración de NaSS se estudió desde 0,175 a 3,6% en peso para el sistema MMA / BA conteniendo 50% en peso de sólidos (capítulo 5). La concentración mínima de NaSS para obtener látex estables se determinó como 0,5%. El grado de incorporación de NaSS en las partículas de polímero aumentó con la concentración de NaSS, probablemente debido al aumento de la fuerza iónica que provocó un cambio del equilibrio de adsorción de los oligoradicales que contenían NaSS hacia las partículas de polímero. Los látex que contenían NaSS exhibían una excelente estabilidad durante el almacenamiento a largo plazo, en ciclos de congelación-descongelación y al añadir sales en comparación con el látex con SDS. La absorción de agua de las películas poliméricas aumentó con la concentración de NaSS y, durante largos períodos, fue inferior a la de la película de SDS. Se encontró que el ángulo de contacto con agua de las películas que contenían hasta un 1,3% de NaSS era similar antes y después del lavado con agua, lo que sugiere que no se observó una migración notable del surfactante formado in situ basado en NaSS. Esto

## Conclusiones

fue confirmado por una mejora del brillo de las películas que contienen NaSS cuando se compara con el látex de control. Las imágenes de AFM mostraron que las interfaces de película-aire de películas que contenían NaSS estaban más limpias que la película de control. La sección transversal de las películas observadas con AFM mostró que las partículas formaban una estructura tipo colmena y los límites de las partículas estaban llenos del polímero rico en NaSS. El recocido de las películas a 60°C resultó en una mejor formación de la película y los límites de las partículas fueran menos perceptibles. Las películas que contenían NaSS exhibían una resistencia a la tracción y un alargamiento de rotura más bajos en comparación con la película de control. A medida que aumentaba la cantidad de NaSS, aumentaba el módulo de Young y la tensión elástica, y el alargamiento a la rotura disminuyó probablemente debido a la estructura de percolación más gruesa formada por la envoltura de NaSS de las partículas de polímero. El recocido aumentó la resistencia a la tracción y la tenacidad de las películas debido a una mejor formación de película y una mejor integridad ganada.

También se exploró la posibilidad de utilizar diferentes monómeros de sulfonatos (Capítulo 6). 3-sulfopropil metacrilato de potasio se usó de una manera similar al NaSS, sin embargo la estabilidad de la congelación-descongelación y de la sal fue menor debido a los efectos Hofmeister. La sal sódica de ácido 2-acrilamido-2-metilpropanosulfónico y la sal sódica del ácido vinilsulfónico condujeron a una coagulación masiva probablemente porque eran demasiado hidrófilas y los

## Conclusiones

oligómeros formados en la fase acuosa no se adsorbían sobre las partículas de polímero.

Se evaluó el rendimiento de los látex MMA / BA / NaSS libres de emulsionantes como aglutinantes en la formulación de pintura exterior y se comparó con un aglutinante de referencia (proporcionado por Synthomer) y un aglutinante de control basado en un emulsionante convencional (SDS). Las pinturas preparadas utilizando aglutinantes que contenían NaSS presentaban un buen desarrollo del color / frotado, una respuesta de espesamiento superior, una excelente estabilidad frente a la intemperie natural y un brillo similar al de la pintura de control y de referencia. Las resistencias a la eflorescencia fueron inferiores a las pinturas a base de emulsionantes, muy probablemente debido a la formación de una red iónica continua que permite la migración de la humedad. Se encontró una excelente estabilidad congelación-descongelación (6 ciclos) para pinturas que contenían látex con más de 0,76% de NaSS. La resistencia al frotado disminuyó con la concentración de NaSS y sólo para una concentración de 0,76% cumplió el rendimiento de la pintura de referencia. Los resultados de otros ensayos como la resistencia al bloque, resistencia al álcali, X-cut adhesión, son comparables con la pintura de referencia.

## Appendix I. Properties of NaSS and Poly(NaSS)

### I.1. Introduction

In order to copolymerize monomers in emulsion polymerization, it is very important to determine precisely their distribution between the phases and how it will be altered by presence of the each other. Quantitatively, the distribution is determined by partitioning coefficient (K), which is the ratio of the concentration of the monomer of interest in the organic phase to that in the aqueous phase (Equation I-1)

$$K_{\text{monomer}} = [\text{Monomer}]_{\text{organic}} / [\text{Monomer}]_{\text{aqueous}} \quad (\text{I-1})$$

K might be affected by temperature, pH, and ionic strength of the medium and relative concentration of other monomers<sup>1</sup> and may influence significantly the extent of polymerization in different phases.

In the following, the preliminary study aimed to determine how NaSS and its homopolymer distribute between water and organic phase (MMA/BA) is presented. In addition, it was checked if NaSS and its homopolymer can form micelles. Surface tension of their aqueous solutions was determined, attempting to determine their surface activity.

## Appendix I

### **I.2. Experimental**

#### **I.2.1. Materials**

The monomers, methyl methacrylate (MMA, purity 99.9%, 45-55 ppm MEHQ, Quimidroga), n-butyl acrylate (BA, purity 99.5%, 10-20 ppm MEHQ, Quimidroga), sodium p-styrene sulfonate (NaSS, purity  $\geq 90\%$ , Sigma Aldrich) and the initiator potassium persulfate (KPS, Sigma Aldrich) were used as received. Hydroquinone (HQ, purity: 99%, Panreac) and 1-pentanol (Fluka, purity  $\geq 99\%$ ) were used without further purification. In critical micellar concentration (CMC) measurements, an aqueous solution of poly(sodium styrene sulfonate) (P(NaSS), average Mw: 70 kDa, Sigma Aldrich, 30 wt% in water) was utilized. Deionized water was used throughout the work.

#### **I.2.2. Methods**

##### **I.2.2.1. Partitioning coefficient of NaSS**

In order to determine  $K_{\text{NaSS}}$ , a series of mixtures containing MMA, BA, water and NaSS were prepared. MMA and BA constitute the organic phase. All the ingredients were weighed into glass bottles (Table I.1). Finally, 115 ppm hydroquinone (HQ) was added to ensure that no polymerization takes place.  $K_{\text{NaSS}}$  were determined at two temperatures, 23°C and 70°C. The mixtures were kept at each temperature in

Appendix I

shaking bath. After 4 hours, the contents were transferred into separatory funnels for extractions. The aqueous phases extracted were diluted with water and analyzed by UV-Vis spectrophotometer (UV-2500 PC Series, Shimadzu).

**Table I.1.** The composition of mixtures prepared to determine  $K_{\text{NaSS}}$  at 23°C and 70°C

NaSS (g)	H <sub>2</sub> O (g)	MMA (g)	BA (g)	
0.125	25	25	0	
		0	25	
		12.5	12.5	
0.25		25	0	
		0	25	
		12.5	12.5	
0.75		25	0	
		0	25	
		12.5	12.5	
0		25	25	-

In order to determine the concentration of NaSS in the aqueous phase  $[\text{NaSS}]_{\text{aqueous}}$ , first a calibration plot based on the absorption of aromatic ring of NaSS at 254.50 nm was prepared. The calibration plot is given in Figure I.1.

Some representative UV absorbance curves of the aqueous parts of a series of NaSS/H<sub>2</sub>O/MMA/BA mixtures are given in Figure I.2.

Appendix I

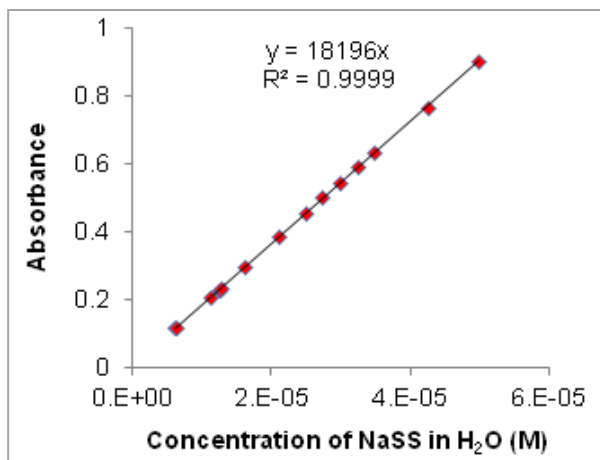


Figure I.1. Calibration plot for absorbance of NaSS solutions in water ( $\lambda = 254.50$  nm)

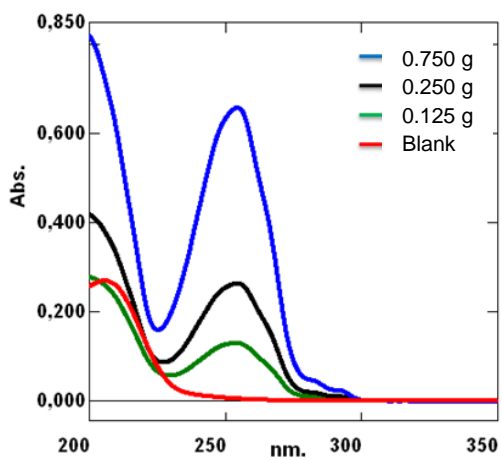


Figure I.2. The absorbance curves of aqueous parts obtained from extractions for NaSS/H<sub>2</sub>O/MMA/BA mixtures at 70°C; blue: 0.75/25/12.5/12.5, black: 0.25/25/12.5/12.5, green: 0.125/25/12.5/12.5 and red: 0/25/25/0 (weight ratios)

## Appendix I

### I.2.2.2. Effect of NaSS amount on monomer partitioning

In order to investigate the effect of NaSS amount on  $K_{\text{MMA}}$ , a series of mixtures containing MMA (25 g), water (25 g), variable NaSS amounts (0-0.75 g) and HQ (115 ppm) were prepared. The mixtures were kept in shaking bath either at 23°C or 70°C. After 4 hours, extractions were performed as described previously. Aqueous phases were diluted with water and analyzed in by Gas Chromatography (Agilent 6890 plus GC equipped with BP-20 column). In order to determine the concentration of MMA in the aqueous phase  $[\text{MMA}]_{\text{aqueous}}$ , first a calibration curve was prepared. 1-pentanol served as the internal standard. The calibration plot used to determine  $[\text{MMA}]_{\text{aqueous}}$  is given in Figure I.3.

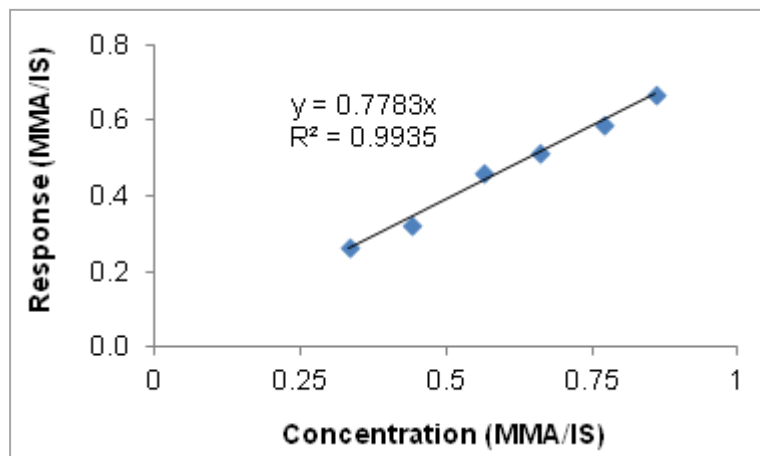


Figure I.3. Calibration plot for the relative response of MMA in gas chromatography as a function of relative concentration (IS: internal standard)

## Appendix I

### **I.2.2.3. Homopolymerization of NaSS**

Free radical polymerization of NaSS was performed in water at a solids content of 3 wt% and a temperature of 70°C by using KPS as initiator (0.8% wbm). The samples were taken at certain intervals for analysis. For conductivity and pH measurements, Crison 5292 conductivity cell and Crison 5209 glass electrode were utilized, respectively. The surface tension of the samples was measured by KSV Sigma 700 tensiometer, using a platinum Du Nouy ring. All measurements were performed at 23°C. The polymerization was followed by <sup>1</sup>H-NMR (Bruker Avance-400 instrument) using deuterium oxide (D<sub>2</sub>O). The conversion of NaSS was calculated by integration of one of the vinyl hydrogen peaks giving doublet at 5.3 ppm in <sup>1</sup>H-NMR spectra.

### **I.2.2.4. Critical Micellar Concentration (CMC)**

In order to determine if NaSS and P(NaSS) form micelles in water, surface tension measurements were performed at 23°C and 55% relative humidity by using a platinum Du Nouy ring in KSV Sigma 700 tensiometer. The change in surface tension was recorded as the aqueous solution of NaSS or P(NaSS) was added by means of a controlled addition pump (Dosimat 665) onto the water in the vial.

### I.3. Results and Discussion

#### I.3.1. Partitioning coefficient of NaSS

$K_{\text{NaSS}}$  values at 23°C and 70°C are given in Table I.2. All K values were very close to 0 showing that the NaSS content the organic phase was negligible regardless of temperature and composition. Some of the K values were found to be negative. This error was due to a high concentration of NaSS in the aqueous phase. Small errors in the concentration in the aqueous phase can lead to huge relative error in the concentration in the organic phase.

**Table I.2.** The amounts of NaSS, MMA and BA in the mixtures and calculated  $K_{\text{NaSS}}$  values at 23°C and 70°C

NaSS (g)	MMA (g)	BA (g)	H <sub>2</sub> O (g)	$K_{\text{NaSS}}$ (at 23°C)	$K_{\text{NaSS}}$ (at 70°C)
0.125	25	0	25	-0.061	-0.030
	0	25		0.016	-0.006
	12.5	12.5		-0.047	-0.033
0.25	25	0		-0.081	0.090
	0	25		-0.034	-0.014
	12.5	12.5		-0.010	0.005
0.75	25	0		0.037	0.009
	0	25		-0.020	-0.014
	12.5	12.5		-0.021	-0.019

## Appendix I

### I.3.2 Effect of NaSS amount on monomer partitioning

$K_{MMA}$  values at 20°C and 70°C for the mixtures with fixed MMA and water but varied NaSS amounts are given in Table I.3. As NaSS content increased, the water solubility of MMA decreased slightly. Since the effect was relatively small, the study was not performed for BA.

**Table I.3.**  $K_{MMA}$  values at 23°C and 70°C for different NaSS amounts in the mixtures

NaSS (g)	H <sub>2</sub> O (g)	MMA (g)	$K_{MMA}$ (at 23°C)	$K_{MMA}$ (at 70°C)
0	25	25	221	236
0.125			237	246
0.250			264	240
0.750			302	275

### I.3.3. Homopolymerization of NaSS

<sup>1</sup>H-NMR spectra of the samples taken during polymerization of NaSS are presented in Figure I.4 and calculated conversions are given in Table I.4. As can be seen, almost 80% of NaSS reacted in the first 60 minutes. Within the next hour, conversion increased to 91%. After 24 hours of reaction time, 97% of NaSS reacted.

Appendix I

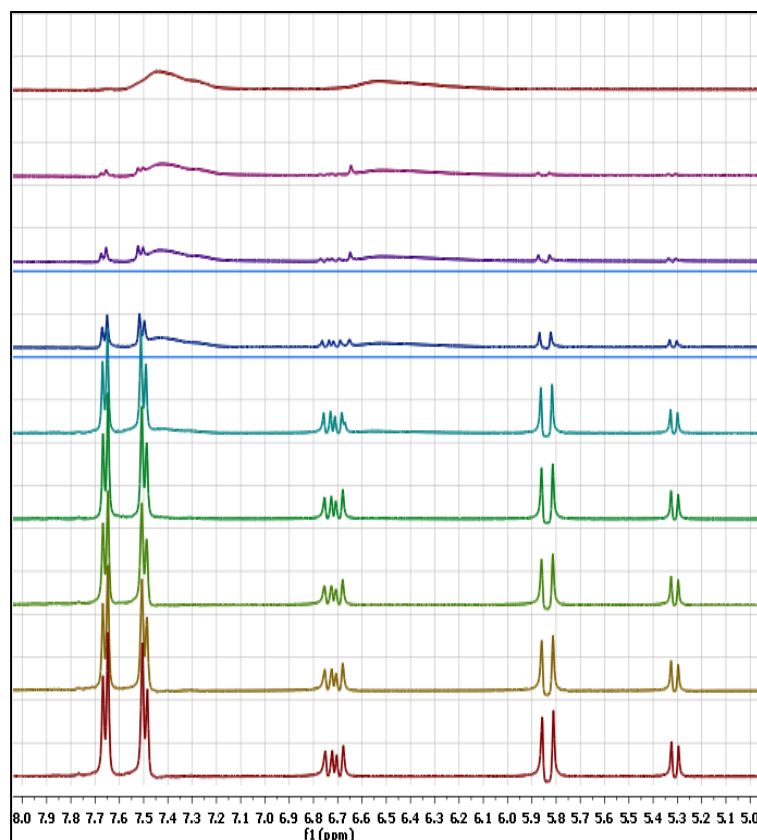


**Table I.4**  
Conversion of NaSS with time

time (min)	Conversion of NaSS (%)
0	0
2	16
5	19
10	21
21	33
40	75
61	79
89	90
121	91
164	95
269	96
420	96
1440	97

Figure I.4. <sup>1</sup>H-NMR spectra for homopolymerization of NaSS. The peaks decrease in intensity as reaction proceeds (from bottom to up)

Figure I.5 depicts conductivity, pH and surface tension evolutions during homopolymerization reaction. The conductivity of the reaction mixture decreased significantly in the first 60 minutes during which 80% of NaSS reacted (Figure I.5a). Although homopolymer was also ionic, the mobility of long chains is significantly less than that of the monomer hence the conductivity was mainly controlled by the amount

## Appendix I

of unreacted NaSS showing a linear decrease with NaSS consumption (Figure I.5b). On the other hand, pH that was around 7.6 in the beginning declined to 4.6. The decrease in pH was not dependent on NaSS content (Figure I.5d) but was mainly determined by the decomposition of KPS as demonstrated by pH vs reaction time plot (Figure I.5c). Figure I.5e shows that at low conversions, there was a linear relationship between surface tension and conversion. Unreacted NaSS was likely adsorbed in air-liquid interface resulting in a lower surface tension. This relationship was lost at high conversions. The scattered surface tension data at high conversions indicate that the measurements could be affected by many parameters such as the amount of NaSS and P(NaSS), the change in pH of the bulk.

Homopolymerization reaction in water showed that P(NaSS) is also completely water soluble.

Appendix I

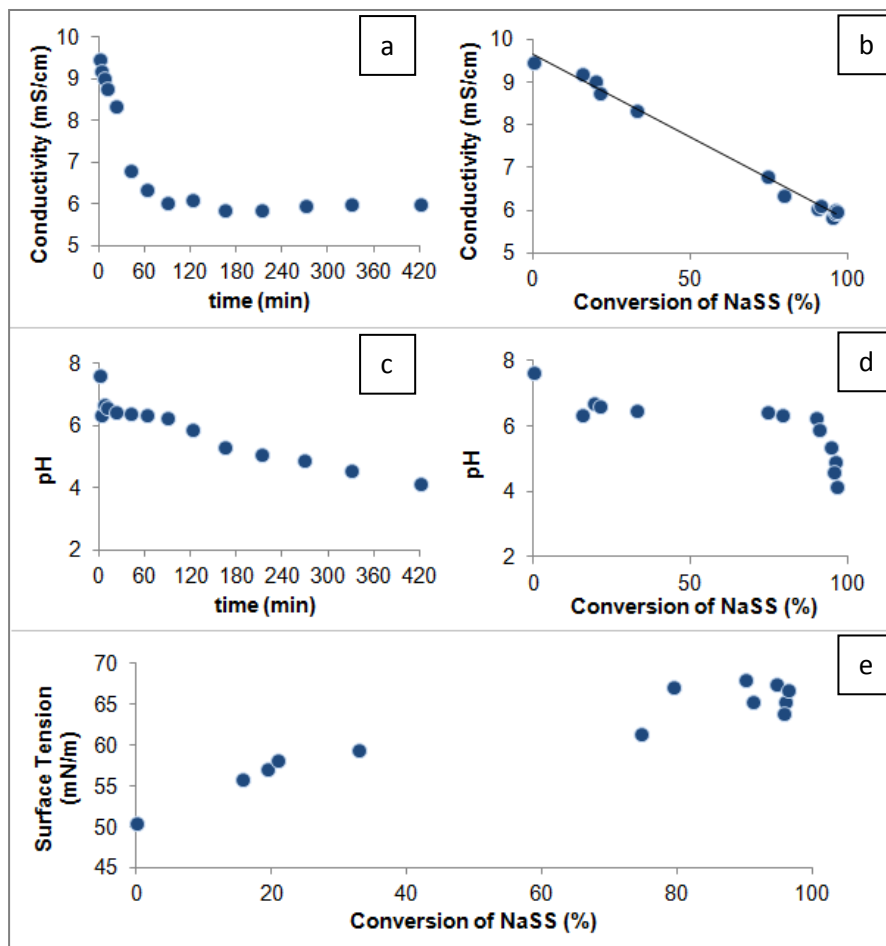


Figure 1.5. a,b) Conductivity, c,d) pH and e) surface tension change during homopolymerization of NaSS

## Appendix I

### I.3.4. Critical Micellar Concentration of NaSS and P(NaSS)

In order to determine if NaSS and its homopolymer P(NaSS) were able form micelles in water, surface tension of their aqueous solutions was measured as a function of concentration (Figure I.6). At low concentrations of NaSS and P(NaSS) surface tension was found to be close to that of water. As concentration increased (after 8.1 g/L for NaSS and 2.5 g/L for P(NaSS)), surface tension values started to decrease monotonically. This behavior differs from that of low molecular weight ionic or nonionic surfactants for which the decrease in surface tension starts at very low concentrations. For water soluble polyelectrolytes such as P(NaSS) surface tension was reported to decrease only at relatively high concentrations.<sup>2</sup>

The decay in surface tension was faster for P(NaSS) than that for NaSS indicating a higher surface activity for P(NaSS). NaSS is highly water soluble small molecule (solubility NaSS: 19.6 wt%)<sup>3</sup> that has only a limited tendency to go to the air/water interface. However, P(NaSS) have a hydrophobic backbone and hydrophilic sulfonate groups in the structure, thus it distributes on the water air interface, where the hydrophobic part is exposed to the air whereas the hydrophilic parts are submerged in the liquid.<sup>4</sup>

Neither NaSS nor P(NaSS) displayed a CMC indicating that they are completely soluble in water in the range of concentrations studied.

Appendix I

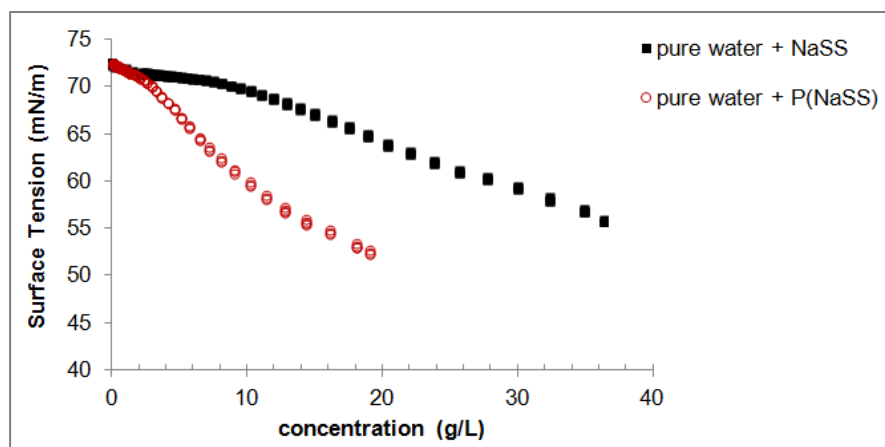


Figure I.6. Surface tension evolution with NaSS / P(NaSS) concentration

## Appendix I

### I.4. References

- [1] Pichot, C., Recent developments in the functionalization of latex particles. *Makromolekulare Chemie. Macromolecular Symposia* **1990**, 35(1), 327-347
- [2] Noskov, B.A., Nuzhnov, S.N., Loglio, G. and Miller, R., Dynamic surface properties of sodium poly (styrenesulfonate) solutions. *Macromolecules* **2004**, 37(7), 2519-2526.
- [3] Spinomar NaSS Brochure, Tosoh USA. Online access:  
<http://www.tosohusa.com/products--services/sodium-styrenesulfonate>
- [4] Yim, H., Kent, M.S., Matheson, A., Stevens, M.J., Ivkov, R., Satija, S., Majewski, J. and Smith, G.S., Adsorption of sodium poly (styrenesulfonate) to the air surface of water by neutron and X-ray reflectivity and surface tension measurements: polymer concentration dependence. *Macromolecules* **2002**, 35(26), 9737-9747.

## **Appendix II. Materials and characterization methods**

### **II.1. Materials**

The monomers, 2-hydroxy ethyl acrylate (2HEA, purity 96%, 200-650 ppm monomethyl ether hydroquinone - MEHQ, Sigma Aldrich), butyl acrylate (BA, purity 99.5%, 10-20 ppm MEHQ, Quimidroga), butyl methacrylate (BMA, purity 99%, 10 ppm MEHQ, Sigma Aldrich), ethyl acrylate (EA, purity 99%, 10-20 ppm MEHQ, Acros), ethyl methacrylate (EMA, purity 99%, 15-20 ppm MEHQ, Sigma Aldrich), methyl acrylate (MA, purity 99%,  $\leq$  100 ppm MEHQ, Sigma Aldrich), methyl methacrylate (MMA, purity 99.9%, 45-55 ppm MEHQ, Quimidroga), styrene (S, purity 99.7%, 10-20 ppm tert-butyl catechol - TBC, Quimidroga), vinyl acetate (VAc, Quimidroga), neodecanoic acid vinyl ester (VeoVa10, Hexion), and sulfonate monomers sodium p-styrene sulfonate (NaSS, purity  $\geq$  90%, Sigma Aldrich), 3-sulfopropyl methacrylate potassium salt (KSPM, purity: 98%, Sigma Aldrich), 2-acrylamido-2-methylpropanesulfonic acid sodium salt (AMPS, 50 wt. % in H<sub>2</sub>O, Sigma Aldrich), vinyl sulfonic acid sodium salt (VS, 25 wt. % in H<sub>2</sub>O, Sigma Aldrich), were used as received.

## Appendix II

The initiators potassium persulfate (KPS, purity  $\geq 99\%$ , Sigma Aldrich), azobisisobutyronitrile (AIBN, purity 98%, Sigma Aldrich), tert-butyl hydroperoxide (TBHP, 70 wt% aqueous solution, Luperox Sigma Aldrich), hydrogen peroxide (H<sub>2</sub>O<sub>2</sub>, 30 wt% aqueous solution, Sigma Aldrich), ascorbic acid (AsAc, purity  $\geq 99\%$ , Acros) were used without further purification.

Sodium dodecyl sulfate (SDS, Sigma-Aldrich), hydroquinone (HQ, purity 99%, Panreac) and dimethyl formamide (DMF, chromatography grade, Fisher) were used as received. The nonionic emulsifier Disponil A3065 was provided by BASF. Deionized water was used throughout the work.

### II.2. Estimation of reactivity ratios of NaSS and various comonomers using Alfrey and Price Q-e scheme

The material balance for NaSS (A) in the aqueous phase is

$$\frac{dA}{dt} = -(k_{pAA} P_A M_A + k_{pBA} P_B M_A) [R]_w \quad (\text{II-1})$$

where A is NaSS, B the comonomer,  $k_{p_{ij}}$  the propagation rate coefficient between radical i and monomer j,  $M_i$  the number of moles of monomer i,  $[R]_w$  the concentration of radicals in the aqueous phase and  $P_i$  the probability of having a radical terminated in monomer i given by

## Appendix II

$$P_A = \frac{k_{PBA} M_A}{k_{PBA} M_A + k_{PAB} M_B} ; \quad P_B = 1 - P_A \quad (II-2)$$

Equation II-2 shows that as  $M_B$  increases  $P_A$  decreases and  $P_B$  increases. Therefore the condition for an increase in the NaSS consumption as  $M_B$  increases is that  $k_{PBA} > k_{PAA}$ .

The reactivity ratios were calculated using the Alfrey and Price Q-e scheme <sup>[1]</sup> using the Q and e values given in Table II.1.

**Table II.1.** Q and e values

	Q	e
NaSS <sup>[2]</sup>	2.0	-0.4
MMA <sup>[1]</sup>	0.78	0.4
EMA <sup>[1]</sup>	0.76	0.17
BMA <sup>[1]</sup>	0.82	0.28
2HEA <sup>[3]</sup>	0.75	0.65
MA <sup>[1]</sup>	0.45	0.64
EA <sup>[1]</sup>	0.41	0.55
BA <sup>[1]</sup>	0.38	0.85
S <sup>[1]</sup>	1.0	-0.8

Table II.2 presents the reactivity ratios of NaSS with different comonomers. In all cases  $r_1 > 1$  and  $r_2 < 1$ . Considering that the homopolymerization rate coefficient of styrenic monomer is substantially lower than those of the (meth)acrylates, <sup>[4]</sup>  $k_{PBA}$  is

## Appendix II

greater than  $k_{pAA}$  for the methacrylate and acrylate monomers. Therefore, NaSS consumption increases as  $M_B$  increases.

**Table II.2.** Estimated reactivity ratios of NaSS with different monomers.

Monomer 1	Monomer 2	r1	r2
NaSS	MMA	1.862	0.283
	EMA	2.095	0.345
	BMA	1.858	0.339
	2HEA	1.752	0.190
	MA	2.932	0.116
	EA	3.336	0.122
	BA	3.192	0.066
S	2.347	0.363	

## II.3. Characterizations

### II.3.1. Characterization of latexes

**The conversion of volatile monomers** was determined gravimetrically. Approximately 1 mL latex samples were withdrawn from the reactor and transferred into aluminum cups having 1-2 drops of aqueous solution of hydroquinone (1 wt% in water). The aliquots in Al cups were kept for 2-3 hours in the fume hood, and then dried in oven at 60°C overnight.

## Appendix II

**The conversion of NaSS** for the final latexes was determined by using  $^1\text{H-NMR}$  Spectroscopy (Bruker Avance-400). In order to quantify the amount of unreacted NaSS in the final latexes, DMF was used as a reference. DMF gives an intense amide hydrogen peak around 7.8 ppm and vinyl hydrogen doublets of NaSS appear at 5.85 and 5.90 ppm.

A set of mixtures were prepared by mixing 10  $\mu\text{L}$  of 142.5 mM DMF reference solution with 5-70  $\mu\text{L}$  of 48.5 mM or 100-500  $\mu\text{L}$  of 0.370 mM NaSS solution directly in NMR tubes. After 50  $\mu\text{L}$   $\text{D}_2\text{O}$  was introduced to each tube, the total volumes of the mixtures were adjusted to 560  $\mu\text{L}$  with ultra pure water. From  $^1\text{H-NMR}$  spectra of the mixtures, the absolute areas for singlet amide peak of DMF at 7.80 ppm and vinyl hydrogen doublets of NaSS appearing at 5.85 and 5.90 ppm were calculated. The calibration curve was obtained by plotting the ratio of these absolute areas against the ratio of NaSS weight to the moles of DMF (Figure II.1).

For the final latexes, 250  $\mu\text{L}$  of latex, 250  $\mu\text{L}$  of deionized water, 10  $\mu\text{L}$  of DMF reference solution and 50  $\mu\text{L}$   $\text{D}_2\text{O}$  was introduced into the NMR tube. The ratio of the areas of the peaks of interest was calculated from  $^1\text{H-NMR}$  spectra and corresponding weight of NaSS in the sample could be determined by using the calibration curve. For the spectra in which vinyl hydrogen doublets at 5.85 and 5.90 ppm were not observed, NaSS was said to be fully converted.

## Appendix II

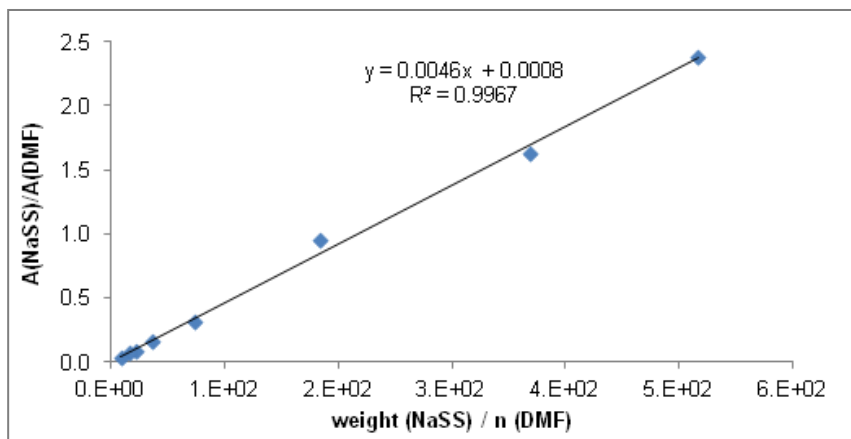


Figure II.1. Calibration curve used for quantification of unreacted NaSS in the final latexes

**The conversion of KSPM** for the final latex (Chapter 6) was determined by using  $^1\text{H-NMR}$  Spectroscopy (Bruker Avance-400) by using a similar method as NaSS. DMF (reference) gives the amide hydrogen peak around 7.8 ppm and one of the hydrogens of the double bond of KSPM appears at 6.0 ppm.

A set of mixtures were prepared by mixing 10  $\mu\text{L}$  of 137.8 mM DMF reference solution with 5-50  $\mu\text{L}$  of 10.4 mg/mL KSPM solution directly in NMR tubes. After 50  $\mu\text{L}$   $\text{D}_2\text{O}$  was introduced to each tube, the total volumes of the mixtures were adjusted to 560  $\mu\text{L}$  with ultra pure water. From  $^1\text{H-NMR}$  spectra of the mixtures, the absolute areas for the amide peak of DMF (7.8 ppm) and for one of the hydrogens of the double bond of KSPM (6.0 ppm) were calculated to make a calibration curve (Figure II.2).

## Appendix II

For the final latexes, 250  $\mu\text{L}$  of latex, 250  $\mu\text{L}$  of deionized water, 10  $\mu\text{L}$  of DMF reference solution and 50  $\mu\text{L}$   $\text{D}_2\text{O}$  was introduced into the NMR tube. The ratio of the areas of the peaks of interest was calculated from  $^1\text{H-NMR}$  spectra and corresponding weight of KSPM in the sample could be determined by using the calibration curve.

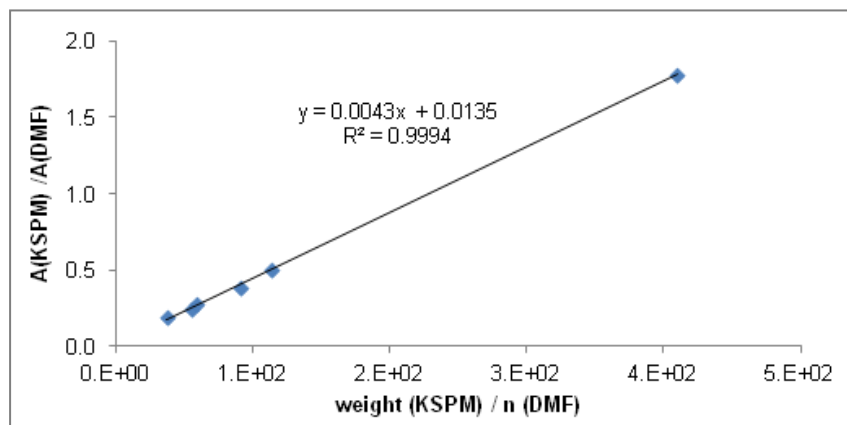


Figure II.2. Calibration curve used for quantification of unreacted KSPM in the final latexes

**Z-average particle diameter** was measured at 25°C by using dynamic light scattering (DLS) Malvern ZetaSizer Nano-S instrument equipped with a 633 nm red laser. Before the analysis, the samples withdrawn from the reactor were diluted 1000 times with deionized water to prevent multiple scattering. The Z-average particle

## Appendix II

diameters measured were used to calculate the evolution of number of particles ( $N_p$ ) during the reactions.

**Particle size distributions** were obtained by using capillary hydrodynamic fractionation in a CHDF-2000 instrument (Matec Applied Sciences). The samples were run at a carrier rate of 1.4 mL/min at 35°C (¼ GR 500 carrier from Matec).

**The amount of coagulum** was calculated based on the total solids content of the latex. The final latex was filtered through a mesh to collect the coagulum. After the discharge of the latex from the reactor, the coagulum around the nitrogen tube, thermocouple, agitator and the reactor wall was also carefully taken. The coagula were combined, washed several times with water, dried in oven at 60°C and weighed.

**The gel fraction** was determined by Soxhlet extraction with THF for 16 hours. The THF-soluble part was kept for molecular weight analysis.

**The molecular weight distribution of the THF-soluble polymer** was measured in a GPC system equipped with three columns in series (Styragel HR2, HR4 and HR6) and a refractive index detector (Waters 2410). THF was used as mobile phase at 1 mL/min flow rate at 35°C. PS standards were used for calibration.

**The molecular weights** of whole polymers were measured in an Agilent PL-GPC 50 integrated Gel Permeation Chromatography system using DMF (10 mM LiBr) as mobile phase at 50°C and a flow rate of 1 mL/min was utilized.

## Appendix II

**The amount of water soluble species** was calculated based on the total solids content of the latex. The diluted latexes (12.5 wt% solids contents) were ultracentrifugated at 30000 RPM for 2 hours at 4°C. The serum parts were carefully taken with a syringe and dried at room temperature for 2 days under air purge and the dry residues were assigned as water soluble species. For each latex, average of 4 measurements was reported.

**The incorporation of NaSS** was calculated by titration of the dialyzed and ion exchanged latexes. The latexes were diluted to 2.5 wt% solids content and dialyzed against ultrapure water by using Spectra-Por®4 membranes (Mw cut-off 12,000-14,000 Da) until constant conductivity. The dialyzed latexes were then passed through a Dowex Marathon MSC cation exchange resin in order to substitute Na<sup>+</sup> of the sulfonate groups by titratable H<sup>+</sup> form. After ion exchange, the latexes were titrated conductimetrically against 5 mM NaOH.

For the latexes in which TBHP/AsAc and H<sub>2</sub>O<sub>2</sub>/AsAc was used as initiator, NaSS incorporation was calculated as  $n/\text{NaSS}_{\text{total}}$ , where n is number of moles of NaOH used in the titration until the end point and NaSS<sub>total</sub> is the total number of moles of NaSS in the formulation.

In Chapter 2, the latexes with 2HEA, MA and BA were also dialyzed by using Spectra-Por®6 membranes with a higher cut-off (50,000 Da) to investigate whether the M<sub>w</sub> cut-off of the membrane had an effect on the cleaning of latexes. No effect of the membrane cut-off on the NaSS incorporated was observed.

## Appendix II

In Chapter 3, for the latexes in which KPS was used, since the consumption of NaOH by sulfate and sulfonate groups were indistinguishable in the titration, the contribution of KPS was subtracted. It was assumed that all decomposed portion of KPS was incorporated chemically onto the polymer particles, so the NaSS incorporation was calculated as  $(n - n_{\text{sulfate}}) / \text{NaSS}_{\text{total}}$  where  $n$  is number of moles of NaOH used in the titration until the end point,  $n_{\text{sulfate}}$  is the number of moles of sulfate groups coming from the decomposed fraction of KPS and  $\text{NaSS}_{\text{total}}$  is the total number of moles of NaSS in the formulation. The decomposed portion of KPS was estimated by the calculation given below:

The amount of KPS remained undecomposed after the reaction [I] is given by the equation:

$$[I] = [I]_0 \exp(-k_d \cdot t) \quad (\text{II-3})$$

where  $[I]_0$  is the initial concentration of KPS,  $k_d$  is the rate constant for decomposition of KPS and  $t$  is the time.

The values used:

$$[I]_0 = 0.01346 \text{ M}$$

$$k_d = 8 \times 10^{15} \exp(-135.0/RT), \text{ at } 70^\circ\text{C } k_d = 2.25 \times 10^{-5} \text{ s}^{-1}$$

$$t = 19800 \text{ s (5.5 h)}$$

## Appendix II

[I] was calculated as  $8.7 \times 10^{-3}$  M which corresponds to 2.512 mmole KPS unreacted. Since the initial amount of KPS is 3.884 mmole, the amount decomposed is 1.372 mmole.

In Chapters 3-5, the ion exchange and titration steps were also performed on as-produced latexes to investigate whether some of NaSS was buried inside the particles. 100% of the sulfonates (and sulfates where applicable) was detected so it was concluded that no NaSS was buried inside the particles.

**The surface tension** of the latex samples was measured in KSV Sigma 700 tensiometer by using a platinum Du Nouy ring.

**Conductivity and pH measurements** were performed by using Crison 5292 conductivity cell and Crison 5209 glass electrode, respectively.

**Salt tolerance tests** Stability of latexes towards electrolyte addition was studied by adding 5 g of a saline solution onto 5 g of latex (as produced). After 24 h of rest at room temperature, the particle size was measured.

**Freze-thaw stability** One cycle consists of exposure of 5 g of as produced latex first to freezing at  $-20^{\circ}\text{C}$  for 24 hours and then thawing at room temperature for 24 hours. Later, the particle size was measured to check the stability.

## Appendix II

### II.3.2. Characterization of polymer films

**Static water contact angle measurements** were performed according to the standard sessile drop method by using Data Physics OCA 20 model goniometer. The films of 120  $\mu\text{m}$  thicknesses were cast from latexes on glass substrates and dried for 24 hours at 23°C and 55% relative humidity. 5  $\mu\text{L}$  deionized water was placed on the films and an average of minimum 10 measurements taken from different locations on the surface was reported. Then, the films were rinsed with deionized water for 20 minutes and dried in the same conditions for another 24 hours. The contact angle measurements were repeated.

**Water uptake measurements** For water uptake test, rectangular samples of dimensions 1cmx4 cm and 0.16 cm thickness were prepared in Teflon molds and dried at 23°C and 55% relative humidity until constant weight. Each sample was left in 100 mL deionized water. At some intervals, the films were taken out of the vials, smoothly blotted with paper and weighed. The water uptake was calculated in relation to the initial dry weight of the sample. After water uptake test, the samples were taken, dried at 23°C and 55% relative humidity for 2 days and then at 60°C for one day. The samples were reweighed to calculate the weight loss compared to the initial weight of the sample before the test.

In Chapter 4, the dimensions of the samples used for water uptake measurements were 1.8cmx4cmx0.1cm. After drying in ambient conditions, the films were kept at 60°C overnight, then the water uptake test was performed.

## Appendix II

**Gloss** 120  $\mu\text{m}$  films were cast on smooth, matte and black substrates (plasticizer-free vinyl chloride /acetate copolymer) and dried at 23°C, 55% relative humidity. After 2 weeks, the measurements were performed by using BYK micro-TRI-gloss meter. Gloss of the substrate is 0.1 (at 20°) and 1.4 (at 60°).

**Atomic force microscopy (AFM)** The films were prepared by casting the latexes into silicone molds and letting them dry until constant weight at a temperature of 23°C and 55% relative humidity. Tapping mode AFM phase and height images of polymers were captured under ambient conditions using a Veeco NanoScope IV MultiMode AFM. Some of the films were rinsed with deionized water for 20 minutes and dried in the same conditions for another 24 hours. The AFM imagings were repeated.

**Thermogravimetric analysis (TGA)** was performed by using a TA instruments Q500 device. The samples were heated from room temperature to 800°C with a heating rate of 10°C/min under  $\text{N}_2$  atmosphere.

**Differential Scanning Calorimeter (DSC)** experiments were performed in a TA instruments Q2000. 3-5 mg of samples, which were placed in aluminum hermetic pans, were first heated to 150°C with a heating rate of 10°C/min and kept isothermal for 2 minutes. Then, they were cooled down to -70°C with a cooling rate of 10°C/min and kept isothermal for 2 minutes. The second heating run carried out at 10°C/min was used to determine the glass transition temperature ( $T_g$ ) of the polymers.

## Appendix II

**Minimum film forming temperature (MFFT)** The measurements were carried out in a bench top instrument which consists of a steel plate with an adjustable temperature gradient along. 120  $\mu\text{m}$  films were applied onto the plate and the visual inspection was performed after 1.5 hours. MFFT was taken as the temperature at which the film was optically clear and mechanical integrity was gained (proven with the help of a metal spatula).

**Mechanical tests** The films were cast in Teflon molds and dried at 23°C and 55% relative humidity for one week, followed by vacuum drying at room temperature for 1 day. Some films were later annealed at 60°C for 2 days and then at 60°C under vacuum for 1 day. Dogbone shaped specimens were punched out of 1 mm thick films. The stress-strain tests were performed in a TA.HD Plus Texture Analyzer, at 23°C and 55% relative humidity, by applying a cross-head speed of 25 mm/min. For each polymer at least five specimens were tested.

**Moisture permeability (P)** was measured using a gravimetric cell. The films with 150  $\mu\text{m}$  thicknesses were cast on polyethylene sheets by using a film applicator and dried in a controlled environment (23°C and 55% relative humidity) for one day. The film was then attached to the open mouth of the gravimetric cell containing water so that the film is exposed to water without touching (100% relative humidity). The cell was well-sealed so that the water could only escape by permeating through the film and it was placed on a balance within a temperature controlled chamber (25°C) to measure the loss of weight during time. The moisture permeability ( $\text{g mm/m}^2 \text{ day}$ )

## Appendix II

was calculated from the slope of the weight loss (water loss) versus time plot by using the formula

$$P = \frac{m f}{A (a_{\text{int}} - a_{\text{ext}})} \quad (\text{II-4})$$

where  $m$  is the slope of the curve,  $f$  is the film thickness,  $A$  is the area of contact between the film and water vapor ( $2.54 \text{ cm}^2$ ),  $a_{\text{int}}$  is the water vapor activity in the headspace of the cell (considered to be 1) and  $a_{\text{ext}}$  is the water vapor activity in the chamber.

**Viscosity** of the latexes was measured at  $25^\circ\text{C}$  by using a TA instruments AR 1500 model rheometer. A stainless steel flat plate with 60 mm diameter was utilized at  $500 \text{ }\mu\text{m}$  gap. A continuous ramp of shear rate from  $8 \times 10^4$  to  $8 \times 10^{-4} \text{ s}^{-1}$  was applied.

## Appendix II

### II.4. References

[1] Greenley R.Z. In Polymer Handbook, 4th ed.; Brandrup J., Immergut E.H., Grulke E.A., Eds.; John Wiley & Sons: USA, 1999; p II-310-314.

[2] Grabiell, C.E. and Decker, D.L., Copolymerization characteristics of sodium styrenesulfonate. *Journal of Polymer Science* **1962**, 59(168), 425-431.

[3] Xinxin, L., Xiaomin, Y., Pingping, W., and Zhewen, H., Effect of temperature on copolymerization parameters of hydroxyethyl acrylate and methyl methacrylate, *Chinese Journal of Polymer Science* **1998**, 16(1), 25-31.

[4] van Herk, A.M., Pulsed initiation polymerization as a means of obtaining propagation rate coefficients in free-radical polymerizations. II Review up to 2000. *Macromolecular Theory and Simulations* **2000**, 9(8), 433-441.

## Appendix III

### III.1. Selection of the seed used in Chapters 3-6

#### III.1.1. Method

A 2 L reactor equipped with a stainless steel 8-bladed frame-type stirrer, a reflux condenser, a N<sub>2</sub> inlet, a temperature probe, a sampling tube and two feeding inlets was first charged with an aqueous solution of NaSS. Then, the MMA/BA mixture was added as a shot and the content was stirred at 200 rpm under N<sub>2</sub> for 20 minutes. The aqueous solutions of reductant and oxidant TBHP/AsAc (0.54% wbm / 0.53% wbm) were fed separately into the reactor for 90 minutes at a temperature of 70°C. The reaction was continued further at the same temperature for 2 hours under stirring. The recipe used to synthesize the seed with 2 wbm % NaSS is given in Table III.1.

The reason to use TBHP/ AsAc redox pair in the seed synthesis is that this redox system forms noncharged radicals and hence the only charged species in the seed are due to the NaSS.

### Appendix III

**Table III.1.** The recipe for seed production in batch at 10wt% solids content

	Initial charge	Feed 2	Feed 3
MMA (g)	75	-	-
BA (g)	75	-	-
NaSS (g)	3	-	-
AsAc (g)	-	0.79	-
TBHP (g)	-	-	0.81
H <sub>2</sub> O (g)	1213	89.2	89.2

#### III.1.2. Results

The details of the seeds synthesized at 10 wt% solids content are given in Table III.2. It can be seen that the as NaSS concentration decreased, final conversion of NaSS and particle size increased. In all cases, coagulation was below 1 wt%.

**Table III.2.** Details of the batch reactions at 10 wt% solids content

Composition (MMA/BA/NaSS)	Z-ave size (nm)	Coagulum (wt%)	Conversion of NaSS (%)
50/50/2.5	120	0.9	77
50/50/2.0	120	0.3	84
50/50/1.5	155	0.4	85
50/50/0.75	170	0.2	87

### Appendix III

Figure III.1 shows that high conversion (98-100%) of volatile monomers (MMA+BA) was achieved and the reaction rates were affected by the concentration of NaSS. Long inhibition times of 40-60 minutes were observed because the monomers used were of industrial grade i.e. containing small amounts of inhibitors, which consumed most of the radicals initially formed.

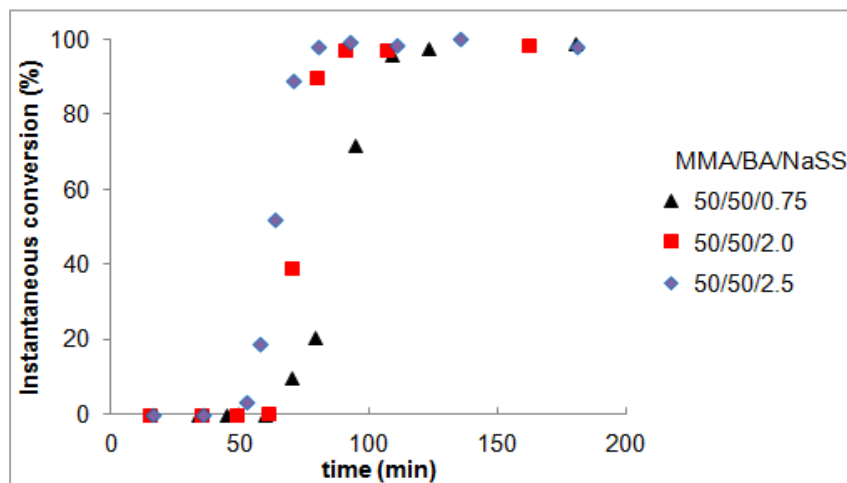


Figure III.1. Time evolution of monomer conversion for batch reactions at 10 wt% solids contents by using different NaSS concentrations

Among the seeds, the one with the smallest size produced by using the lowest concentration of NaSS (2% wbm) was selected to be used in all seeded semicontinuous polymerizations.

Appendix III

### **III.2. Effect of initiator concentration and feed time/strategy on the chemical incorporation of sodium styrene sulfonate onto MMA/BA particles**

#### **III.2.1. Method**

A 1 L reactor equipped with a stainless steel two-stage three-bladed Ekato MIG impeller, a reflux condenser, a N<sub>2</sub> inlet, a temperature probe, and three feeding inlets, was first charged with the seed and purged with N<sub>2</sub> for 20 minutes under 200 rpm agitation. When the temperature reached 70°C, the reactants were added in three separated feeds. Feed 1 was MMA+BA. Feed 2 was the aqueous solution of TBHP and feed 3 was the aqueous solution of NaSS+AsAc. At the end of the feedings, the system was allowed to react batchwise for 2 hours.

For the investigation of the initiator concentration, the concentration of initiator was varied from 1.1% to 0.27% wbm while NaSS concentration in the formulation was kept constant at 1.3 wbm% and the feedings were performed for 5 hours.

For the investigation of the feed time/strategy, the concurrent feed times of MMA+BA and NaSS were varied from 5 to 2 hours in three reactions. In a fourth run, a different feed strategy was applied. MMA/BA, TBHP and AsAc were fed for 3.5 hours whereas the feeding of NaSS was made for 2 hours. In these reactions, the concentration of NaSS was 1.3 wbm% and initiator concentration was 0.54 wbm%.

### Appendix III

A representative recipe is given in Table III.3 for the reaction with the following concentrations: [NaSS]= 1.3 wbm% and [I]= 0.54 wbm%.

**Table III.3.** Representative recipe for high solids content seeded semicontinuous reactions

	Initial charge	Feed 1	Feed 2	Feed 3
Seed (g)	225	-	-	-
MMA (g)	-	129.2	-	-
BA (g)	-	129.2	-	-
NaSS (g)	-	-	3.21	-
AsAc (g)	-	-	0.69	-
TBHP (g)	-	-	-	0.7
H <sub>2</sub> O (g)	-	-	54.5	29.3

#### III.2.2. Results

The total concentration of initiator used in seeded semicontinuous reactions was varied from 1.1% to 0.27% wbm while NaSS concentration in the formulation was kept constant at 1.3 wt%. Figure III.2 shows that the higher the initiator concentration, the higher the instantaneous conversion of MMA+BA, and when [I]  $\geq$  0.54 wbm% the process was under starved conditions (Figure III.3). In all cases, the number of particles slightly decreased during the feed process, indicating some particle coagulation (Figure III.4).

Appendix III

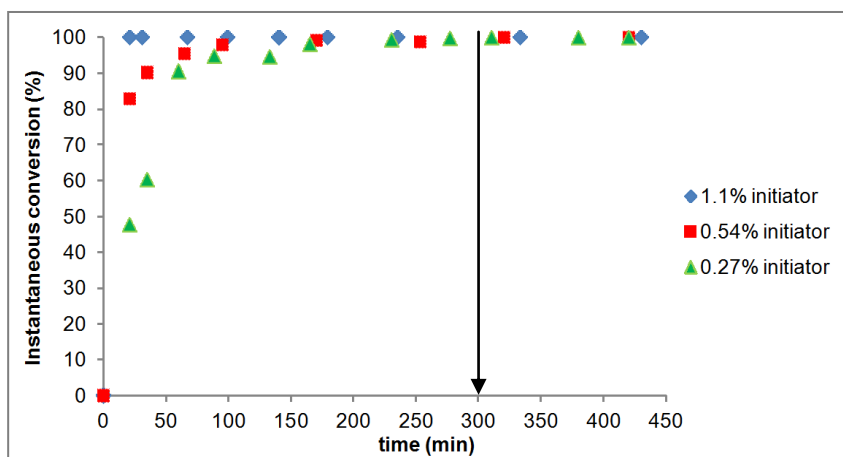


Figure III.2. Time evolution of monomer conversion for seeded semicontinuous reactions by using different initiator concentrations. Reaction conditions: [NaSS]= 1.3 wbm%, feed time= 5 h. The arrow indicates the end of feedings.

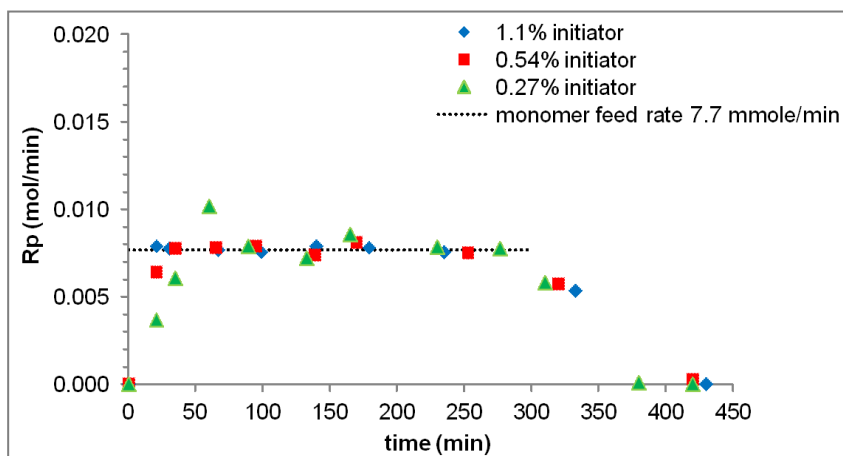


Figure III.3. Rate of polymerization as a function of time for seeded semicontinuous reactions by using different initiator concentrations. Reaction conditions: [NaSS]= 1.3 wbm%, feed time= 5 h.

### Appendix III

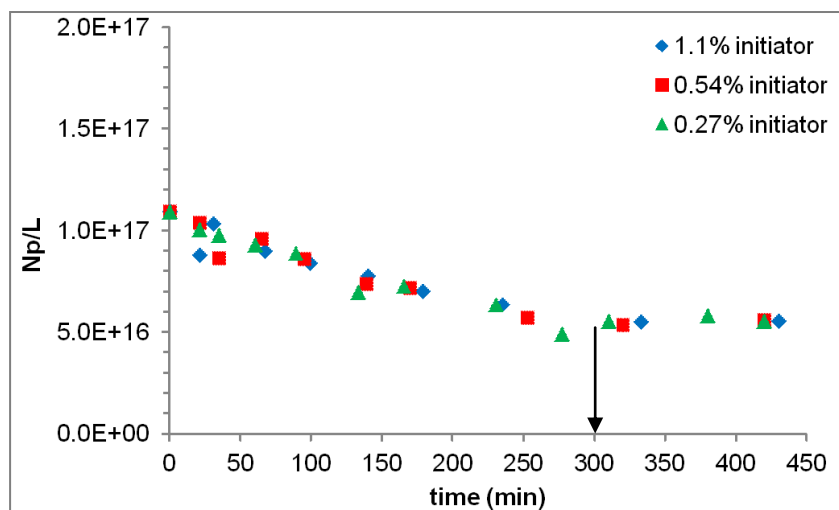


Figure III.4. Time evolution of number of particles for seeded semicontinuous reactions by using different initiator concentrations. Reaction conditions: [NaSS]= 1.3 wbm%, feed time= 5 h. The arrow indicates the end of feedings

The characteristics of the latexes are given in Table III.4. Although the conversion of NaSS decreased with the decrease in initiator concentration, there is a slight increase in incorporation indicating that the yield was slightly higher as less initiator was used. It is also seen that as the initiator concentration decreased, the surface tension which can be associated to the in-situ formed emulsifier that is dissolved in the aqueous phase increased. These can be explained by the lower comonomer conversion obtained at low initiator concentration. As the concentration of hydrophobic comonomers in the aqueous phase are higher, more hydrophobic namely, less water soluble oligomers are formed. This effect may be reinforced by the

### Appendix III

longer molecular weights of the oligoradicals (at low [I], molecular termination is less).

Therefore, there may be more chance of chemical incorporation of NaSS.

Similar final particle sizes were obtained. Molecular weights of the polymers were measured in DMF and refer to the whole system. They decreased as initiator concentration increased, likely due to increased entry rates of the radicals, that resulted in an increase in termination rates in the particles; thus, the average lifetime of the growing chains decreased and as well as the molecular weights. The coagulation was higher than 1wt% when [I] =0.27 wbm%. This may be related with slow reaction kinetics in the initial stages of the reaction, resulting in a slow formation of stabilizing copolymer.

By considering the molecular weights, conversion values and coagulation concentrations, an initiator concentration of 0.54 wbm% was selected to be used in the subsequent reactions.

**Table III.4.** Properties of latexes produced by different initiator concentrations

Initiator amount (% wbm)	NaSS amount (wbm%)	MMA+BA feed time (h)	NaSS feed time (h)	Coag. (%)	NaSS conv. (%)	NaSS inc. (%)	Surface tension (mN/m)	Size by CHDF (nm)	M <sub>w</sub>	Đ
1.1	1.3	5	5	0.2	97	70.3	51.5 ± 0.1	245.5 ± 19.2	257,000	2.4
0.54				0.6	95	71.5	54.0 ± 0.1	247.4 ± 17.4	355,600	2.5
0.27				2.1	92	72.4	56.4 ± 0.2	248.0 ± 15.2	451,000	2.5

### Appendix III

The concurrent feed times of MMA+BA and NaSS were varied from 5 to 2 hours while the other parameters were kept constant, namely  $[\text{NaSS}] = 1.3\% \text{ wbm}$  and  $[\text{I}] = 0.54\% \text{ wbm}$ . In a fourth run, a different feed strategy was applied; MMA/BA, TBHP and AsAc were fed for 3.5 hours whereas the feeding of NaSS was made for 2 hours. The instantaneous conversion of volatile monomers is presented in Figure III.5 as a function of relative time for the sake of comparison. The time scale was normalized by taking the end of the comonomer feedings (MMA+BA) as relative time =1 for all the cases. There was no significant difference in the instantaneous conversion of volatile monomers except that the final conversion stayed at 99.5% in the reaction with 2 hours of concurrent feeds. All systems displayed monomer starved conditions (Figure III.6).

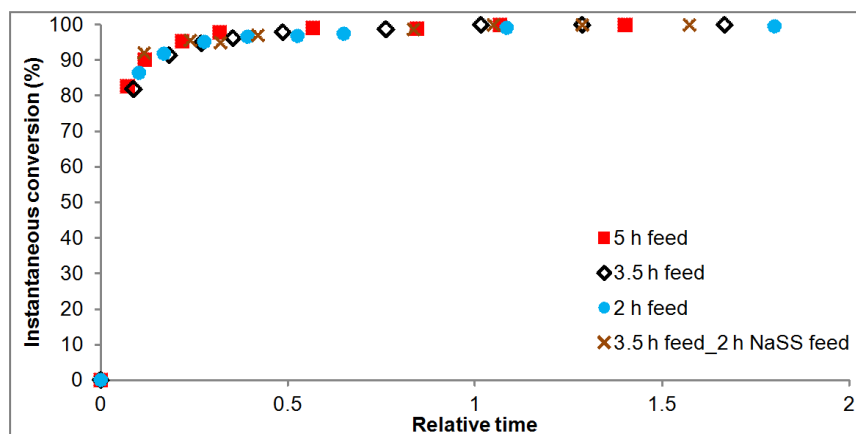


Figure III.5. Monomer conversion as a function of relative time for seeded semicontinuous reactions by using different feed time/strategy. Reaction conditions:  $[\text{NaSS}] = 1.3\% \text{ wbm}$ ,  $[\text{I}] = 0.54\% \text{ wbm}$ . Relative time =1 indicates the end of monomer feedings (MMA+BA).

Appendix III

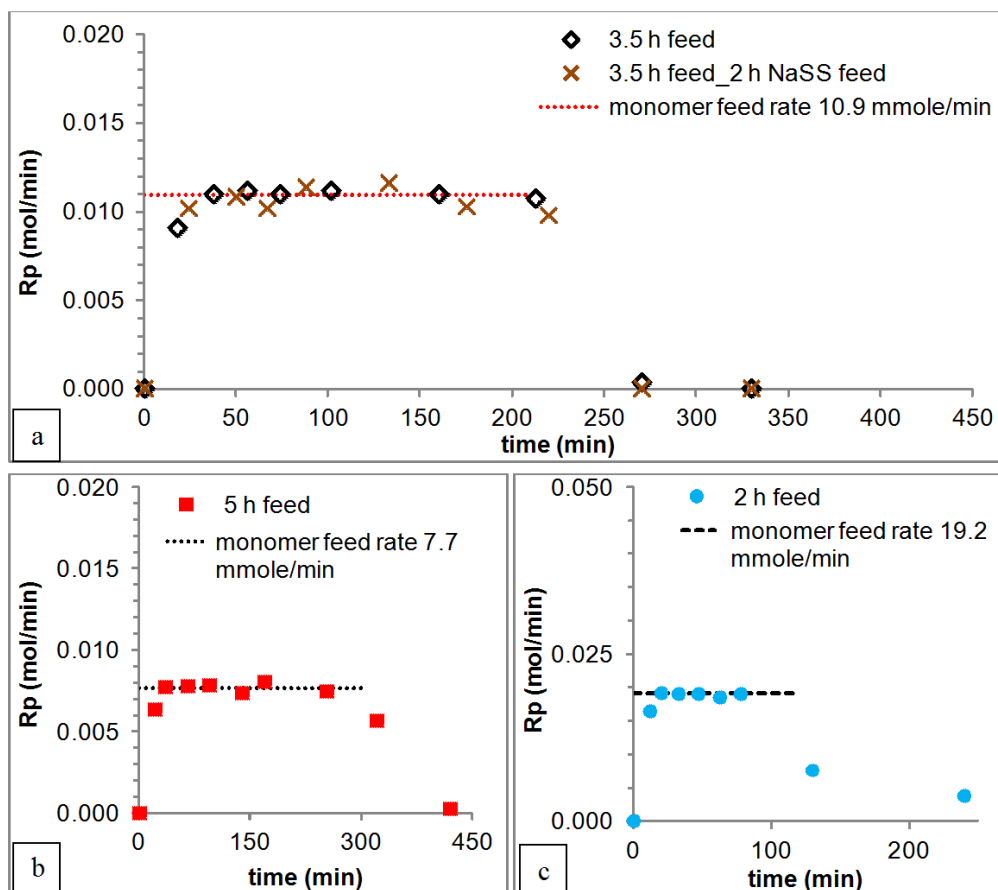


Figure III.6. Rate of polymerization as a function of time for seeded semicontinuous reactions by using different feed time/ strategy. Reaction conditions:  $[NaSS] = 1.3$  wbm%,  $[I] = 0.54$  wbm%.

The number of particles decreased continuously during the feed process in all reactions indicating some particle coagulation, except the reaction where NaSS was fed faster (Figure III.7). This strategy gave a higher number of particles at the

### Appendix III

beginning of the reactions (up to 60 min), but later  $N_p$  approached to the value obtained with 3.5 h feeding.

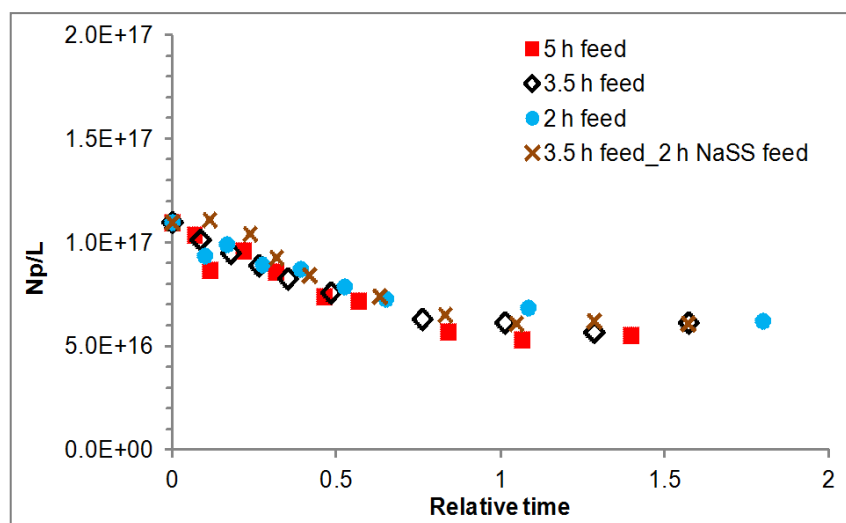


Figure III.7. Number of particles as a function of relative time for seeded semicontinuous reactions by using different feed time/strategy. Reaction conditions:  $[NaSS]= 1.3$  wbm%,  $[I]= 0.54$  wbm%. Relative time =1 indicates the end of monomer feedings (MMA+BA)

Table III.5 shows that the process time could be substantially reduced from 5 hours to 3.5 hours without observing any significant effect on the final conversion of NaSS achieved. However, a feeding time of 2 hours resulted in lower conversions of NaSS (91%). In the reaction where NaSS was fed faster, the highest value for both NaSS conversion (99%) and NaSS incorporation (73.2%) was achieved. The former

### Appendix III

can be explained by the fact that the feeding of initiators continued although NaSS feeding was finished and the latter is because there was plenty of hydrophobic comonomer in the aqueous phase for NaSS to react with, which favor the chemical incorporation. Consistent with the extent of NaSS incorporation, the surface tension values increased slightly as faster feedings were made.

**Table III.5.** Properties of latexes produced by different feed time/strategy

Initiator amount (% wbm)	NaSS amount (wbm%)	MMA+BA feed time (h)	NaSS feed time (h)	Coag. (%)	NaSS conv. (%)	NaSS inc. (%)	Surface tension (mN/m)	Size by CHDF (nm)	M <sub>w</sub>	Đ
0.54	1.3	5	5	0.6	95	71.5	54.0 ± 0.1	247.4 ± 17.4	355,600	2.5
		3.5	3.5	0.7	95	72.5	54.8 ± 0.2	243.7 ± 19.2	368,000	2.7
		3.5	2	1.3	99	73.2	55.6 ± 0.2	245.1 ± 18.5	365,500	2.6
		2	2	0.6	91	72.6	55.7 ± 0.5	244.8 ± 19.0	368,900	2.9

There was no significant effect of feed time/strategy on the final particle sizes and the molecular weights of the polymers. A coagulation amount >1 wt% observed in the reaction in which a faster feed of NaSS was applied. This might be related with slightly higher ionic strength of the reaction medium compared to the systems with concurrent feedings.

## Appendix IV. Supporting Information for Chapter 7

**Table IV.1.** Observations made during water blanching test of the latex films

<b>Code</b>	<b>Initial</b>	<b>30 min</b>	<b>60 min</b>	<b>3 hours</b>	<b>4 hours</b>	<b>24 hours</b>
<b>0.5%</b>	transp.	Slight white coloration	Slightly bluish	bluish	bluish, some blistering	whitening, some blistering
<b>0.76%</b>	transp.	Slightly bluish	bluish	bluish	bluish, some blistering	whitening, some blistering
<b>1%</b>	transp.	Slightly white coloration	Slightly bluish	bluish	bluish	whitening
<b>1.3%</b>	transp.	Slightly white coloration	Slightly bluish	bluish	bluish	bluish
<b>3.6%</b>	transp.	whitening, partial delamination	delamination	delamination	delamination	delamination
<b>HPO</b>	transp.	Slightly white coloration, blistering	white coloration, blistering	white coloration, blistering, wrinkles	white coloration, blistering, wrinkles	whitening, wrinkles, delamination
<b>KPS</b>	transp.	no change	no change	no change	no change	bluish, some blistering
<b>SDS</b>	opaque	Slightly white coloration, cracks	cracks, whitening	cracks, whitening, blistering	blistering, wrinkles, delamination	whitening, blistering, wrinkles, delamination
<b>Syn-A</b>	slightly opaque	Slightly white coloration	wrinkles at the edges	wrinkles, blistering	wrinkles, blistering	wrinkles, blistering

Appendix IV

Table IV.2. Data for storage stability test of the paints

	3.6%	1.3%	1%	0.76%	0.5%	HPO	KPS	SDS	Syn-A
Phase sep. (mm) 2 weeks	0.3	0.3	0.25	0.25	0.25	0.8	0.6	0.6	0.4
Phase sep. (mm) 4 weeks	0.6	0.7	0.4	0.55	0.7	0.8	0.5	0.6	0.6
pH (initial)	9.68	9.7	9.76	9.74	9.71	9.65	9.75	9.66	9.45
pH (5 days)	9.47	9.33	9.3	9.35	9.54	9.3	9.44	9.31	9.16
pH (2 weeks)	9.33	9.43	9.48	9.48	9.45	9.41	9.52	9.39	9.34
pH (4 weeks)	8.87	8.80	8.94	9.13	9.02	8.92	9.01	9.22	9.10
Drop in pH, 4 weeks	-0.8	-0.9	-0.8	-0.6	-0.7	-0.7	-0.7	-0.4	-0.4
Viscosity (kU) (initial)	95.4	95.7	94.2	92.6	92.2	95.4	99.8	92.6	95.5
Viscosity (5 days)	96.3	95	94.5	93.3	91.3	95.3	100.7	91.6	96.2
Viscosity (2 weeks)	93.9	92.6	93.1	90.5	88	95.4	98.5	89.6	93.9
Viscosity (4 weeks)	95.4	93.6	93.9	91.3	89	95.1	100.4	86.3	96.1
Drop in viscosity,4 weeks	0	-2.1	-0.3	-1.3	-3.2	-0.3	0.6	-6.3	0.6
Lightness (initial)	94.83	95.07	94.69	94.68	94.59	94.48	95.04	94.58	94.54
L (1 week)	94.48	93.33	93.68	93.51	94.21	94.06	94.12	93.34	93.85
L (15 days)	94.18	94.19	94.06	94.23	94.21	94.24	94.21	94.34	94.44
L (4 weeks)	94.04	93.86	94.21	94.47	94.00	93.83	94.26	93.82	94.32
delta L (4 weeks)	-0.80	-1.22	-0.48	-0.22	-0.58	-0.65	-0.78	-0.76	-0.22
a (initial)	-0.16	-0.22	-0.08	-0.01	0.21	0.08	-0.21	0.07	0.19
a (1 week)	-0.02	0.48	0.34	0.43	0.35	0.30	0.39	0.47	0.55
a (15 days)	0.05	0.11	0.22	0.07	0.24	0.14	0.26	0.17	0.33
a (4 weeks)	0.18	0.13	-0.03	-0.22	0.27	0.01	0.10	0.34	0.24
delta a (4 weeks)	0.34	0.35	0.05	-0.22	0.07	-0.07	0.31	0.27	0.05
b (initial)	0.05	0.20	-0.03	0.17	-0.19	-0.10	-0.07	-0.24	-0.39
b (1 week)	0.51	-0.49	-0.13	-0.15	-0.14	0.03	-0.29	-0.77	-0.63
b (15 days)	0.68	0.59	0.47	0.78	0.31	0.58	0.20	0.62	-0.08
b (4 weeks)	0.70	0.51	0.61	0.97	0.40	0.36	0.31	0.43	-0.03
delta b (4 weeks)	0.65	0.31	0.64	0.80	0.58	0.46	0.38	0.67	0.36
ΔE (4 weeks)	1.08	1.30	0.80	0.86	0.83	0.80	0.91	1.05	0.42
WI (initial)	87.43	87.17	87.50	86.44	88.12	87.43	88.54	88.40	89.11
WI (1 week)	84.04	86.74	85.67	85.37	86.97	85.71	87.60	88.37	88.77
WI (15 days)	82.55	83.01	83.38	82.25	84.56	83.17	85.15	83.18	87.17
WI (4 weeks)	82.11	82.68	82.90	81.59	83.66	83.44	84.67	83.05	86.67
delta WI	-5.31	-4.49	-4.60	-4.85	-4.46	-3.99	-3.88	-5.35	-2.44
YI (initial)	0.18	0.43	0.10	0.53	0.02	0.07	-0.07	-0.19	-0.40
YI (1 week)	1.23	-0.37	0.23	0.27	0.22	0.51	-0.06	-0.96	-0.60
YI (15 days)	1.58	1.46	1.31	1.80	1.01	1.46	0.82	1.56	0.32
YI (4 weeks)	1.72	1.32	1.40	1.95	1.20	0.92	0.90	1.32	0.35
delta YI	1.54	0.89	1.30	1.42	1.18	0.85	0.98	1.51	0.75
Contrast ratio % (initial)	90.67	88.35	90.53	89.12	85.69	88.55	87.83	90.67	87.49
CR % (1 week)	89.61	90.00	91.23	93.07	89.71	89.21	91.61	95.17	88.41
CR % (15 days)	85.15	91.04	93.10	93.17	89.74	92.72	91.72	92.33	90.79
CR % (4 weeks)	85.76	86.00	87.75	88.86	87.03	81.06	88.15	80.45	86.04
Gloss 20° (initial)	1.40	1.40	1.40	1.40	1.40	1.40	1.40	1.40	1.40
Gloss 60° (initial)	4.20	4.60	4.50	4.40	4.50	4.30	4.80	4.20	4.40
Gloss 85° (initial)	2.70	3.20	3.10	3.20	3.20	3.10	3.10	2.70	2.50
Gloss 20° (1 week)	1.4	1.4	1.4	1.4	1.4	1.4	1.5	1.4	1.5
Gloss 60° (1 week)	4.2	4.2	4.1	4	4.2	4.2	4.7	4.3	4.6
Gloss 85°(1 week)	2.6	2.7	2.6	2.8	3.1	3	2.8	2.6	2.5
Gloss 20° (15 days)	1.50	1.50	1.50	1.50	1.50	1.50	1.50	1.50	1.50
Gloss 60° (15 days)	4.70	4.60	5.10	4.80	4.90	4.80	4.8	4.70	5.10
Gloss 85° (15 days)	3.20	3.30	3.60	3.60	3.80	3.50	3.00	3.20	3.30
Gloss 20° (4 weeks)	1.4	1.4	1.5	1.5	1.5	1.5	1.4	1.4	1.5
Gloss 60° (4 weeks)	4.5	4.6	4.7	4.5	4.8	4.4	4.5	4.7	4.8
Gloss 85° (4 weeks)	3.1	3.3	3.3	3.4	3.8	3.1	2.7	3.2	3.1
Gloss retention 60°	107	100	104	102	107	102	94	112	109
Gloss retention 85°	115	103	106	106	119	100	87	119	124

Appendix IV

**Table IV.3.** Data for natural weathering test of the paints

	3.60%	1.30%	1%	0.76%	0.50%	HPO	KPS	SDS	Syn-A
Lightness (initial)	95.96	95.89	95.98	95.74	95.95	95.73	96.11	95.74	95.73
L (2 weeks)	95.73	95.62	95.55	95.48	95.68	95.37	95.44	94.58	94.25
L (4 weeks)	95.07	95.27	95.01	95.09	95.19	94.01	94.74	93.74	93.27
delta L (4 weeks)	-0.89	-0.62	-0.97	-0.65	-0.75	-1.72	-1.38	-2.01	-2.46
a (initial)	-0.27	-0.20	-0.17	-0.23	-0.25	-0.12	-0.09	-0.23	-0.17
a (2 weeks)	-0.54	-0.20	-0.53	-0.25	-0.54	-0.44	-0.40	-0.25	-0.16
a (4 weeks)	0.01	-0.18	-0.08	-0.23	0.02	-0.07	-0.13	-0.11	-0.12
delta a (4 weeks)	0.28	0.02	0.09	0.00	0.26	0.05	-0.04	0.12	0.06
b (initial)	1.57	1.41	1.48	1.44	1.26	1.30	1.33	1.44	0.94
b (2 weeks)	1.76	1.72	1.75	1.79	1.83	1.71	1.60	1.65	1.63
b (4 weeks)	1.62	1.93	1.73	1.86	1.79	1.88	1.72	1.76	1.77
delta b (4 weeks)	0.06	0.52	0.25	0.42	0.53	0.59	0.39	0.32	0.83
ΔE (4 weeks)	0.94	0.81	1.00	0.77	0.96	1.82	1.43	2.03	2.60
WI (initial)	81.71	82.37	82.22	81.90	83.38	82.70	83.39	81.90	84.65
WI (2 weeks)	80.16	80.15	79.79	79.44	79.67	79.61	80.38	78.22	77.56
WI (4 weeks)	79.39	78.21	78.73	78.18	78.79	75.74	78.19	75.76	74.73
deltaWI (4 weeks)	-2.32	-4.16	-3.49	-3.72	-4.59	-6.96	-5.20	-6.13	-9.91
YI (initial)	3.03	2.80	2.95	2.82	2.46	2.63	2.70	2.82	1.90
YI (2 weeks)	3.19	3.38	3.19	3.48	3.33	3.19	2.99	3.23	3.28
YI (4 weeks)	3.38	3.81	3.51	3.65	3.69	3.85	3.46	3.59	3.61
deltaYI (4 weeks)	0.35	1.01	0.56	0.83	1.23	1.21	0.76	0.77	1.71
Gloss 20° (initial)	1.5	1.5	1.5	1.5	1.6	1.5	1.6	1.6	1.5
Gloss 60° (initial)	4.5	4.9	5.0	4.7	4.8	4.7	5.3	4.9	4.8
Gloss 85° (initial)	2.4	3.4	2.7	3.2	2.8	2.1	2.5	3.3	2.6
Gloss 20° (2 weeks)	1.5	1.6	1.6	1.5	1.5	1.5	1.6	1.5	1.5
Gloss 60° (2 weeks)	4.3	4.9	5.0	4.7	5.0	4.6	5.2	4.9	4.7
Gloss 85° (2 weeks)	3.3	3.8	3.4	3.8	4.4	3.7	4.0	3.4	3.3
Gloss 20° (4 weeks)	1.4	1.5	1.5	1.5	1.5	1.5	1.5	1.5	1.5
Gloss 60° (4 weeks)	4.4	4.8	4.9	4.7	4.8	4.5	5.2	4.8	4.7
Gloss 85° (4 weeks)	3.3	4	3.6	4	4.3	4	4.2	3.9	3.5
Gloss retention 60° (4 weeks)	98	98	98	100	100	96	98	98	98